



**US Army Corps
of Engineers®**
Engineer Research and
Development Center

Flood and Coastal Storm Damage Reduction R&D Program

Adaptation of the Levee Erosional Equivalence Method for the Hurricane Storm Damage Risk Reduction System (HSDRRS)

Steven A. Hughes

May 2011



Adaptation of the Levee Erosional Equivalence Method for the Hurricane Storm Damage Risk Reduction System (HSDRRS)

Steven A. Hughes

*Coastal and Hydraulics Laboratory
U.S. Army Engineer Research and Development Center
3909 Halls Ferry Road
Vicksburg, MS 39180-6199*

Final report

Approved for public release; distribution is unlimited.

Abstract: This report describes a rational methodology for evaluating the strength and resiliency of earthen levees against wave overtopping forces during hurricanes. The new methodology was developed by extending Dean, et al.'s (2010) concept of "cumulative excess work," which hypothesized that damage to grass-covered slopes is caused by cumulative work done by the overtopping waves in excess of some tolerable level. The erosional equivalence method is able to account for the fact that (1) earthen levees can tolerate certain levels of wave overtopping without any soil erosion, (2) earthen levees can survive some duration of increased wave overtopping with allowable erosion, and (3) earthen levees will eventually suffer slope damage if the overtopping level is high and overtopping duration is sufficiently long. A predictive capability for estimating the cumulative excess wave volume (or excess work) as a function of time for prescribed wave, surge, and levee parameters was developed for the cases of wave-only overtopping, combined wave and surge overtopping, and realistic storms with time-varying parameters. Application of the methodology is illustrated by worked examples. The erosional equivalence methodology provides a useful (but perhaps conservative) tool for comparative analyses of different reaches of the HSDRRS to identify which reaches would benefit from additional slope armoring.

DISCLAIMER: The contents of this report are not to be used for advertising, publication, or promotional purposes. Citation of trade names does not constitute an official endorsement or approval of the use of such commercial products. All product names and trademarks cited are the property of their respective owners. The findings of this report are not to be construed as an official Department of the Army position unless so designated by other authorized documents.

DESTROY THIS REPORT WHEN NO LONGER NEEDED. DO NOT RETURN IT TO THE ORIGINATOR.

Contents

Figures and Tables	vi
Preface	x
List of symbols	xi
Unit Conversion Factors	xv
1 Introduction	1
Background	1
Study purpose	3
Report contents.....	4
2 Concept of Levee Erosion Equivalence	6
Steady overflow - grass	6
Steady overflow - other slope protection.....	11
3 Dean et al. (2010) Application to Wave Overtopping	15
Unsteady wave overtopping.....	15
Linking the velocities to storm parameters	18
Some background on friction factors.....	20
4 Proposed Application to the HSDRRS	22
Idealized overtopping wave	22
Excess wave volume in an individual wave.....	25
Cumulative excess overtopping wave volume criterion.....	28
5 Application for Wave-Only Overtopping	30
Estimation of individual overtopping wave volumes (V_{Wn})	30
Incident wave periods ($T_{m-1,0}$ and T_m).....	31
Wave runup ($R_{u2\%}$).....	31
Average wave overtopping discharge (q).....	32
Levee freeboard (R_c).....	33
Individual wave overtopping volume (V_w)	33
Estimation of individual wave overtopping durations (T_{on})	35
Wave-only overtopping calculation procedure	38
Required parameters.....	39
Calculation of constant parameters.....	39
Monte Carlo simulation of the overtopping event	40
Example 1: Wave-only overtopping calculation	41
Calculation of constant parameters.....	41
Monte Carlo simulation of the overtopping event	44
Results of the wave-only overtopping example	46

Equivalent steady flow	50
Influence of storm and levee parameters.....	52
<i>Effect of average wave overtopping discharge</i>	52
<i>Effect of grass quality</i>	53
<i>Effect of significant wave height</i>	55
<i>Effect of friction factor</i>	57
<i>Effect of landward-side slope</i>	58
6 Application for Combined Wave Overtopping and Surge Overflow.....	60
Estimation of individual overtopping wave volumes (V_{Wn})	60
<i>Steady overflow discharge (q_s)</i>	61
<i>Average combined wave overtopping and surge overflow discharge (q_{ws})</i>	61
<i>Individual wave overtopping volume (V_w)</i>	61
Estimation of individual wave overtopping durations (T_{on})	62
Combined wave and surge overtopping calculation procedure.....	63
<i>Required parameters</i>	64
<i>Calculation of constant parameters</i>	64
<i>Monte Carlo simulation of the overtopping event</i>	65
Example 2: Combined wave and surge overtopping calculation	66
<i>Calculation of constant parameters</i>	66
<i>Monte Carlo simulation of the overtopping event</i>	68
<i>Results of the combined wave and surge overtopping example</i>	69
7 Application for Time-Varying Waves and Surge	73
Simulation method for time-varying waves and surge	73
Simulation of a hypothetical storm	73
Simulation variations due to slope protection types	76
8 Comparison of Methodology to Wave Overtopping Simulator Results	78
The Dutch Wave Overtopping Simulator	78
Dutch overtopping simulator test conditions.....	79
Comparison of the erosional equivalence methodology to OTS results.....	81
Comparison using larger critical threshold velocity.....	84
Dutch cumulative hydraulic load methodology.....	87
Conclusions	89
9 Uncertainties of the Methodology.....	91
Assumed damage mechanism	91
Definitions of damage and failure.....	93
Friction factors.....	96
Individual overtopping wave duration	96
<i>Effect of shorter overtopping durations</i>	96
<i>Case 1: Critical threshold velocity, $u_c = 1.8$ m/s</i>	99
<i>Case 2: Critical threshold velocity, $u_c = 5.0$ m/s</i>	102
<i>Conclusions</i>	103
Other uncertainties	104

10 Improvement of the Methodology	106
Improvements based on Colorado State University testing program	106
<i>Testing sequences</i>	107
<i>Acquired test information</i>	108
<i>Analysis of test results</i>	109
<i>Roadblocks</i>	110
<i>Postscript on the 2010 CSU Wave Overtopping Simulator tests</i>	111
Improvements based on Hurricane Katrina observations	111
Improvements based on Dutch overtopping simulator results	112
Summary	113
11 Summary and Conclusions	114
Summary	114
Caveats and uncertainties	117
Conclusions	119
References	121
Appendix: The Relationship Between Flow Work and Stream Power	123
Report Documentation Page	

Figures and Tables

Figures

Figure 1. Limiting velocity versus overflow duration for grass	6
Figure 2. Erosion resistance of grass-lined spillways	7
Figure 3. Dean et al. (2010) best fit of Equation (3) to Hewlett et al. (1987) curves.	10
Figure 4. Schematic representation of the Hewlett et al. (1987) curve for good grass.	11
Figure 5. Original limiting velocity curves from Hewlett et al. (1987).....	12
Figure 6. Best-fit to the Hewlett et al. (1987) curves for mats.....	14
Figure 7. Schematic representation of the work accumulation during wave overtopping.....	16
Figure 8. Definition of average wave overtopping discharge used by Dean et al. (2010).....	18
Figure 9. Flow depth, velocity, and calculated discharge	22
Figure 10. Flow parameters of an idealized overtopping wave.	23
Figure 11. Excess wave volume above the threshold for a realistic individual wave.....	25
Figure 12. Excess wave volume above the threshold for an idealized individual wave.	25
Figure 13. Variation of exponent m in Equation (29).	27
Figure 14. Wave volume exceedance probability distribution for wave-only overtopping.....	35
Figure 15. Individual wave overtopping duration for negative freeboard.....	38
Figure 16. Results of the wave-only overtopping example.	47
Figure 17. Twenty repeats of the wave-only overtopping example.....	48
Figure 18. Best simulation and limits from the wave-only overtopping example.....	48
Figure 19. Time histories of individual wave volumes and durations for a simulation.....	49
Figure 20. Effect of average overtopping discharge for wave-only overtopping example.....	53
Figure 21. Effect of grass quality on levee resiliency for wave-only overtopping example.....	54
Figure 22. Effect of different wave heights for same average overtopping discharge.	56
Figure 23. Effect of different wave heights for threshold velocity, $u_c = 4$ m/s.....	57
Figure 24. Effect of different landward-side slope friction factors.	59
Figure 25. Effect of different landward-side slopes.....	59
Figure 26. Individual overtopping volumes for combined wave and surge overtopping.....	63
Figure 27. Results from the combined wave and surge overtopping example.....	70
Figure 28. Time histories of wave volumes and durations for combined example.....	71
Figure 29. Storm parameters represented as discrete 1-hr steps.....	74
Figure 30. Result of hypothetical hurricane simulation for good grass.	75
Figure 31. Individual wave volumes and overtopping durations for storm simulation.	76
Figure 32. Variations between different grass qualities.	77
Figure 33. Comparison between good grass and open mat simulations.	77
Figure 34. The Dutch Wave Overtopping Simulator in action	79
Figure 35. Wave Overtopping Simulator experiments.	82

Figure 36. Slope damage at St. Philipsland after $q = 50$ l/s/m test	83
Figure 37. Slope damage at Boonweg after $q = 75$ l/s/m test.....	85
Figure 38. Individual wave volumes and overtopping durations for the OTS simulation.	86
Figure 39. Wave Overtopping Simulator experiments with $u_c = 5.0$ m/s.....	87
Figure 40. Difference due to overtopping duration reduction.	99
Figure 41. Wave periods from Bosman Equation (56) for Case 1 first run.	99
Figure 42. Wave periods from Bosman Equation (56) reduced using $\gamma_T = 0.5$ for Case 1.	100
Figure 43. Cumulative excess wave volume estimates for $u_c = 1.8$ m/s.	100
Figure 44. Rank-ordered values of q_c/q_p from the first Case 1 simulation.....	101
Figure 45. Cumulative excess wave volume estimates for $u_c = 5.0$ m/s.	103
Figure 46. Rank-ordered values of q_c/q_p from the first Case 2 simulation.....	104
Figure 47. Dimensions and orientation of test trays.....	107
Figure 48. Colorado State University Overtopping Test Facility.....	107

Tables

Table 1. Results for the best-fit of Equation (3) to the Hewlett et al. (1987) grass curves.	9
Table 2. Results for the best-fit of Equation (3) to the Hewlett et al. (1987) mat curves.....	14
Table 3. Required input parameters for wave-only overtopping.	39
Table 4. Input parameters for wave-only overtopping example.	42
Table 5. Calculated parameters for wave-only overtopping example.....	46
Table 6. Required input parameters for combined wave and surge overtopping.	64
Table 7. Input parameters for combined wave and surge overtopping example.....	66
Table 8. Calculated parameters for combined wave and surge overtopping example.....	70
Table 9. Parameters for hypothetical time-varying hurricane.	74
Table 10. Comparison of wave overtopping parameters for three average discharges.....	80

Executive Summary

Report summary

This report describes a rational methodology for evaluating the strength and resiliency of earthen levee protection against wave overtopping forces during severe hurricanes. The new methodology was developed by applying and extending the concept of “cumulative excess work” originally proposed by Dean et al. (2010). They hypothesized that damage to grass-covered slopes was caused by cumulative work done by the overtopping waves on the levee slope, in excess of some tolerable work level. Once the initiation of erosion threshold has been exceeded during an overtopping event, there is a certain amount of allowable erosion that can occur without causing damage to the slope protection. However, if overtopping persists, at some point the cumulative erosion results in slope damage.

A predictive capability for estimating the cumulative excess wave volume (or excess work) as a function of time for prescribed wave, surge, and levee parameters was developed for the cases of wave-only overtopping, combined wave and surge overtopping, and realistic storms with time-varying parameters. Application of the methodology is illustrated by worked examples.

Descriptions and provisional results from the Dutch testing of actual dike slopes using the Wave Overtopping Simulator (OTS) provided insight into the progression of slope damage. Simulations using the erosional equivalence methodology showed good correspondence to the Dutch testing when a higher value of critical threshold velocity was used.

There are several uncertainties in the erosional equivalence predictive methodology. One uncertainty pertains to how we define the conditions of initial erosion, damage progression, and damage limit for the various types of levee slope protection. Another uncertainty is whether or not the physical processes causing damage for wave overtopping are similar to the damage processes for steady overflow. The turbulence levels in overtopping waves are higher, and this could accelerate the erosion processes. The key uncertainty in the methodology is using the values of critical threshold velocity and erosional damage limit derived for steady overflow. These

important thresholds will need to be adjusted, if possible, based on full-scale testing and analysis of field observations.

Report conclusions

Armoring portions of the HSDRRS to provide greater resiliency for storm events that exceed the established design level is a critical mission for Task Force Hope. Previously, no design guidance existed that would provide a rational method for assessing where levee armoring should be placed to provide adequate resiliency against extreme storm events. Furthermore, no methods existed that could estimate the duration of overtopping that can be tolerated before slope damage becomes problematic.

The erosional equivalence method is able to account for the fact that (1) earthen levees can tolerate certain levels of wave overtopping without any soil erosion, (2) earthen levees can survive some duration of increased wave overtopping with a certain amount of allowable erosion, and (3) earthen levees will eventually suffer damage to the slope protection if the overtopping level is high enough and the overtopping persists for sufficient duration.

A predictive tool based on the erosional equivalence concept was developed to simulate the accumulation of excess wave volume for the cases of wave-only overtopping, combined wave and surge overtopping, and time-varying wave and surge conditions. The methodology provisionally uses critical threshold velocity and erosional limits derived from steady overflow conditions. However, these thresholds are most likely conservative and will predict damage sooner than should be expected because the critical threshold velocities are quite small. Nevertheless, the methodology provides a useful (but perhaps conservative) tool for comparative analyses of different reaches of the HSDRRS to identify which reaches will be likely candidates for additional slope armoring.

If fully validated using full-scale test results and other comparisons, the erosional equivalence methodology could provide a logical basis for selecting appropriate armoring options for all reaches of the HSDRRS exposed to potential wave overtopping. Like any engineering design tool, it would be prudent to include some factor of safety when using methodology results to determine levee armoring requirements.

Preface

This technical report summarizes and applies the “erosional equivalence” method proposed by Dean et al. (2010) as a methodology for evaluating resiliency of grass-covered levees subjected to wave overtopping. Explicit details of the application are provided, and worked examples are given for the cases of wave-only overtopping, wave overtopping combined with surge overflow, and time-varying storm simulations. The study was conducted by the U.S. Army Engineer Research and Development Center (ERDC), Coastal and Hydraulics Laboratory (CHL), Vicksburg, MS, for the U.S. Army Engineer District, New Orleans (MVN), and Task Force Hope (TFH). The intent of this report is to provide a viable framework for evaluation of armoring requirements for the Hurricane Storm Damage Risk Reduction System (HSDRRS) that can be refined when more full-scale data become available. A review draft of this report was submitted to TFH on 13 July 2010. The second draft incorporating comments and suggestions by the Internal Technical Review was completed during the period 10 - 18 January 2011, and the third draft with final comments incorporated was completed on 9 February 2011.

Dean Arnold, Task Force Hope, MVN, was the point of contact for the sponsoring New Orleans District, and he provided study oversight and arranged for independent technical review. Dr. Jentsje W. van der Meer provided valuable comments and suggestions for improving the report.

The technical report was written by Dr. Steven A. Hughes, Navigation Division (HN), CHL, during the period May 2010 through July 2010 under the direct supervision of Dr. Jackie S. Pettway, Chief, Harbors, Entrances, and Structures Branch, Navigation Division, CHL. Administrative supervision was provided by Dr. William D. Martin, Director, CHL, and Dr. M. Rose Kress, Chief, Navigation Division, CHL. Publication was funded through the Flood and Coastal Storm Damage Reduction R&D Program. Dr. Cary A. Talbot was Program Manager and William R. Curtis was Acting Technical Director.

COL Kevin Wilson was Commander and Executive Director of ERDC.
Dr. Jeffery P. Holland was Director.

List of symbols

a	Empirical overtopping wave volume distribution scale factor [-]
a	Exponent for idealized individual wave flow thickness formula [-]
b	Exponent for idealized individual wave flow velocity formula [-]
b_V	Weibull distribution shape factor for individual wave volumes [-]
C_Z	Chezy's roughness coefficient [$\text{m}^{1/2}/\text{s}$]
c_V	Weibull distrib. scale factor for individual wave volumes [m^3/m]
E_u	Erosion rate proportional to excess velocity [$\text{m}^3/\text{s}/\text{m}$]
E_W	Erosion rate proportional to excess work [$\text{m}^3/\text{s}/\text{m}$]
E_τ	Erosion rate proportional to excess shear stress [$\text{m}^3/\text{s}/\text{m}$]
f_D	Weisbach-Darcy Friction Factor [-]
f_F	Fanning's friction factor [-]
g	Gravitational acceleration [m/s^2]
H_L	Cumulative hydraulic loading [m^2/s^2]
H_{m0}	Energy-based significant wave height [m]
h	Instantaneous flow thickness [m]
h_p	Peak flow thickness of an individual wave [m]
K_u	Proportionality coefficient for excess velocity [m/s]
K_W	Proportionality coefficient for excess work [m^3/kg]
K_τ	Proportionality coefficient for excess shear stress [$\text{m}^2 \cdot \text{s}/\text{kg}$]
k_I	Fraction of incident wave parameter, $T_{0.2\%}$ [-]
$L_{m-1,0}$	Deepwater wave length based on mean spectral wave period [m]
m	Exponent for idealized individual wave discharge formula [-]
N	Summation limit [-]

N_{ow}	Number of overtopping waves [-]
N_W	Total number of waves [-]
n	Summation counter [-]
n	Manning's roughness coefficient [-]
P	Probability [-]
P_{ov}	Probability of overtopping waves [-]
P_S	Stream power per unit area [$N \cdot m/s/m^2$]
P_{Sc}	Critical threshold stream power per unit area [$N \cdot m/s/m^2$]
P_{Sn}	Stream power per unit area of the n th individual wave [$N \cdot m/s/m^2$]
P_T	Probability of a given individual overtopping wave duration [-]
P_{TE}	Exceedance probability of an individual wave duration [-]
P_V	Probability of a given overtopping wave volume [-]
P_{VE}	Exceedance probability of an individual wave volume [-]
q	Average wave-only overtopping discharge per unit length [$m^3/s/m$]
q_c	Critical threshold discharge per unit length [$m^3/s/m$]
q_n	Average discharge per unit length of the n th wave [$m^3/s/m$]
q_p	Peak discharge per unit length of an individual wave [$m^3/s/m$]
q_s	Steady overflow discharge per unit length [$m^3/s/m$]
q_{ws}	Average combined wave/surge overtopping discharge per unit length [$m^3/s/m$]
R	Hydraulic radius [m]
R_c	Crest freeboard [m]
$R_{u2\%}$	Runup elevation exceeded by 2% of the waves [m]
S_f	Friction slope (slope of the energy-grade line) [-]
S_0	Friction slope at steady flow terminal velocity ($= \sin \theta$) [-]
s	Coordinate parallel to the landward-side levee slope [m]

$T_{1/3}$	Average of highest 1/3 wave periods [s]
$T_{2\%}$	Wave period exceeded by 2% of incident waves [s]
T_c	Duration over which the critical threshold discharge is exceeded for an individual wave [s]
T_m	Mean wave period [s]
$T_{m-1,0}$	Mean spectral energy wave period [s]
T_o	Overtopping duration of an individual wave [s]
$T_{o2\%}$	Overtopping duration exceeded by 2% of individual waves [s]
T_{on}	Overtopping duration of the n th individual wave [s]
$T_{o,rms}$	Root-mean-square individual overtopping wave duration [s]
T_p	Peak spectral wave period [s]
t	Time [s]
t_E	Duration of storm event [hr]
t_n	Time increment of the n th overtopping wave [s]
u	Instantaneous velocity [m/s]
u_c	Critical threshold velocity for excess work assumption ($=u_{c,W}$) [m/s]
$u_{c,u}$	Critical threshold velocity for excess velocity assumption [m/s]
$u_{c,W}$	Critical threshold velocity for excess work assumption [m/s]
$u_{c,\tau}$	Critical threshold velocity for excess shear stress assumption [m/s]
u_n	Average velocity of the n th overtopping wave volume [m/s]
u_p	Peak flow velocity of an individual overtopping wave [m/s]
u_{pn}	Peak flow velocity of the n th individual overtopping wave [m/s]
V	Wave volume per unit length [m ³ /m]
V_E	Excess wave volume per unit length [m ³ /m]
V_W	Overtopping wave volume per unit length [m ³ /m]
V_{Wmax}	Maximum overtopping wave volume per unit length [m ³ /m]

V_{Wn}	Overtopping wave volume per unit length of the n th wave [m^3/m]
W	Steady overflow stream power per unit area [$\text{N}\cdot\text{m}/\text{s}/\text{m}^2$]
W_c	Critical threshold overflow stream power per unit area [$\text{N}\cdot\text{m}/\text{s}/\text{m}^2$]
α	Seaward structure slope angle [-]
α_τ	Shear stress proportionality coefficient [kg/m^3]
β_W	Work proportionality coefficient [kg/m^3]
Δ	Mathematical symbol for small increment [-]
γ_b	Reduction factor for influence of berm [-]
γ_f	Reduction factor for influence of roughness [-]
γ_T	Fraction of individual wave overtopping duration [-]
γ_v	Reduction factor for influence of vertical wall [-]
γ_w	Specific weight of water [kN/m^3]
γ_β	Reduction factor for influence of angle of wave attack [-]
θ	Landward-side levee slope angle [-]
$\xi_{m-1,0}$	Iribarren number based on deepwater wave length and mean energy period [-]
ρ	Density of water [kg/m^3]
τ	Steady overflow shear stress [N/m^2]
τ_c	Critical threshold shear stress [N/m^2]
τ_0	Instantaneous shear stress [N/m^2]

Unit Conversion Factors

Multiply	By	To Obtain
cubic feet	0.02831685	cubic meters
cubic feet per second per ft	0.0929	cubic meters per second per meter
cubic feet per second per ft	92.90	liters per second per meter
feet	0.3048	meters
inches	0.0254	meters
square feet	0.09290304	square meters
square inches	6.4516 E-04	square meters
yards	0.9144	meters

1 Introduction

Background

Task Force Hope (TFH) at the U.S. Army Engineer District, New Orleans (MVN), is responsible for overseeing the Corps of Engineers' \$14.6 billion hurricane protection system work in New Orleans and Southeast Louisiana, as well as performing the long-term planning of coastal restoration and hurricane damage reduction. This broad mission includes repairing and strengthening all components of the Hurricane Storm Damage Risk Reduction System (HSDRRS). Components of the HSDRRS include earthen levees, flood walls, flood gates, surge barriers, pumping systems, and all other structures needed to provide integrated and safe storm and flood protection to Southeast Louisiana.

An important part of strengthening the HSDRRS is a rigorous and scientific analysis of the probable hydrodynamic loading that could occur anywhere throughout the HSDRRS for hurricanes of specified intensity. Equally important is an assessment of how the levee system will respond to the projected hydrodynamic loading.

Paramount to the engineering analysis and design of the HSDRRS is the goal that every component must be strong enough to resist failing under extreme conditions. Failure in the context of earthen levees subjected to battering by hurricane force waves and elevated surge levels is defined as

Earthen levee failure: A loss of significant quantities of soil due to hydrodynamic forces resulting in either a decrease of levee crown elevation or a breaching of the levee itself that causes catastrophic damage.

Failure is typically the end result of damage to the earthen levee slope caused by soil erosion or removal of slope protection by hydrodynamic forces such as: (1) waves breaking on the flood-side slope, (2) waves overtopping the levee when the surge level is lower than the levee crown elevation, (3) surge overflow when the surge level exceeds the levee crown elevation, or (4) a combination of surge overflow and wave overtopping. Other failure modes resulting from hurricanes could include seepage

failure or geotechnical slip surface failure, but these failure modes will not be addressed in this report.

Damage is distinctly different from failure. The following is a general definition of damage that has been applied specifically to earthen levees.

Earthen levee damage: Degradation of the levee slope protective (grass cover or protective armoring) surface due to hydrodynamic loading either above or below the design level.

Damaged levees can continue to fulfill their designed function of preventing catastrophic flooding until such time the damage becomes so severe that failure occurs. The distinction between damage and failure is sometimes not communicated effectively to the general public, and often damage is equated to failure even though the structure continued to perform its primary design function. Depending on the degree of damage, immediate repairs may be needed to minimize the risk of failure during subsequent storms.

Well-designed levees are not expected to be damaged until the design conditions have been exceeded. However, there are abundant uncertainties in levee design that can lead to damage during conditions beneath the design level. The capability of an earthen levee to continue to fulfill its function after sustaining damage or being subjected to conditions greater than intended in the design is known as resiliency.

Earthen levee resiliency: The capability for any component of the HSDRRS earthen levees to maintain its intended functionality without failure when subjected to hydrodynamic loading greater than that of the design level. Damage can occur; but the damage should not interfere with the component functionality, and the damage should be repairable.

It was recognized by TFH that providing adequate earthen levee resiliency requires sound engineering analysis and judgment to determine (1) the capability of grass covers to protect the levees during wave and surge overtopping, (2) locations on the HSDRRS where additional slope protection beyond grass is required, and (3) the types of additional protection that will provide the necessary resiliency. This mission is the responsibility of the TFH Armoring Program Delivery Team.

The overall goal of the Armoring Program Delivery Team is...

...to develop and execute an armoring program that integrates the results of armoring studies, research and physical tests into armoring design recommendations and guidance, and to implement this guidance in the construction of the HSDRRS programmatic armoring components.

The armoring program addresses armoring requirements for the 100-year system designs, and it will determine where additional levee slope armoring can best be used to increase the HSDRRS resiliency against wave overtopping and breach failures that could result from less frequent, more intense, storm events. An additional concern is levee resiliency during multiple storm events within the same season.

Study purpose

Conventional design guidance for allowable wave overtopping at an earthen levee is given in terms of tolerable average wave overtopping discharge for different quality grass surfaces (TAW 2002). The 100-year design elevations of the HSDRRS levees were established based on the TAW (2002) criteria, which are considered to be very conservative. Whereas the TAW criteria can be used to provide a safe design for a specified set of conditions and associated risk, there is no similar guidance for evaluating levee resiliency once the design criteria have been exceeded.

The purpose of the study described in this report was to develop and propose a rational methodology for evaluating the strength and resiliency of earthen levee protection against wave overtopping forces during severe hurricanes. The methodology is based on the concept that cumulative work done by the overtopping waves on the levee slope, in excess of some tolerable level, is the cause of slope damage. Once the initiation of erosion threshold has been exceeded during an overtopping event, there is a certain amount of allowable erosion that can occur without causing damage to the slope protection. However, if overtopping persists, at some point the cumulative erosion results in slope damage.

The methodology developed in this report initially uses thresholds for initiation of erosion and the onset of damage that were derived from limiting velocity versus duration curves for stability of grass slopes exposed to steady overflow. Application of these steady overflow thresholds to unsteady overtopping by irregular waves assumes an “erosional

equivalence” between the two diverse types of hydrodynamic loading, and there is uncertainty about the veracity of these thresholds. In addition, the critical thresholds and erosional limits are necessarily a function of grass species and soil erodibility; and thus, there can be no universal set of thresholds that will be valid over a wide range. Fortunately, the methodology developed here can be adjusted to specific grass slopes using more reliable thresholds for initiation of erosion and onset of damage that arise from full-scale wave overtopping tests or direct field observations. Until such time that reliable thresholds are available for specific grass conditions found in the HSDRRS, the methodology provides a useful tool for comparative analyses of different reaches of the HSDRRS to assess which reaches will be likely candidates for additional slope armoring.

Report contents

This report begins with an examination of the “erosional equivalence” concept, proposes how the concept can be developed into a practical engineering tool for evaluating armoring needs, describes how to apply the methodology for different wave and surge overtopping scenarios, and compares results to field tests conducted on dikes in The Netherlands. Each chapter is briefly described below.

Chapter 2 overviews the concept of erosional equivalence as introduced by Dean et al. (2010). The development is described, and thresholds are determined for various types of slope protection based on steady overflow observations. Chapter 3 reviews how Dean et al. applied the concept to wave overtopping by linking the excess work done on the slope to parameters of the incident waves and water level.

Chapter 4 develops easy-to-apply mathematical equations that relate the cumulative excess overtopping wave volume (or excess flow work) to the summation of individual overtopping wave volumes and associated overtopping durations. Chapter 5 provides the vital link between the storm parameters and the excess overtopping volume as a function of the wave-only overtopping event duration. Chapter 6 does the same linkage for the case of surge overflow combined with wave overtopping. Application of the methodology for a realistic storm where the surge level, wave height, and wave period vary in time is described in Chapter 7.

Chapter 8 compares the erosional equivalence methodology to actual results obtained from full-scale testing of Dutch dikes using the Wave

Overtopping Simulator. Uncertainties of the presently-described methodology are listed and discussed in Chapter 9. Chapter 10 outlines how the methodology can be improved using full-scale Overtopping Simulator test results or direct field observations of storm damage. A summary and some conclusions are presented in Chapter 11.

2 Concept of Levee Erosion Equivalence

Dean et al. (2010) developed a methodology that provisionally equates observed performance of grass-covered slopes during steady overflow to predicted performance during intermittent, unsteady wave overtopping. This chapter summarizes the key aspects of this important development in understanding and predicting overtopping erosional stability on earthen levees.

Steady overflow - grass

The principle guidance for erosional stability of grass-covered slopes is a design nomogram presented in Hewlett et al. (1987). This nomogram used full-scale steady overflow test data to develop stability curves for various grass qualities and other slope protection surfaces (turf reinforcement mats and concrete block systems). Each curve presents the limiting steady overflow velocity as a function of overflow duration that results in an acceptable level of erosion without putting the grass cover at risk of failure. Figure 1 shows the limiting velocity curves for grass as given in Hewlett et al. (1987).

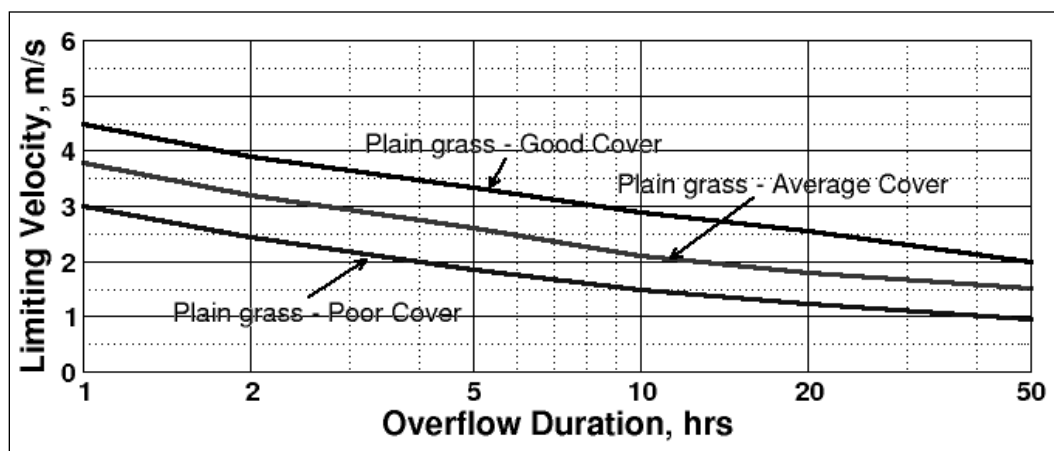


Figure 1. Limiting velocity versus overflow duration for grass (after Hewlett et al. 1987).

Hewlett et al. (1987) had curves for good-, average-, and poor-cover plain grass as shown in Figure 1. As might be expected, the grasses tolerate faster steady velocities for only short durations, whereas slower velocities can be tolerated for longer durations. Hewlett et al. described the grass qualities as follows:

Good grass cover is assumed to be a dense, tightly-knit turf established for at least two growing seasons. Poor grass cover consists of uneven tussocky grass growth with bare ground exposed or a significant proportion of non-grass weed species. Newly sown grass is likely to have poor cover for much of the first season. (Hewlett et al. 1987)

The Hewlett et al. curves are based on earlier work by Whitehead et al. (1976). Figure 2, reproduced from the original Whitehead et al. report, includes the sparse data points on which the curves are based. Superimposed on the Whitehead et al. graph are the three grass curves as presented by Hewlett et al. (shown by heavy colored lines). It is interesting to note that the Hewlett et al. curves for grass were adjusted downward on the low-duration side of the plots in comparison to the curves and data given by Whitehead et al. (1976). There is no explanation for this adjustment, but the result is that the Hewlett curves become more conservative on the low-duration end when compared to the guidance given by Whitehead et al. (1976).

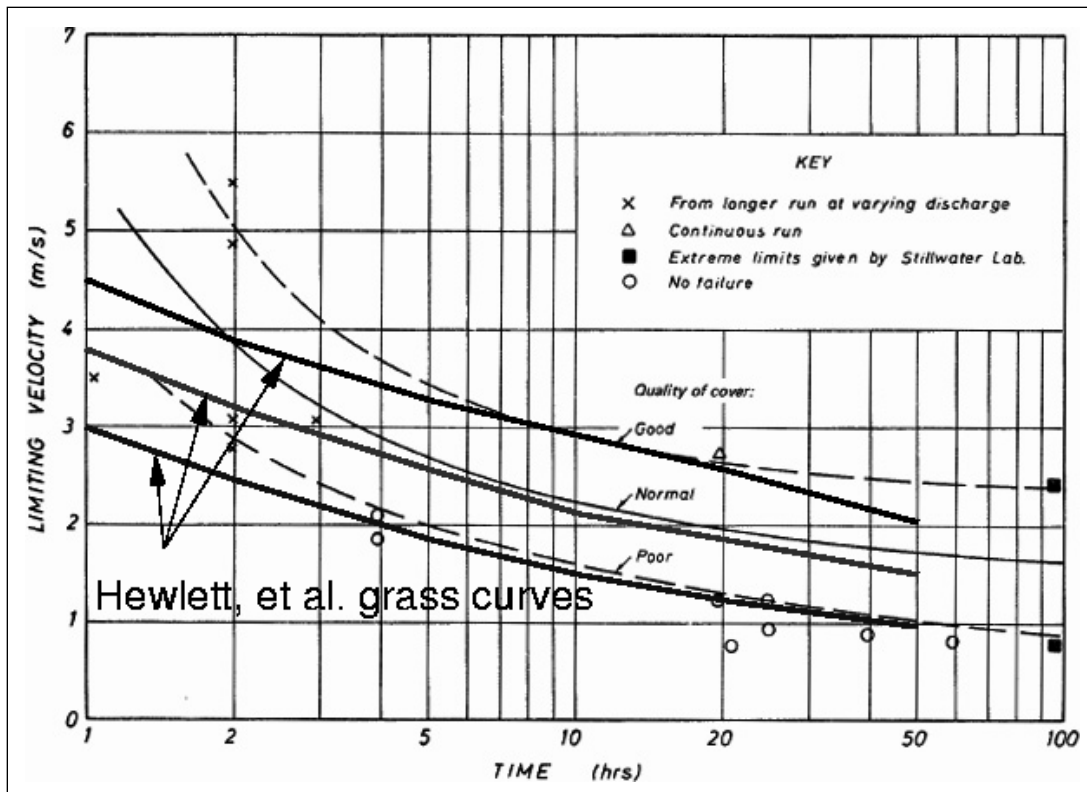


Figure 2. Erosion resistance of grass-lined spillways (from Whitehead et al. 1976).

Dean et al. (2010) used numerical values manually extracted from the Hewlett et al. grass-cover curves (Figure 1) to examine the underlying

physical mechanism that might be responsible for the form of the curves. Three possibilities were investigated: (a) flow velocity above a certain threshold, (b) shear stress above a certain threshold, and (c) flow work above a certain threshold. For each case, the acceptable slope erosion was assumed to be in the following forms

Excess Velocity

$$E_u = K_u (u - u_{c,u}) t \quad \text{for } u > u_{c,u} \quad (1)$$

Excess Shear Stress

$$E_\tau = K_\tau (\tau - \tau_c) t = K_\tau \alpha_\tau (u^2 - u_{c,\tau}^2) t \quad \text{for } u > u_{c,\tau} \quad (2)$$

Excess Work

$$E_W = K_W (W - W_c) t = K_W \beta_W (u^3 - u_{c,W}^3) t \quad \text{for } u > u_{c,W} \quad (3)$$

where the E and K variables are unknown coefficients, α_τ is a grouping of terms that includes water mass density and a shear stress coefficient, and β_W is a grouping of terms that includes water mass density and a shear stress coefficient.

Whereas Dean et al. did not give the exact forms of α_τ and β_W , we can derive them. Assume that shear stress is given by the usual formula for fully turbulent open-channel flow as

$$\tau_o = \frac{1}{8} \rho f_D u^2 \quad (4)$$

where ρ is the mass density of water and f_D is the Weisbach-Darcy friction factor. From Equation (2) we can assume

$$\alpha_\tau = \frac{1}{8} \rho f_D \quad (5)$$

Stream power is the time rate of flow work per unit surface area, and it is defined as the shear stress multiplied by the flow velocity. Thus, from Equation (4) stream power has the form

$$P_s = \frac{dW}{dt} = \tau_o \cdot u = \frac{1}{8} \rho f_D u^2 \cdot u = \frac{1}{8} \rho f_D u^3 \quad (6)$$

Equation (6) indicates that the symbol W in Equation (3) is actually stream power per unit area rather than work, and the excess work per unit area done by the flow is proportional to $(W - W_c) \cdot t$. From Equation (6) we conclude that β_W in Equation (3) is given as

$$\beta_W = \frac{1}{8} \rho f_D \quad (7)$$

which is the same as α_τ . Appendix A presents more information about stream power applied to the landward-side slopes of overtopped levees.

Dean et al. (2010) fit Equations (1) - (3) to the Hewlett et al. curves for grass covers, and appropriate values were determined for the threshold velocities ($u_{c,u}$; $u_{c,\tau}$; $u_{c,W}$) and erosion limits [E_u/K_u ; $E_\tau/(K_\tau \alpha_\tau)$; $E_W/(K_W \beta_W)$] so that the error of the curve fit was minimized. The analysis showed that the assumption of excess work (Equation 3) had the smallest standard error by a significant margin when the three equations were fitted to all three grass quality curves. The resulting best-fit values for the excess work assumption are shown in Table 1.

Table 1. Results for the best-fit of Equation (3) to the Hewlett et al. (1987) grass curves.

Plain Grass	Threshold velocity - u_c (m/s)	Erosion Limit - $E_W / (K_W \beta_W)$ (m ³ /s ²)	Std. Error in Velocity (m/s)
Good Cover	1.80	0.492 x 10 ⁶	0.38
Average Cover	1.30	0.229 x 10 ⁶	0.12
Poor Cover	0.76	0.103 x 10 ⁶	0.04

For convenience, the subscript W has been dropped from threshold velocity, i.e., $u_c = u_{c,W}$.

This best-fit analysis of Equations (1) - (3) led Dean et al. (2010) to conclude that cumulative work done on the slope by the flowing water, in excess of some critical value of work, was the physical mechanism responsible for the trends given in the Hewlett et al. (1987) limiting velocity versus duration curves. Figure 3 shows the best-fit obtained by Dean et al. compared to the original Hewlett et al. curves for three types of grass. The heavy solid lines are the Hewlett, et al. curves, and the symbols connected by lighter dashed lines are the best-fit values. Note the very good fits for average and poor grass.

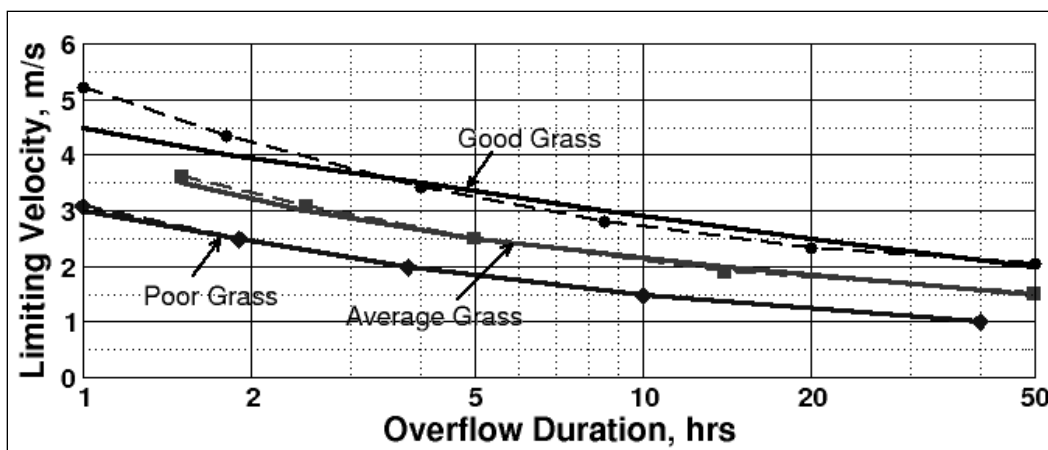


Figure 3. Dean et al. (2010) best fit of Equation (3) to Hewlett et al. (1987) curves.

Dean et al. (2010) included a similar plot that showed that the most deviation between velocities predicted using the best fit of Equation (3) and the original Hewlett velocities occurred at the short durations, and this is seen in Figure 3 for good grass. Given that the Hewlett curves have lower velocities at short-durations when compared to the Whitehead et al. curves (see Figure 2), this over-prediction by the best-fit procedure for good grass at short durations should not be too much of a concern. Note that there could be additional “almost” best-fits of the two-parameter equation that might result in different values for the threshold velocity and the erosion limit.

A schematic representation of the Dean et al. conclusion is illustrated in Figure 4 for the Hewlett et al. curve corresponding to good grass cover. The range of cumulative work between the no-damage work threshold and the grass-damage threshold represents a range of tolerable slope erosion that can occur before grass damage. The duration over which tolerable erosion can occur is related to the cumulative work done by a steady overflow of given velocity. The lines representing different values of velocity are linear because flow work done on the slope accumulates at a constant rate for steady overflow. (This will not be the case for intermittent wave overtopping during actual storm events when the rate of overtopping varies with surge level and storm intensity.)

The formulation based on cumulative excess work might imply that the grass surface is fairly homogeneous in structure and strength. If this were the case, then we should expect erosion to be somewhat uniform, and grass damage would occur nearly simultaneously over the entire region subjected to the same flow conditions. Of course, this is not the case, and

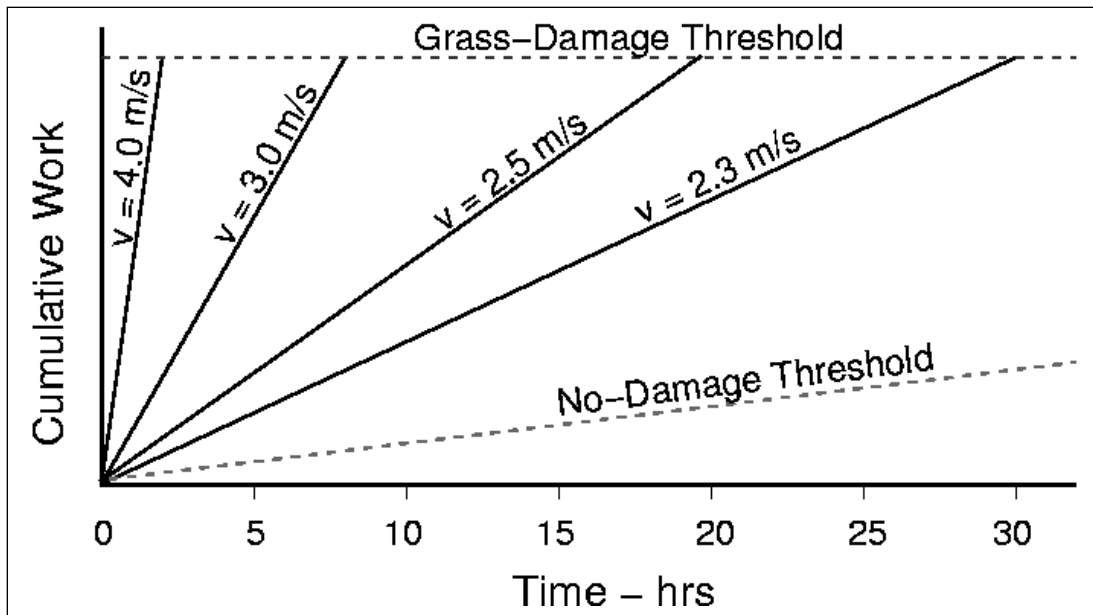


Figure 4. Schematic representation of the Hewlett et al. (1987) curve for good grass.

erosion will occur sporadically at isolated “hot spots.” The implicit assumption of the Dean et al. excess work model is that the model gives an indication when the isolated grass cover damage begins to become locally problematic as determined by analysis of the original full-scale test data.

Steady overflow - other slope protection

Dean et al. (2010) did not perform a similar analysis for other slope protection alternatives such as turf reinforcement mats (TRMs) and articulated concrete blocks (ACBs), so we shall do that in this section. Hewlett et al. (1987) included curves on their design nomogram for concrete block systems, open mats, and filled mats. These curves are shown in Figure 5, which is the original Hewlett et al. nomogram reproduced from their report.

Note that concrete block systems are a function only of limiting steady overflow velocity, and not duration. This implies that system damage for a concrete block system is not the result of accumulated flow work that erodes the slope, but rather a sudden (perhaps catastrophic) damage when the limiting velocity is exceeded. More recent steady overflow tests on concrete block systems are now available, and these data should be reanalyzed to establish time dependency damage. For example, damage for some systems might be defined as the loss of a prescribed amount of underlying soil that occurs over time.

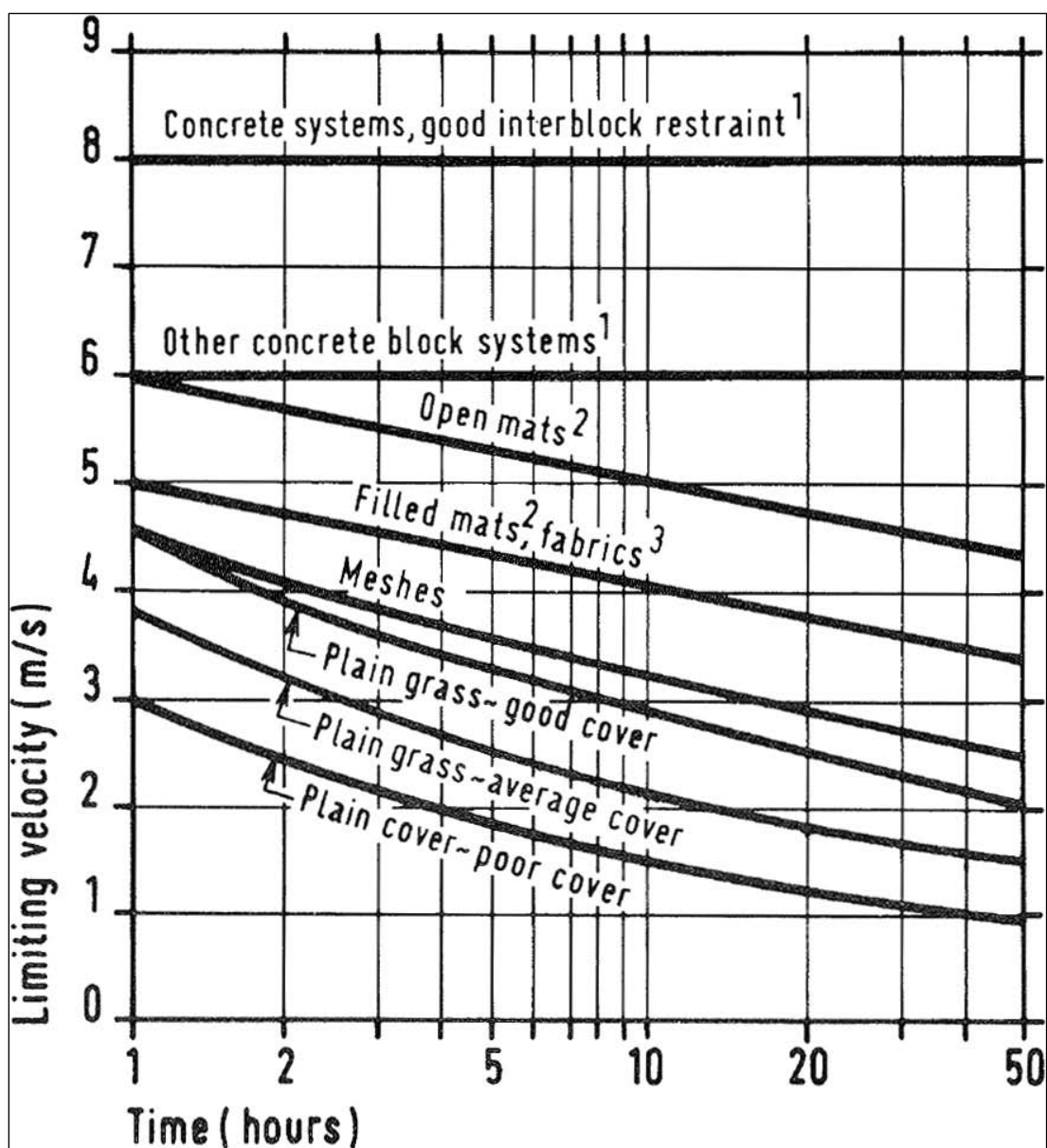


Figure 5. Original limiting velocity curves from Hewlett et al. (1987).

Open mats were described by Hewlett et al. as “synthetic mats which are subsequently filled with topsoil.” They recommended a nominal minimum mat thickness of 20 mm with the mat installed near the soil surface. The advantages of open mats are (1) good contact with the underlying soil because the mats are filled after installation, and (2) open mats are more permeable, and this helps prevent the buildup of water pressure in the soil. Filled mats were defined by Hewlett et al. as “synthetic mats filled with bitumen-bound gravel.” These mats should be at least 20 mm thick. Fabrics are basically woven geotextiles, and they should be installed within 20 mm of the soil surface.

Hewlett et al. (1987) stated that the limiting condition for open and filled mats is failure due to uplifting, and they included descriptions of full-scale tests of a variety of mat products in a report appendix. The following statement in Hewlett et al. appears to be the basis for the open mat and filled mat design curves.

The limited information from the field trials suggests that the risk of uplift failure becomes significant when average velocity of flow exceeds about 5- to 6-m/s (velocity head or stagnation pressure about 1.5 m). Given this present state of knowledge, the recommended design approach is based on limiting flow velocity to this threshold, and minimum geotextile opening size to 0.5 mm. (Hewlett et al. 1987)

Looking at the curves for open and filled mats in Figure 5, it appears that the 5- and 6-m/s thresholds were used to anchor the curves at the 1-hr duration, and then straight lines were drawn on the semi-log axis with slopes similar to those of the grass-cover curves. In other words, the supporting data for the curves are sparse to non-existent. (This statement is speculation by the author of this report and is not necessarily fact.)

A MatLab[®] script was written that performed the same optimization on the two Hewlett, et al. (1987) curves for mats that Dean et al. (2010) did for the three types of grass quality. As a check on the script veracity, the velocity versus duration data listed in the Dean et al. paper were reanalyzed, and the same results given by Dean et al. (Table 1) were obtained.

Results of the optimization based on the “excess work” formula (Equation 3) are given in Table 2 for the open and filled mat/fabric curves. The two curves for mats are essentially parallel to one another with a 1-m/s separation as seen in Figure 5. The 1 m separation between the curves might explain why the threshold velocities for the two curves differ by about 1-m/s. The best-fit threshold velocities and erosion limits for the two mat types are considerably higher than grass-only cover layers as should be expected. There may be additional pairs of threshold velocity and erosion limit that provides nearly as good a fit.

The best-fit parameters in Table 2 were substituted into Equation (3) to calculate velocity as a function of duration for both types of mat. Figure 6 compares the velocity estimates to the original Hewlett et al. curves. The symbols connected by light-weight dashed lines are the estimates, and the heavy lines are the original curves from Hewlett et al. (1987).

Table 2. Results for the best-fit of Equation (3) to the Hewlett et al. (1987) mat curves.

Mat Type	Threshold velocity - u_c (m/s)	Erosion Limit - $EW / (KW \beta W)$ (m^3 / s^2)	Std. Error in Velocity (m/s)
Open Mat	4.23	1.231×10^6	0.66
Filled Mat/Fabric	3.32	0.730×10^6	0.53

For convenience, the subscript W has been dropped from threshold velocity, i.e., $u_c = u_{c,W}$.

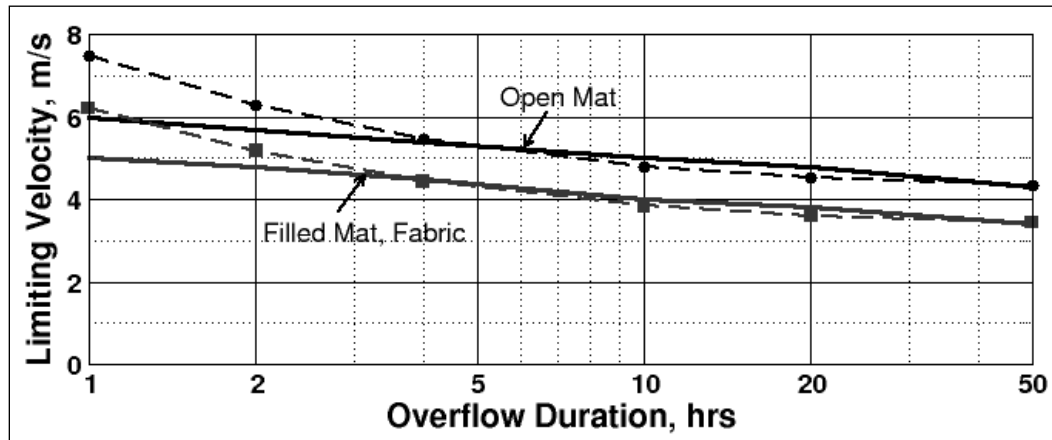


Figure 6. Best-fit to the Hewlett et al. (1987) curves for mats.

The Figure 6 comparison shows the same trend as found by Dean et al. for good grass-covered slopes. The largest deviation between predictions and the original curves occurs at the short-duration side of the plots. However, the upward trending in limiting velocity at the short-duration side seems to mimic the data for grass slopes presented by Whitehead et al. (1976) as shown in Figure 2. The deviations are greater than those seen for the grass best-fits because the original mat lines have no curvature like the grass limit-state lines.

The parameters given in Table 2 for the mats should be considered to be less reliable than those for grass slopes because the data used to establish the curves are not as abundant as the grass data. Also, the straight line nature of the curve raises suspicion that there is not a substantial basis for these curves.

3 Dean et al. (2010) Application to Wave Overtopping

The first important result from the Dean et al. (2010) paper was the parameterizations of the Hewlett et al. (1987) grass performance curves into an equation based on accumulation of flow work above some threshold work level (see previous chapter). The second important result was the adaptation of this accumulation of excess work concept to intermittent wave overtopping.

Unsteady wave overtopping

Dean et al. (2010) assumed that any flow work above the threshold limit done by an overtopping wave should be added to the cumulative total. Acceptable erosion occurs on the landward-side slope until such time that the cumulative excess work exceeds the grass-damage threshold. Thus, for every overtopping wave in which the flow velocity is greater than the critical velocity, there will be a contribution to the accumulated total work. Dean et al. proposed the following equation for assessing the tolerable limit of cumulative excess work for overtopping waves.

$$\sum_{n=1}^N (u_n^3 - u_c^3) \Delta t_n \leq \frac{E_W}{K_W \beta_W} \quad (8)$$

The subscript n refers to an individual overtopping wave, N is the number of overtopping waves, Δt_n is the overtopping wave duration, and the parameters u_c and $E_W/(K_W \beta_W)$ are taken from Table 1 for the particular grass type (or Table 2 for a mat type). Both sides of Equation (8) have units of m^3/s^2 . Note that the subscript, W , has been dropped from u_c , but this threshold velocity is the same as the Dean et al. $u_{c,W}$ term.

Because of the intermittent nature of overtopping waves, the variation of levee freeboard during a storm event, and the variation in overtopping wave volumes; the accumulation of flow work during an overtopping event might be similar to the sketch shown in Figure 7 rather than the straight lines seen for steady overflow as illustrated in Figure 4. In this particular hypothetical example, the initial overtopping for the first 1.5 hrs does not cause any erosion; but as the storm surge and wave height increase, slope

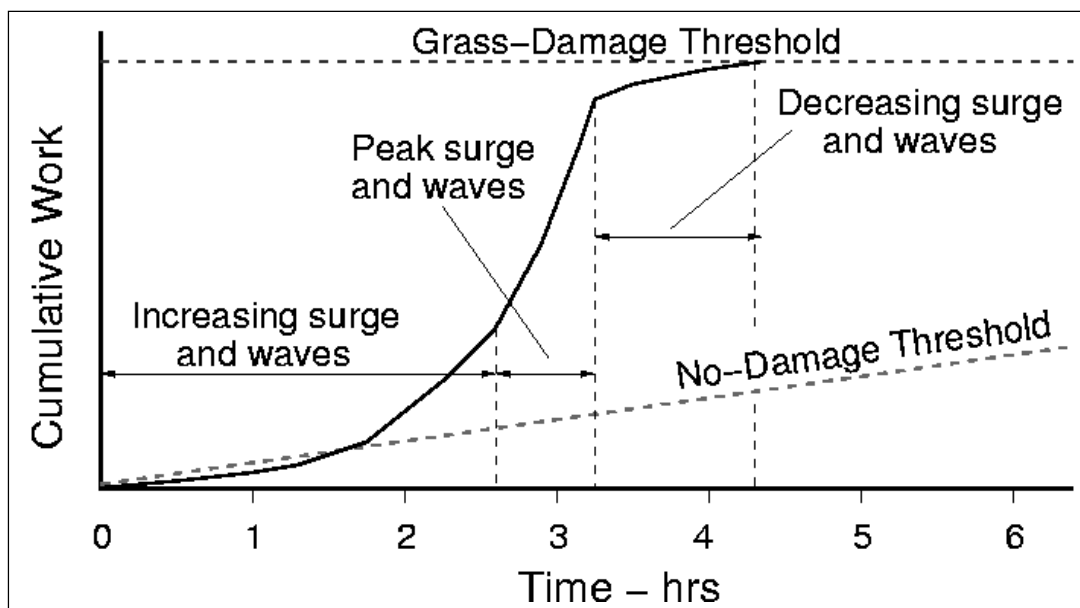


Figure 7. Schematic representation of the work accumulation during wave overtopping.

erosion starts to occur. The most rapid erosion is during the peak of the storm when overtopping is the greatest. However, in this hypothetical example, erosion continues at a slower rate as the storm peak is passed, and the grass-damage threshold is reached as the surge is falling. In other cases, damage may occur while the storm surge is still rising, and the initial damage may lead to levee failure if the storm is severe.

Dean et al. (2010) noted that Equation (8) can be expressed in terms of overtopping discharge under the conservative assumption that the flow velocity of the overtopping wave had reached terminal velocity, and the force balance described by the steady flow resistance equation was piecewise applicable to unsteady wave overtopping. The steady flow resistance equation at terminal velocity is essentially the same as the Chezy equation with the Chezy coefficient represented by a friction factor, i.e.,

$$u^3 = \left(\frac{8g}{f_D} \sin \theta \right) q = \left(\frac{2g}{f_F} \sin \theta \right) q \quad (9)$$

where q is volumetric discharge per unit length of levee, θ is the landward-side levee slope angle, g is gravitational acceleration, f_D is the Weisbach-Darcy friction factor, and f_F is the Fanning friction factor. The two friction factors are related by the expression $f_D = 4 f_F$. The Fanning friction factor commonly appears in the European overtopping literature.

Substituting Equation (9) for velocities in Equation (8) yields

$$\sum_{n=1}^N \left[\left(\frac{2g \sin \theta}{f_F} \right) q_n - u_c^3 \right] \Delta t_n \leq \frac{E_W}{K_W \beta_W} \quad \text{for } q_n > \left(\frac{f_F u_c^3}{2g \sin \theta} \right) \quad (10)$$

An alternative version of Equation (10) is

$$V_{ET}(t) = \sum_{n=1}^N (q_n - q_c) \Delta t_n \leq \frac{E_W}{K_W \beta_W} \left(\frac{f_F}{2g \sin \theta} \right) \quad \text{for } q_n > q_c \quad (11)$$

where

$$q_c = \left(\frac{f_F u_c^3}{2g \sin \theta} \right) \quad (12)$$

It is interesting to note that both sides of Equation (11) have units of m^3/m , so the terms inside the summation represent all the water volume (per unit levee length) in the individual wave above a critical discharge volume that is given by $q_c \cdot \Delta t_n$. The parameter V_{ET} is used to designate the summation in Equation (11), and it means “cumulative (or total) excess wave volume.”

The upper sketch of Figure 8 illustrates time variation of overtopping discharge for an individual wave. The duration of overtopping is denoted by Δt_n . The average discharge for the wave, q_n , is shown relative to the critical discharge, q_c . Average discharge is defined as

$$q_n = \frac{1}{\Delta t_n} \int_0^{\Delta t_n} q(t) dt \quad (13)$$

The integral in Equation (13) is the volume of the individual wave, V_{Wn} , so

$$V_{Wn} = q_n \Delta t_n \quad (14)$$

Therefore, Equation (11) can also be expressed as

$$V_{ET}(t) = \sum_{n=1}^N [V_{Wn} - (q_c \Delta t_n)] \leq \frac{E_W}{K_W \beta_W} \left(\frac{f_F}{2g \sin \theta} \right) \quad \text{for } \frac{V_{Wn}}{\Delta t_n} > q_c \quad (15)$$

where the critical discharge volume is defined as $q_c \cdot \Delta t_n$.

The bottom sketch of Figure 8 is a schematic representation of the terms contained in the summation of Equation (15). Erosion on the levee slope is assumed to be caused by the flow work associated with the excess wave volume represented by the labeled box. If both sides of Equation (15) were multiplied by the specific weight of the water, the equation would become a cumulative flow work equation with units of kN-m/m² in the SI system.

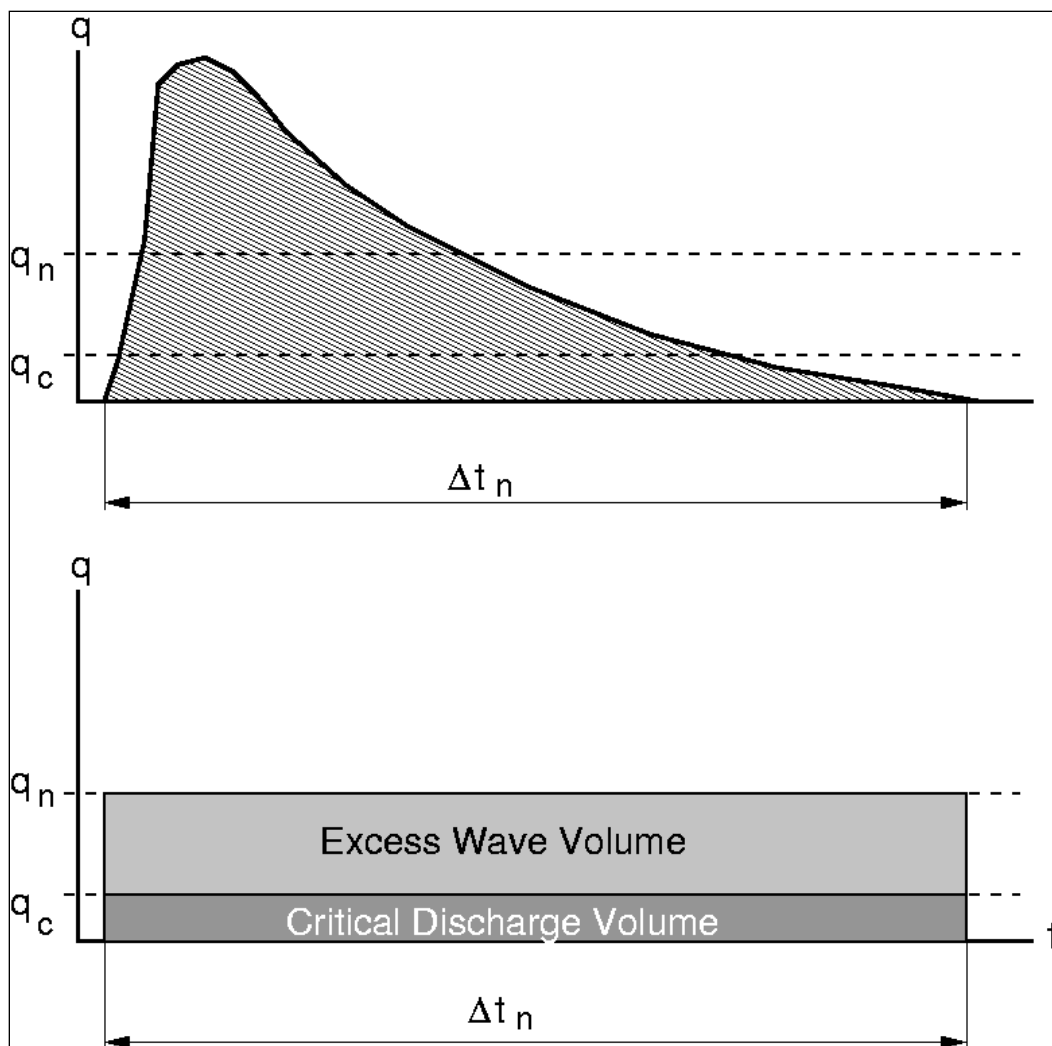


Figure 8. Definition of average wave overtopping discharge used by Dean et al. (2010).

Linking the velocities to storm parameters

Application of the cumulative excess work formulation requires some method to link the storm parameters (significant wave height, peak wave peak, and levee freeboard) and the levee geometry (flood-side slope and

friction factor) to the velocities (or discharge) of individual overtopping waves. Dean et al. (2010) started with empirical equations (de Waal and van der Meer 1992) for estimating the wave runup elevation exceeded by 2% of the waves. Based on earlier research, they assumed wave runup followed a Rayleigh distribution, and this allowed them to estimate which of the incident waves would overtop the levee. They then developed a correlation between the distribution of overtopping waves and the cumulative overtopping as estimated by the established TAW (2002) formula for average wave overtopping discharge (also see Pullen et al. 2007).

The method described in Dean et al. is fairly involved. The final result is an expression for the individual wave average discharge that exceeds the threshold. The individual wave discharge is a function of excess wave runup elevation (difference in runup elevation and levee crown elevation), the duration of overtopping for that wave, and a proportionality factor that relates the summation of all of the individual overtopping wave runups to the average overtopping discharge determined by the TAW (2002) formula. Duration of individual wave overtopping was assumed to be the product of the representative incident wave period and two reduction factors. One reduction factor related to the portion of time that the individual runup elevation exceeds the levee crown elevation, and the second reduction factor was based on the proportion of time that overtopping occurs.

Dean et al. (2010) concluded their paper with two example applications of their methodology. These examples included time-varying storm surge hydrographs and wave heights, and the examples differed only by the duration of the peak storm surge and maximum wave height. The variations due to grass cover quality and peak storm surge duration were examined for different average wave overtopping discharge, and the differences were quantified in terms of relative levee crown elevation requirements necessary to prevent damage occurring on the grass slope.

Dean et al. (2010) cautioned that the methodology should be calibrated/verified using observed erosion and damage caused by full-scale wave overtopping on specific grass surfaces before applying the method to actual design. However, they noted that the methodology could be used to analyze the relative differences that arise due to grass quality and time-varying storm characteristics. They also noted that alternate methods could be used to link the storm parameters to the excess work formulation.

Some background on friction factors

One difficulty with the cumulative excess wave volume equations expressed in terms of discharge (Equations 10 - 12) is specifying a suitable value for the friction factor. Friction factors appropriate for grass and mats are implicitly included in the Hewlett et al. velocity curves, but we do not know what they are. Furthermore, the friction factor can be shown to be a function of flow depth (see below), and it will vary in magnitude during individual wave overtopping. Dean et al. (2010) did not state explicitly what friction factor they used for the two levee examples in their paper, but earlier in the paper they mentioned a Weisbach-Darcy friction factor of $f_D = 0.08$ (or $f_F = 0.02$) when evaluating whether the flow on the levee landward-side slope would be supercritical. It is assumed that the same friction factor was applied to the examples.

European overtopping research indicated that the friction factor has a significant influence on flow velocity across the levee crown and down the backside slope. The small-scale experiments of Schüttrumpf et al. (2002) had a structure surface constructed of wood fiberboard, and the friction factor was determined experimentally to be $f_F = 0.0058$ (Schüttrumpf and Oumeraci 2005). The structure in the companion large-scale experiments was constructed with a bare, compacted clay surface; and experimental results gave the friction factor as $f_F = 0.01$ (Schüttrumpf et al. 2002). Schüttrumpf and Oumeraci (2005) also list the following representative values for the Fanning friction coefficient: $f_F = 0.02$ (smooth slopes), $f_F = 0.1 - 0.6$ (rough revetments and rubble-mound slopes). From this we can speculate that grass-covered slopes would have a Fanning friction coefficient somewhere between $f_F = 0.01$ and 0.10

Hewlett et al. (1987) recommended a value of Manning's $n = 0.02$ for grass-covered slopes steeper than 1:3. Manning's n can be related to the Chezy coefficient, C_z , by the expression (e.g., Henderson 1966)

$$C_z = \frac{R^{1/6}}{n} \quad (16)$$

where R is the hydraulic radius, and n is given in metric units. For wide channels, R is essentially the same as the flow thickness, h . The Chezy coefficient is also given as (Henderson 1966)

$$C_z = \sqrt{\frac{8g}{f_D}} = \sqrt{\frac{2g}{f_F}} \quad (17)$$

Equating Equations (16) and (17), substituting h for R , and using the value of $n = 0.02$ results in an equation (in metric units) relating friction factor to flow depth h in meters for grass slopes.

$$f_D = \frac{8gn^2}{h^{1/3}} = \frac{8(9.816)(0.02)^2}{h^{1/3}} = \frac{0.0314}{h^{1/3}} \quad (18)$$

or

$$f_F = \frac{2gn^2}{h^{1/3}} = \frac{2(9.816)(0.02)^2}{h^{1/3}} = \frac{0.0079}{h^{1/3}} \quad (19)$$

From Equation (19), flow thicknesses over the levee of 0.15 m (0.5 ft), 0.3 m (1.0 ft), and 0.6 m (2.0 ft) have friction factors of $f_F = 0.015$, 0.012, and 0.009, respectively. Therefore, it seems reasonable as an initial assumption to use a friction factor in the range of $f_F = 0.01 - 0.02$ ($f_D = 0.04 - 0.08$) as a representative average for overtopped grass-covered levee slopes. The above estimates assume Manning's n remains constant for different flow thickness, and this may not be entirely true in some situations.

4 Proposed Application to the HSDRRS

Idealized overtopping wave

Measurements of wave overtopping at earthen dikes and levees have revealed that the time-varying flow thickness and velocity of overtopping waves resemble saw-tooth shapes, as shown in Figure 9. At the leading edge of the overtopping wave, flow thickness (depth on levee crest) and velocity increase from zero to maximum values for each wave in a very short time span. The continuous decrease from the maximum values takes a relatively long time compared to the initial rise time. Notice that the decrease in magnitude is often concave rather than linear.

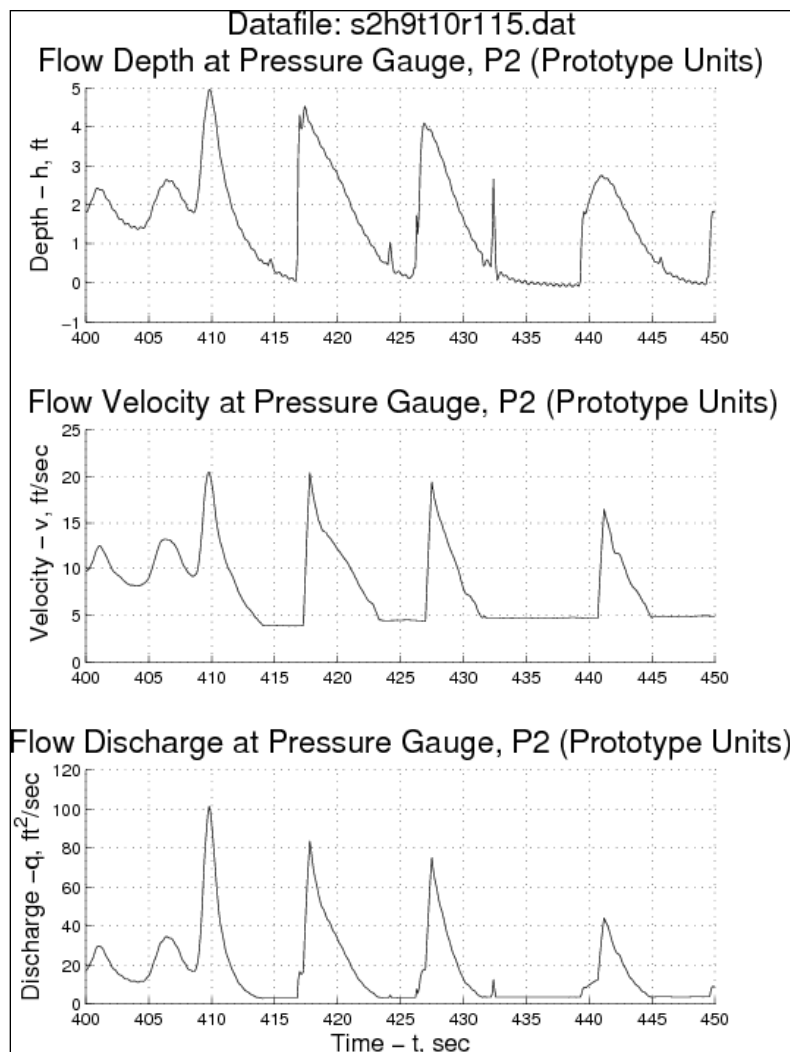


Figure 9. Flow depth, velocity, and calculated discharge (laboratory measurements).

If we feel justified in representing the initial rapid increase in flow depth and velocity of an individual wave as a nearly instantaneous jump, we can perhaps idealize the slope-parallel flow thickness hydrograph and the slope-parallel flow velocity time variation as shown in the upper and middle diagrams, respectively, of Figure 10. The bottom diagram in Figure 10 is the time-variation of the idealized overtopping discharge per unit levee length of a single wave. Discharge is simply the product of the flow thickness and velocity at each instant in time.

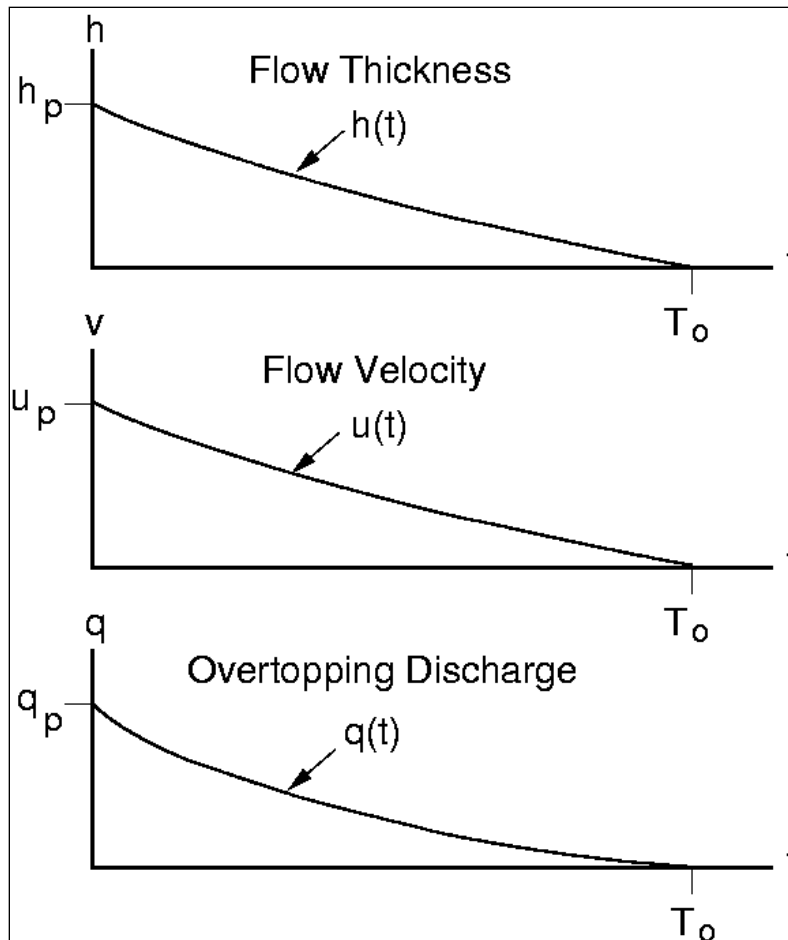


Figure 10. Flow parameters of an idealized overtopping wave.

In each diagram of Figure 10, the maximum (or peak) value at the wave leading edge is identified by the subscript, p . The overtopping duration for an individual wave is denoted by the symbol, T_o . This period will be shorter than the corresponding period associated with the wave before it reaches the levee.

A simple mathematical power-curve representation for the flow depth and velocity hydrographs is proposed in order to characterize the overtopping of waves analytically, i.e.,

$$h(t) = h_p \left[1 - \frac{t}{T_o} \right]^a \quad \text{for } 0 \leq t \leq T_o \quad (20)$$

and

$$u(t) = u_p \left[1 - \frac{t}{T_o} \right]^b \quad \text{for } 0 \leq t \leq T_o \quad (21)$$

When the exponents a and b have values of unity, the decreases in flow thickness and velocity are linear (which turns out to be a reasonable assumption). Combining Equations (20) and (21) gives the individual wave volumetric discharge per unit levee length, i.e.,

$$q(t) = h_p u_p \left[1 - \frac{t}{T_o} \right]^{a+b} = q_p \left[1 - \frac{t}{T_o} \right]^m \quad \text{for } 0 \leq t \leq T_o \quad (22)$$

where the product of the peak flow thickness and peak velocity has been replaced with the peak discharge, q_p , and the exponent, $m=a+b$.

The volume (per unit levee length) of the individual overtopping wave is simply the integration of the discharge hydrograph with respect to time, or

$$V_w = \int_0^{T_o} q(t) dt = \int_0^{T_o} q_p \left[1 - \frac{t}{T_o} \right]^m dt = \frac{q_p}{(T_o)^m} \int_0^{T_o} [T_o - t]^m dt \quad (23)$$

Carrying out the integration and evaluating at the limits yields

$$V_w = \frac{q_p}{(T_o)^m} \left[\frac{(T_o - t)^{m+1}}{(m+1)(-1)} \right]_0^{T_o} = \frac{q_p (T_o)^{m+1}}{(m+1)(T_o)^m} \quad (24)$$

$$V_w = \frac{q_p T_o}{(m+1)}$$

Excess wave volume in an individual wave

Figure 11 illustrates the discharge time history of an individual wave. The instantaneous discharge is greater than the threshold discharge, q_c , for a duration denoted as T_c . Integration of the instantaneous discharge minus the threshold discharge, q_c , over the duration T_c is the total excess wave volume per unit levee length associated with this individual wave (shown hatched in Figure 11). This excess wave volume is proportional to excess flow work with the proportionality factor being the water specific weight.

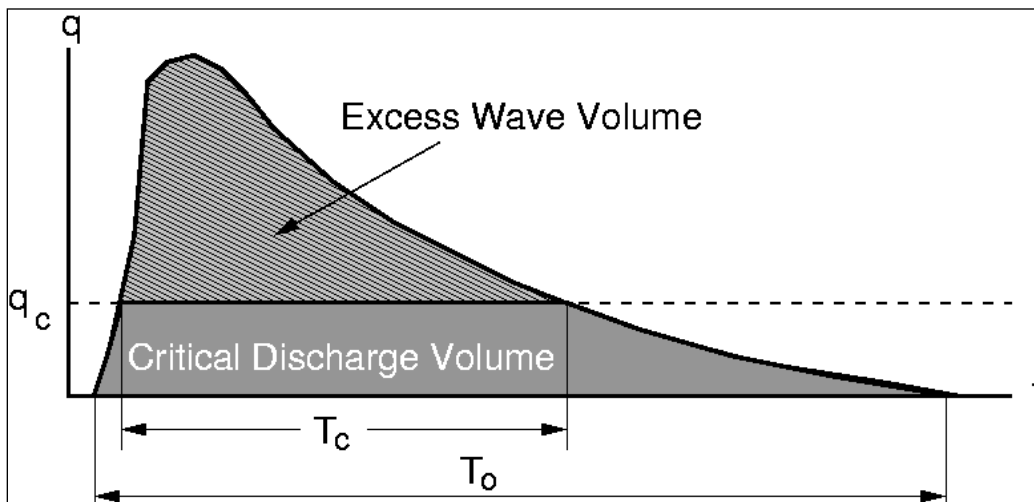


Figure 11. Excess wave volume above the threshold for a realistic individual wave.

Figure 12 is an idealization of the actual instantaneous discharge using the idealized instantaneous discharge given by Equation (22).

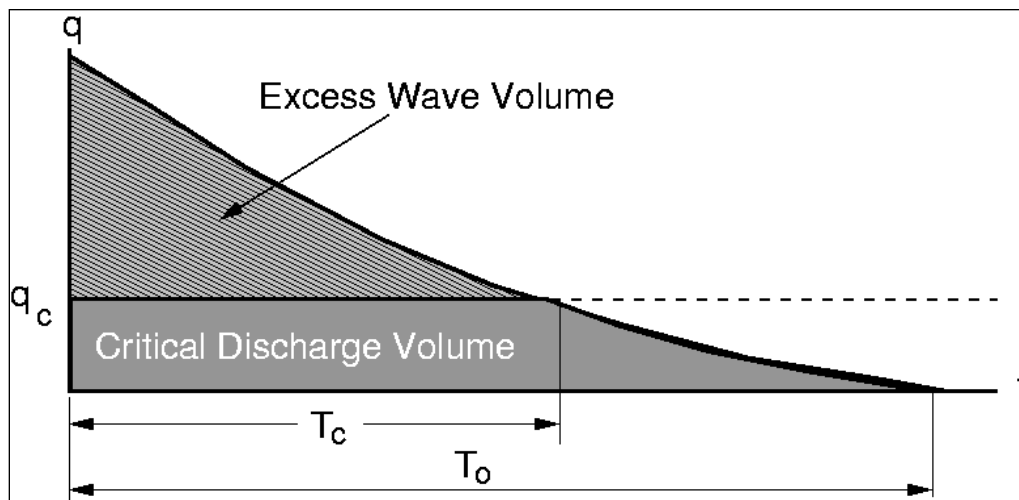


Figure 12. Excess wave volume above the threshold for an idealized individual wave.

The duration T_c is found by solving Equation (22) when $t = T_c$ and $q(T_c) = q_c$, i.e.,

$$q_c = q_p \left[1 - \frac{T_c}{T_o} \right]^m \quad \Rightarrow \quad T_c = T_o \left[1 - \left(\frac{q_c}{q_p} \right)^{1/m} \right] \quad (25)$$

An analytical expression for the excess wave volume, V_E , given by the hatched area in Figure 12 can be found by integrating between zero and T_c ,

$$V_E = \int_0^{T_c} [q(t) - q_c] dt = \int_0^{T_c} q_p \left[1 - \frac{t}{T_o} \right]^m dt - \int_0^{T_c} q_c dt \quad (26)$$

Carrying out the integration gives...

$$V_E = \frac{q_p}{T_o^m} \left[\frac{(T_o - t)^{m+1}}{-(m+1)} - q_c t \right]_0^{T_c} \quad (27)$$

Evaluating Equation (27) at the limits, substituting for the duration T_c from Equation (25), and performing some algebraic manipulations yields

$$V_E = \frac{T_o}{(m+1)} \left\{ q_p - q_c - m q_c \left[1 - \left(\frac{q_c}{q_p} \right)^{1/m} \right] \right\} \quad (28)$$

Using the derived expression for the total volume of the wave (Equation 24), Equation (28) can be rearranged into the form

$$V_E = V_W \left[1 - (m+1) \left(\frac{q_c}{q_p} \right) + m \left(\frac{q_c}{q_p} \right)^{\frac{m+1}{m}} \right] \quad \text{for } q_p > q_c \quad (29)$$

Equation (29) provides an effective means of evaluating the importance of the exponent m . If both the velocity and the flow thickness of an overtopping wave decrease linearly ($a = 1$ and $b = 1$), then the lower limit of the exponent is $m = a + b = 2$. A reasonable upper limit might be $m = 4$, which could correspond to velocity and flow thickness decreasing as squares ($a = 2$ and $b = 2$).

Figure 13 shows plots of Equation (29) for three values of the exponent m over the entire range of equation applicability. Varying the exponent between 2 and 4 has only a minor effect. Therefore, it would be reasonable and practical to set the exponent to $m = 2$ to simplify the application of the Dean et al. methodology to the HSDRRS levees. This gives a slightly larger estimate of excess wave volume, so it would be a bit conservative. Setting $m = 2$ in Equation (29) gives

$$V_E = V_W \left[1 - 3 \left(\frac{q_c}{q_p} \right) + 2 \left(\frac{q_c}{q_p} \right)^{3/2} \right] \quad \text{for } q_p > q_c \quad (30)$$

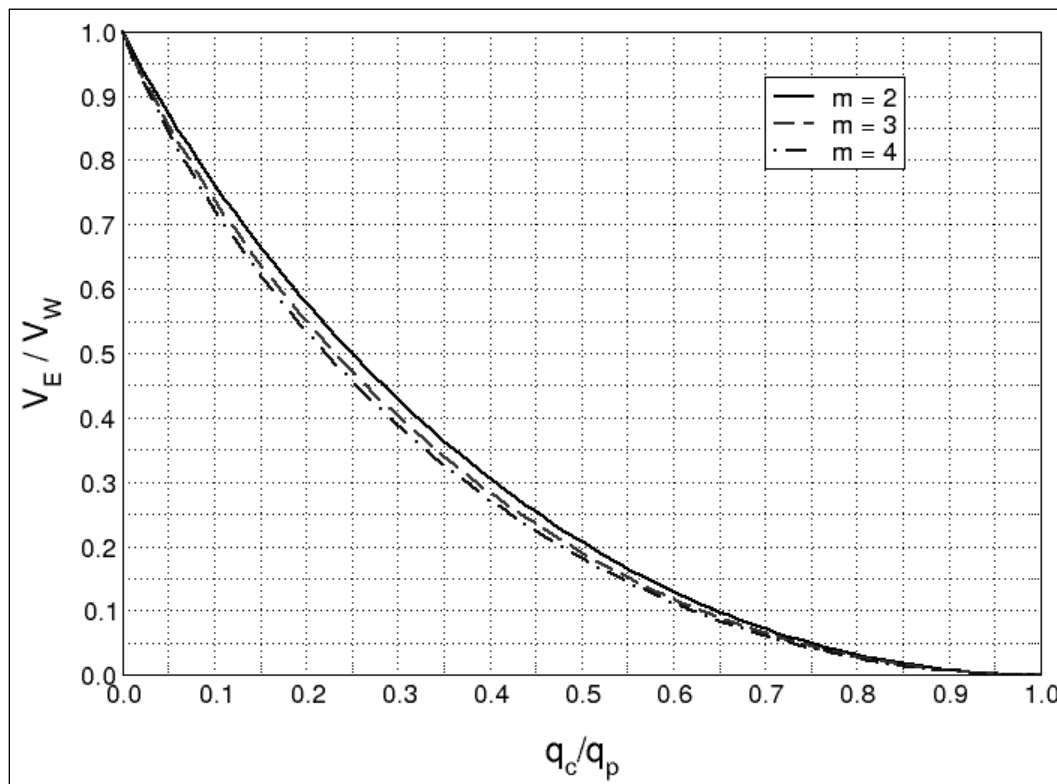


Figure 13. Variation of exponent m in Equation (29).

Estimation of the excess wave volume for overtopping waves using Equation (30) requires the total wave volume per unit levee length and the peak instantaneous discharge of each wave. An alternative version in terms of wave volume and duration of overtopping is found by substituting for q_p from Equation (24) with $m = 2$, i.e.,

$$V_E = V_W \left[1 - \left(\frac{q_c T_o}{V_W} \right) + \frac{2}{3^{3/2}} \left(\frac{q_c T_o}{V_W} \right)^{3/2} \right] \quad \text{for} \quad \frac{3 V_W}{T_o} > q_c \quad (31)$$

Thus, application of Equation (31) requires that the wave volume per unit levee length and associated overtopping duration for each wave be known.

It is interesting to note that the first two terms on the right-hand side of Equation (31) are the same as used by Dean et al. (2010) as shown in Equation (15). The third term represents the additional excess wave volume that arises from a slightly more accurate representation of the wave volume above a given discharge threshold. Specifically, the third term is a result of considering the duration T_c when the discharge is above the critical discharge and using the actual time variation of discharge instead of the average discharge for the wave.

Cumulative excess overtopping wave volume criterion

The cumulative excess wave volume per unit levee length for irregular wave overtopping is the summation of the excess wave volume of individual overtopping waves (V_E) as expressed by Equation (31). This summation is analogous to the Dean et al. (2010) excess wave volume as represented by the summation in Equation (11). Making this substitution into Equation (11) gives the following criterion for evaluating levee protective surfaces

$$V_{ET}(t) = \sum_{n=1}^N V_{Wn} \left[1 - \left(\frac{q_c T_{on}}{V_{Wn}} \right) + \frac{2}{3^{3/2}} \left(\frac{q_c T_{on}}{V_{Wn}} \right)^{3/2} \right] \leq \left(\frac{E_W}{K_W \beta_W} \right) \left(\frac{f_F}{2g \sin \theta} \right) \quad (32)$$

where

$$q_c = \left(\frac{f_F u_c^3}{2g \sin \theta} \right) \quad (33)$$

and V_{Wn} and T_{on} are the total volume and overtopping duration, respectively, of the n th individual overtopping wave.

Required inputs for applying Equation (32) to a specific levee reach are the time histories of overtopping wave volumes (V_{Wn}) and associated overtopping durations (T_{on}), a representative friction factor (f_F), and the landward-side slope angle (θ). The parameters u_c and $E_W/(K_W \beta_W)$ are

constants related to the specific levee protective surface, and they are provisionally given in Table 1 for grass and Table 2 for open and filled mats. The above required inputs are the same for wave overtopping with either positive or negative freeboard.

The following two chapters provide guidance on applying the cumulative excess wave volume formulation to wave-only overtopping (positive freeboard) and combined wave overtopping and storm surge overflow (negative freeboard). Worked examples help illustrate the application.

5 Application for Wave-Only Overtopping

The two key variables needed for application of the cumulative excess overtopping wave volume given by Equations (32) and (33) are the individual wave overtopping volumes (V_{Wn}) and the associated overtopping durations (T_{on}). In this section, these required inputs will be specified for the case of wave-only overtopping when the levee crown elevation is above the still water elevation of the storm surge (positive freeboard).

Estimation of individual overtopping wave volumes (V_{Wn})

The distribution of overtopping wave volumes (V_{Wn}) is a function of the following variables:

- H_{m0} = Energy-based significant wave height
- T_p = Incident peak spectral wave period
- T_m = Incident mean wave period
- $T_{m-1.0}$ = Incident mean spectral wave period
- $\tan \alpha$ = Slope of the flood-side levee face
- $R_{u2\%}$ = Runup elevation exceeded by 2% of the runups
- R_c = Freeboard (levee crown elevation minus still water level)
- q = Average wave overtopping discharge per unit levee length
- $\gamma_b, \gamma_f, \gamma_\beta$ = Wave runup reduction factors

For a given reach of the HSDRRS, it is necessary to specify H_{m0} , T_p , $\tan \alpha$, and either q or R_c . Depending on the levee cross section, it may be necessary to nominate appropriate wave runup reduction factors ($\gamma_b, \gamma_f, \gamma_\beta$). The rest of the parameters are calculated.

Well-tested empirical equations are available in the technical literature for estimating wave runup and wave overtopping on levee-type structures, along with the associated distribution of overtopping wave volumes. These equations are based mostly on abundant small- and large-scale laboratory measurements, and they are widely accepted and commonly used for critical design of coastal structures. Below are all the equations needed for estimating the individual overtopping wave volumes. The equations are in the approximate order in which they are used in the application to wave-

only overtopping. The application procedure is described after the equations are presented and discussed.

Incident wave periods ($T_{m-1,0}$ and T_m)

Strictly speaking, the mean wave period, T_m , should be determined from up-crossing analysis of the measured sea surface elevation time series; and the mean spectral period, $T_{m-1,0}$, should be estimated from the corresponding wave frequency spectrum. However, for single-peaked wave spectra (typical of storms) it was suggested by TAW (2002) and in Pullen et al. (2007) that the mean spectral period can be approximated as

$$T_{m-1,0} = \frac{T_p}{1.1} \quad (34)$$

when only the peak spectral, T_p , period is known or specified. Pullen et al. (2007) also noted that the ratio $T_p/T_m = 1.1$ to 1.25. For convenience we will assume for this application that

$$T_m = T_{m-1,0} = \frac{T_p}{1.1} \quad (35)$$

Wave runup ($R_{u2\%}$)

Irregular wave runup typically is expressed by the parameter, $R_{u2\%}$, which is defined as the vertical elevation above the still water level that is exceeded by 2-percent of the waves running up an imaginary, infinitely-long levee flood-side slope. The following wave runup relationships were recommended by TAW (2002) and in Pullen et al. (2007) for deterministic design or safety assessment. They are slightly modified versions of runup equations introduced originally by de Waal and van der Meer (1992).

$$\frac{R_{u2\%}}{H_{m0}} = 1.75 \gamma_b \gamma_f \gamma_\beta \xi_{m-1,0} \quad (36)$$

with a maximum given by

$$\frac{R_{u2\%}}{H_{m0}} = 1.0 \gamma_f \gamma_\beta \left(4.3 - \frac{1.6}{\sqrt{\xi_{m-1,0}}} \right) \quad (37)$$

In Equations (36) and (37) γ_b , γ_f , γ_β are runup reduction factors that account for a fronting berm, slope roughness, and oblique wave approach, respectively. For a standard trapezoidal grass-covered levee cross section with waves approaching head-on, all of the γ -factors are assumed equal to unity. The runup equations also include the Iribarren number

$$\xi_{m-1,0} = \frac{\tan \alpha}{\sqrt{H_{m0} / L_{m-1,0}}} \quad (38)$$

where the wave length is given by the deepwater linear theory equation

$$L_{m-1,0} = \frac{g}{2\pi} T_{m-1,0}^2 \quad (39)$$

Equations (36) and (37) include a safety margin of about one standard deviation above the mean of the empirical data used to establish the equations (Pullen et al. 2007).

Average wave overtopping discharge (q)

Average wave overtopping discharge, q , is the total volume of water per unit levee length that overtops a structure divided by the total duration of the overtopping event. This is a useful parameter for estimating inundation of the protected region, and it is presently used as a very conservative indicator of tolerable wave overtopping for grass-covered levees.

TAW (2002) and Pullen et al. (2007) recommended slightly revised versions of overtopping equations originally developed by van der Meer and Janssen (1995). The following equations were recommended for deterministic design or safety assessment, and they include a safety margin of about one standard deviation above the mean of the experimental data.

$$\frac{q}{\sqrt{gH_{m0}^3}} = \frac{0.067}{\sqrt{\tan \alpha}} \gamma_b \cdot \xi_{m-1,0} \cdot \exp \left[-4.3 \frac{R_c}{\xi_{m-1,0} H_{m0} \gamma_b \gamma_f \gamma_\beta \gamma_v} \right] \quad (40)$$

with a maximum of

$$\frac{q}{\sqrt{gH_{m0}^3}} = 0.2 \cdot \exp \left[-2.3 \frac{R_c}{H_{m0} \gamma_f \gamma_\beta} \right] \quad (41)$$

The reduction factor γ_v pertains to vertical walls, and it can be set to unity for application to earthen levees.

Levee freeboard (R_c)

Estimation of average wave overtopping discharge (Equations 40 and 41) requires that levee freeboard be known. Some applications of the erosional equivalence methodology may specify the average discharge, and it will be necessary to calculate the corresponding freeboard associated with that discharge for specified wave conditions and levee slope. Inverting Equations (40) and (41) yields

$$R_c = - \left(\frac{\xi_{m-1,0} H_{m0} \gamma_b \gamma_f \gamma_\beta \gamma_v}{4.3} \right) \ln \left[\left(\frac{q}{\sqrt{g H_{m0}^3}} \right) \frac{\sqrt{\tan \alpha}}{0.067 \gamma_b \cdot \xi_{m-1,0}} \right] \quad (42)$$

with a maximum of

$$R_c = - \left(\frac{H_{m0} \gamma_f \gamma_\beta}{2.3} \right) \ln \left[\frac{5q}{\sqrt{g H_{m0}^3}} \right] \quad (43)$$

Individual wave overtopping volume (V_w)

Franco et al. (1994) and van der Meer and Janssen (1995) used the Weibull distribution with a shape factor of 0.75 to represent the cumulative probability distribution of water volume in individual waves. The probability of an overtopping wave volume, V , being less than or equal to a specified volume, V_w , is expressed as

$$P_V = P(V \leq V_w) = 1 - \exp \left[- \left(\frac{V_w}{a} \right)^{0.75} \right] \quad (44)$$

and the corresponding exceedance probability (defined as $P_{VE} = 1 - P_V$) that an overtopping wave volume, V , is greater than a specified volume, V_w , is given as

$$P_{VE} = P(V > V_w) = \exp \left[- \left(\frac{V_w}{a} \right)^{0.75} \right] \quad (45)$$

In Equations (44) and (45), the scale factor, a , is given by the empirical equation

$$a = 0.84 \cdot T_m \cdot \left(\frac{q}{P_{ov}} \right) = 0.84 \cdot T_m \cdot q \cdot \left(\frac{N_W}{N_{ow}} \right) = 0.84 \cdot q \cdot \left(\frac{t_E}{N_{ow}} \right) \quad (46)$$

In Equation (46), N_W is the total number of incident waves, N_{ow} is the number of overtopping waves, t_E is the total duration of the storm (overtopping) event, and P_{ov} is the probability of overtopping per wave given by the formula

$$P_{ov} = \exp \left[- \left(\sqrt{-\ln(0.02)} \frac{R_c}{R_{u2\%}} \right)^2 \right] \quad (47)$$

Equation (47) is based on the assumption that wave runup is Rayleigh distributed, and that it uses the 2-percent runup value, $R_{u2\%}$, instead of R_{rms} as the scale factor. Also note from Equation (46) the following relationships

$$P_{ov} = \frac{N_{ow}}{N_W} \quad \text{and} \quad N_W = \frac{t_E}{T_m} \quad (48)$$

Inverting the exceedance probability function of Equation (45) gives the individual wave volume associated with a given probability of exceedance, P_{VE} , i.e.,

$$V_W = a \left[-\ln(P_{VE}) \right]^{4/3} \quad (49)$$

The distribution of wave volumes represented by Equation (49) is shown graphically in Figure 14. At very low probabilities of exceedance, the curve approaches infinity, and the wave volumes are large compared to most of the waves. However, keep in mind these rare large overtopping volumes contribute substantially to the average overtopping discharge.

The maximum overtopping wave volume has been approximated as a function of the number of overtopping waves during a storm event.

$$V_{W_{\max}} = a \left[\ln(N_{ow}) \right]^{4/3} \quad (50)$$

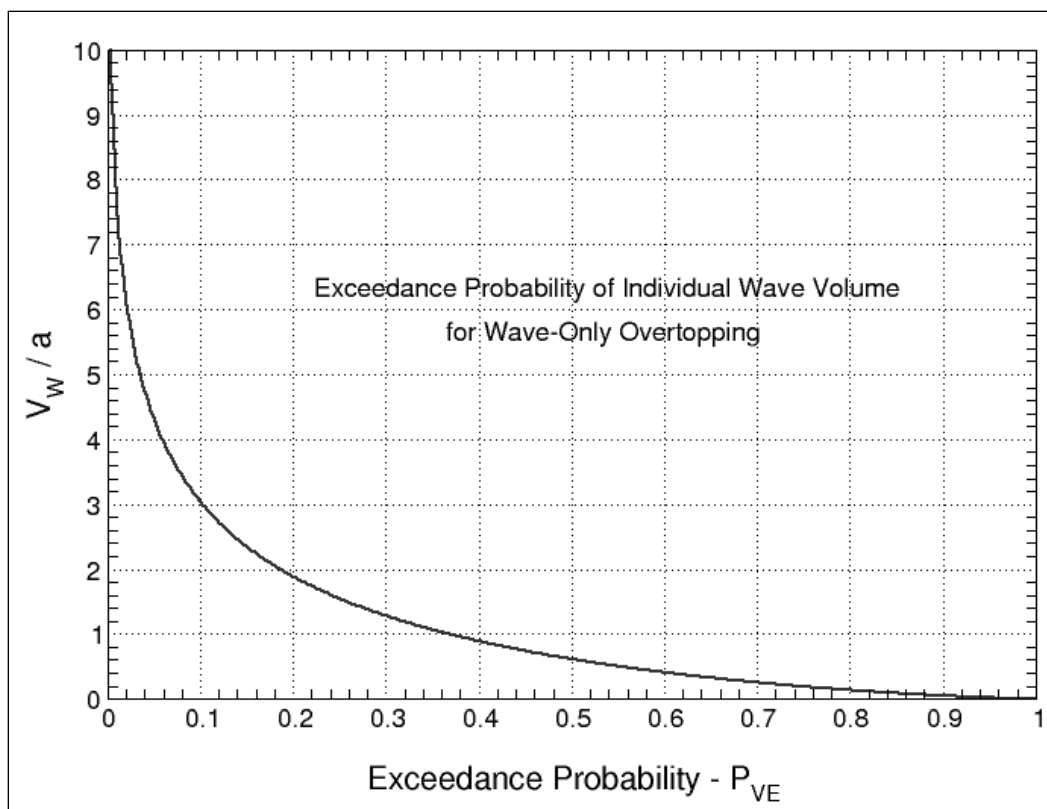


Figure 14. Wave volume exceedance probability distribution for wave-only overtopping.

As the number of overtopping waves increases, either because of decreased freeboard or longer storm duration, the maximum wave volume will increase. Pullen et al. (2007) noted that Equation (50) has considerable uncertainty because it pertains to the extreme tail of the cumulative probability distribution.

Estimation of individual wave overtopping durations (T_{on})

The duration of overtopping for each individual wave is the other key parameter needed for implementation of the methodology (see Figure 12 for a definition of T_o). For wave-only overtopping, we follow a procedure for estimating the individual wave overtopping duration based on analysis of limited laboratory test results. Bosman (2007) and Bosman et al. (2008) analyzed five of the overtopping tests conducted by van Gent (2002), and they proposed the following formula for the duration exceeded by 2-percent of the overtopping wave durations

$$\frac{T_{o2\%}}{T_{m-1,0}} = 1.15 \sqrt{\frac{(R_{u2\%} - R_c)}{H_{m0}}} \quad \text{for } R_{u2\%} > R_c \quad (51)$$

The validity of Equation (51) has not been confirmed independently, and there is some speculation that predicted overtopping durations are too large. Assuming that the individual wave overtopping durations follow a Rayleigh distribution (same as assumed for wave runup), the cumulative probability function for overtopping duration is written as

$$P_T = P(T \leq T_o) = 1 - \exp\left[-\left(\frac{T_o}{T_{o,rms}}\right)^2\right] \quad (52)$$

Equation (52) gives the probability that an individual overtopping wave duration is less than the specified duration, T_o . By noting that $P_T = 0.98$ when $T_o = T_{02\%}$, the root-mean-square period is found from the Rayleigh distribution to be

$$T_{o,rms} = \frac{T_{02\%}}{\sqrt{-\ln(0.02)}} \quad (53)$$

Substituting Equation (53) into Equation (52) gives the individual wave overtopping duration cumulative probability distribution in terms of $T_{02\%}$, i.e.,

$$P_T = P(T \leq T_o) = 1 - \exp\left[-\left\{\sqrt{-\ln(0.02)}\left(\frac{T_o}{T_{02\%}}\right)\right\}^2\right] \quad (54)$$

and the corresponding exceedance probability is $P_{TE} = (1 - P_T)$, or

$$P_{TE} = P(T > T_o) = \exp\left[\ln(0.02)\left(\frac{T_o}{T_{02\%}}\right)^2\right] \quad (55)$$

Solving Equation (55) for the duration associated with a given exceedance probability yields

$$T_o = T_{02\%} \sqrt{\frac{\ln(P_{TE})}{\ln(0.02)}} \quad \text{for } R_{u2\%} > R_c \quad (56)$$

The exceedance probabilities for wave overtopping volume (P_{VE}) and wave overtopping duration (P_{TE}) must be the same, i.e., $P_{VE} = P_{TE}$, because both

are based on the Rayleigh distribution with the onset of wave overtopping defined as $R_{u2\%} = R_c$. This suggests a direct relationship between overtopping wave volume and flow duration. Equating the exceedance probability functions given in Equations (45) and (55) and rearranging gives

$$\frac{T_o}{T_{o2\%}} = \frac{1}{\sqrt{-\ln(0.02)}} \left(\frac{V_W}{a} \right)^{3/8} \quad \text{for } R_{u2\%} > R_c \quad (57)$$

Replacing the scale factor, a , with Equation (46) and substituting the peak spectral wave period for mean period, T_m , from Equation (35) yields

$$\frac{T_o}{T_{o2\%}} = 0.56 \left(\frac{V_W P_{ov}}{q T_p} \right)^{3/8} \quad \text{for } R_{u2\%} > R_c \quad (58)$$

Equation (58) gives the same result as Equation (56) when $P_{VE} = P_{TE}$ and V_W is calculated from Equation (49).

For the special cases of small positive freeboard where every wave overtops, or for negative freeboard with combined wave overtopping and surge overflow, the probability of overtopping, $P_{ov} = 1$, and $T_{o2\%}$ is some fraction of the incident wave parameter $T_{2\%}$, i.e., $T_{2\%} = k_1 \cdot T_{o2\%}$. For Rayleigh distributed incident wave periods,

$$\frac{T_{2\%}}{T_{1/3}} = \frac{\sqrt{-\ln(0.02)}}{1.416} = 1.397 \quad (59)$$

Substituting $T_{2\%} = k_1 \cdot T_{o2\%}$ into Equation (59), replacing $T_{o2\%}$ in Equation (58) with Equation (59), and noting that $T_{1/3} \approx T_p$ (Pullen et al. 2007) gives an expression that could be appropriate for situations where every wave is overtopping the levee if the value of k_1 could be determined, i.e.,

$$\frac{T_o}{T_p} = 0.78 k_1 \left(\frac{V_W}{q T_p} \right)^{3/8} \quad \text{for } P_{ov} = 1 \quad (60)$$

Figure 15 shows individual wave overtopping data collected during experiments of combined wave overtopping and surge overflow (Hughes and Nadal 2009). The 2,092 data points in Figure 15 were from tests with

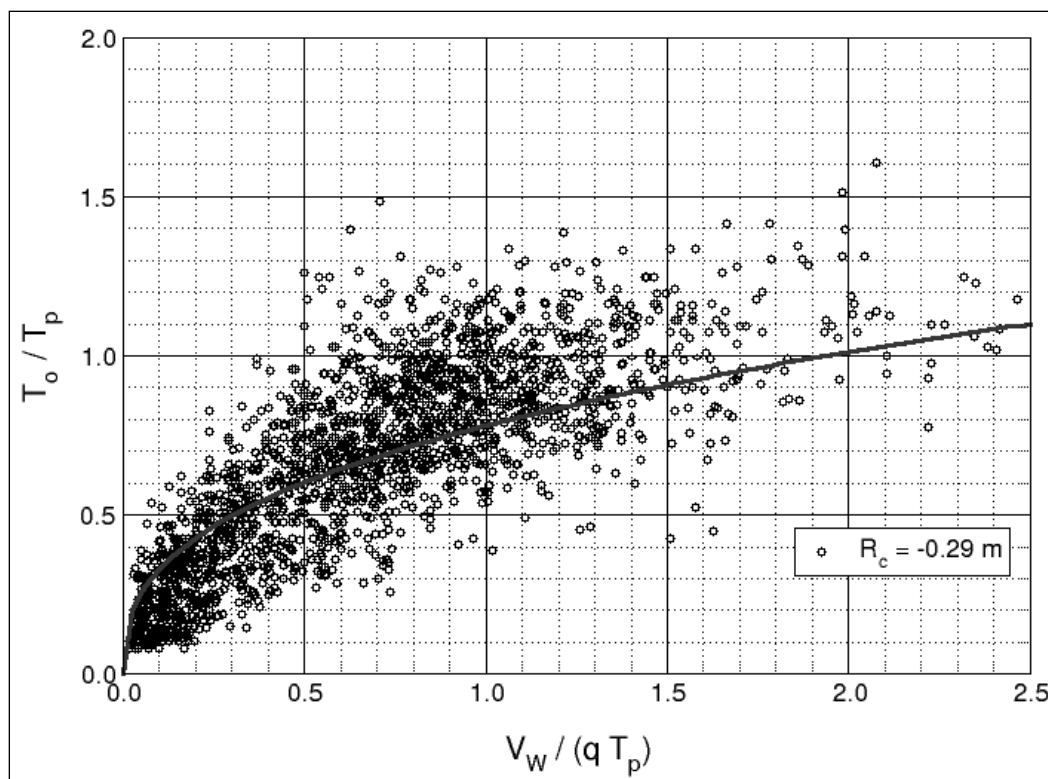


Figure 15. Individual wave overtopping duration for negative freeboard.

the surge level approximately 0.3 m (1.0 ft) above the levee crown (scaled to prototype). The heavy solid line is Equation (60) with $k_l = 1$ (of course k_l should be less than 1). Equation (60) generally under-predicts overtopping durations, but the trend is at least reassuring given the uncertainty about Bosman's (2007) original formulation (Equation 51), the assumption of durations being Rayleigh distributed, and application to severe overtopping cases with negative freeboard. Overtopping durations should be expected to be somewhat longer with negative freeboards because there is less runup and rundown between waves, and the steady overflow contributes to the duration as well. Given the uncertainty, use of Equation (56) or (58) to estimate individual wave overtopping durations is provisional until such time that experimental validation can be obtained. A sensitivity analysis of overtopping durations is presented in Chapter 9.

Wave-only overtopping calculation procedure

Estimation of the cumulative excess wave volume contributing to levee landward-side slope erosion and damage is a two-phase process. The first phase is calculation of parameters that remain constant throughout the overtopping event duration (assuming the incident wave conditions and

surge elevation do not change). The second phase is repeated calculation of individual overtopping wave volumes, durations, and excess wave volumes in the style of a Monte Carlo simulation. The result is a plot of cumulative excess wave volume as a function of storm event duration.

Required parameters

This calculation procedure requires specification of the parameters listed in Table 3. The first 4 parameters pertain to the storm event. Either average wave discharge or levee freeboard must be specified. The only reason for selecting average discharge would be to evaluate a specific design condition based on the allowable overtopping discharge criterion, or to evaluate results from controlled Wave Overtopping Simulator tests. The next 4 parameters are related to levee geometry, slope roughness, and oblique wave approach. The final two parameters quantify the initial and limiting erosion criteria for the specific type of grass cover or levee protection alternative being evaluated.

Table 3. Required input parameters for wave-only overtopping.

H_{m0}	–	Energy-based significant wave height
T_p	–	Incident peak spectral wave period
t_E	–	Duration of storm event
q or R_c	–	Average wave discharge or levee freeboard
$\tan \alpha$	–	Slope of the flood-side levee face
$\tan \theta$	–	Slope of the landward-side levee face
f_F	–	Landward-side levee face friction factor
$\gamma_b, \gamma_t, \gamma_\beta$	–	Wave runup reduction factors
u_c	–	Threshold velocity for levee grass or armoring alternative
$E_w / (K_w \beta_w)$	–	Erosion limit for levee grass or armoring alternative

Calculation of constant parameters

The following steps give the procedure for calculating the constant parameters for a storm event simulation.

1. Calculate the erosional limit from the rightmost side of Equation (32) for the type of levee protection.

2. Calculate the critical discharge (q_c) based on threshold velocity from Equation (33).
3. Calculate the mean spectral wave period ($T_{m-1,o}$) and the mean wave period (T_m) from Equations (34) and (35), respectively.
4. Calculate the deepwater wave length ($L_{m-1,o}$) based on mean spectral wave period from Equation (39) and the Iribarren number ($\xi_{m-1,o}$) from Equation (38).
5. Estimate the 2-percent runup value ($R_{u2\%}$) using Equations (36) and (37). Select the smaller of the two estimates.
6. If average wave overtopping discharge is specified instead of freeboard, estimate the levee freeboard (R_c) from Equations (42) and (43). Select the smaller of the two estimates.
7. If levee freeboard is specified instead of discharge, estimate the average wave overtopping discharge (q) using Equations (40) and (41). Select the smaller of the two estimates.
8. Calculate the probability of individual wave overtopping (P_{ov}) using Equation (47).
9. Calculate the wave volume cumulative probability distribution scale factor (a) from Equation (46).
10. Calculate the total number of waves in the storm event (N_W) and the number of overtopping waves (N_{ow}) from Equation (48). These values need to be rounded down to integers.
11. Calculate the 2-percent overtopping duration ($T_{o2\%}$) from Equation (51).

Monte Carlo simulation of the overtopping event

Once all of the constant parameters for the simulation are computed, a Monte Carlo procedure is used to simulate the overtopping of individual waves. We assume that the ordering of the waves selected from the overtopping wave volume cumulative distribution is completely random, provided the distribution of volumes is represented correctly. Thus, any wave grouping effects are absent. The following repetitive steps are required for the total number (N_{ow}) of overtopping waves.

1. Using a random number generator, select an exceedance probability in the range ($0 < P_{VE} < 1$).
2. Calculate the volume (V_{Wn}) for the individual wave using Equation (49).
3. Calculate the associated overtopping duration (T_{on}) using either Equation (56) or (58).
4. Calculate the excess wave volume as the term inside the summation of Equation (32) for each wave in which $(3V_W / T_o) > q_c$. This is the

contribution of the wave to the running cumulative total. Add this amount to the cumulative excess wave volume total (V_{ET}) in Equation (32). Note that waves not meeting this criterion contribute zero volume.

5. Terminate the calculation after processing N_{ow} waves.
6. Compare the cumulative excess wave volume to the erosion limit excess wave volume determined for the levee slope protection.

The overtopping of N_{ow} waves takes place over a storm event duration that is longer than the summed overtopping durations, i.e., $t_E > \sum (T_{on})$. For plotting purposes we will distribute the contributions of individual overtopping waves evenly over the total storm event duration. In nature, overtopping waves will not be evenly distributed in time. This compromise has minor effect on the estimation of when the erosional limit is exceeded.

Example 1: Wave-only overtopping calculation

Determine if a levee protected with good-quality grass will suffer damage during a specified storm. Assume that the storm surge and incident wave conditions remain constant during a storm lasting 4 hours, and use the threshold velocity and erosional limit for good grass shown in Table 1. The calculation input parameters are shown on Table 4. Calculations were performed using a MatLab[®] script.

Calculation of constant parameters

The following steps give the procedure for calculating the constant parameters for a storm event simulation. SI units are used in the example.

1. Calculate the erosional limit from the rightmost side of Equation (32) for good grass cover.

$$\left(\frac{E_w}{K_w \beta_w} \right) \left(\frac{f_F}{2g \sin \theta} \right) = \left[0.492 (10)^6 \text{ m}^3 / \text{s}^2 \right] \left[\frac{0.015}{2(9.815 \text{ m/s}^2) \sin(18.4^\circ)} \right] = 1,189 \text{ m}^3 / \text{m}$$

2. Calculate the critical discharge (q_c) based on threshold velocity from Equation (33).

$$q_c = \left(\frac{f_F u_{c,w}^3}{2g \sin \theta} \right) = \left[\frac{0.015 (1.8 \text{ m/s})^3}{2(9.815 \text{ m/s}^2) \sin(18.4^\circ)} \right] = 0.014 \text{ m}^3 / \text{s/m}$$

Table 4. Input parameters for wave-only overtopping example.

Parameter	SI Units	English Units
H_{m0}	2.0 m	6.56 ft
T_p	8.0 s	8.0 s
t_E	4.0 hr	4.0 hr
q	$q = 100 \text{ l/s/m (0.1 m}^3\text{/s/m)}$	1.08 cfs/ft
$\tan \alpha$	1/4	1/4
$\tan \theta$	1/3	1/3
f_F	0.015	0.015
$\gamma_b, \gamma_f, \gamma_\beta$	1.0, 1.0, 1.0	1.0, 1.0, 1.0
u_c	1.8 m/s	5.9 ft/s
$E_w / (K_w \beta_w)$	0.492 (10) ⁶ m ³ /s ²	17.37 (10) ⁶ ft ³ /s ²

3. Calculate the mean spectral wave period ($T_{m-1,0}$) and the mean wave period (T_m) from Equations (34) and (35), respectively.

$$T_{m-1,0} = T_m = \frac{T_p}{1.1} = \frac{8.0\text{s}}{1.1} = 7.27\text{s}$$

4. Calculate the deepwater wave length ($L_{m-1,0}$) based on mean spectral wave period from Equation (39) and the Iribarren number ($\xi_{m-1,0}$) from Equation (38).

$$L_{m-1,0} = \frac{g}{2\pi} T_{m-1,0}^2 = \frac{(9.815\text{m/s}^2)}{2\pi} (7.27\text{s})^2 = 82.6\text{m}$$

$$\xi_{m-1,0} = \frac{\tan \alpha}{\sqrt{H_{m0} / L_{m-1,0}}} = \frac{(1/4)}{\sqrt{(2.0\text{m}) / (82.6\text{m})}} = 1.607$$

5. Estimate the 2-percent runup value ($R_{u2\%}$) using Equations (36) and (37). Select the smaller of the two estimates.

$$R_{u2\%} = 1.75 H_{m0} \gamma_b \gamma_f \gamma_\beta \xi_{m-1,0} = 1.75 (2.0\text{m}) (1.0) (1.0) (1.0) (1.607) = 5.62\text{m}$$

or

$$R_{u2\%} = 1.0 H_{m0} \gamma_f \gamma_\beta \left(4.3 - \frac{1.6}{\sqrt{\xi_{m-1.0}}} \right) = 1.0(2.0\text{ m})(1.0)(1.0) \left(4.3 - \frac{1.6}{\sqrt{1.607}} \right) = 6.08\text{ m}$$

Use the smaller value of $R_{u2\%} = 5.62\text{ m}$.

6. Because average wave overtopping discharge is specified instead of freeboard, estimate the levee freeboard (R_c) from Equations (42) and (43). Select the smaller of the two estimates.

$$\begin{aligned} R_c &= - \left(\frac{\xi_{m-1.0} H_{m0} \gamma_b \gamma_f \gamma_\beta \gamma_v}{4.3} \right) \ln \left[\left(\frac{q}{\sqrt{g H_{m0}^3}} \right) \frac{\sqrt{\tan \alpha}}{0.067 \gamma_b \cdot \xi_{m-1.0}} \right] \\ &= - \left(\frac{(1.607)(2.0\text{ m})(1)(1)(1)(1)}{4.3} \right) \ln \left[\left(\frac{(0.1\text{ m}^3/\text{s/m})}{\sqrt{(9.815\text{ m/s}^2)(2.0\text{ m})^3}} \right) \frac{\sqrt{(1/4)}}{0.067(1.0)(1.607)} \right] \\ &= -(0.747\text{ m}) \ln(0.0524) = 2.2\text{ m} \end{aligned}$$

or

$$\begin{aligned} R_c &= - \left(\frac{H_{m0} \gamma_f \gamma_\beta}{2.3} \right) \ln \left[\frac{5q}{\sqrt{g H_{m0}^3}} \right] = - \left(\frac{(2.0\text{ m})(1)(1)}{2.3} \right) \ln \left[\frac{5(0.1\text{ m}^3/\text{s/m})}{\sqrt{(9.815\text{ m/s}^2)(2.0\text{ m})^3}} \right] \\ &= -(0.87\text{ m}) \ln(0.0564) = 2.5\text{ m} \end{aligned}$$

Use the smaller value of $R_c = 2.2\text{ m}$.

7. If levee freeboard is specified instead of discharge, estimate the average wave overtopping discharge (q) using Equations (40) and (41). Select the smaller of the two estimates.

(Skip this step because q was specified)

8. Calculate the probability of individual wave overtopping (P_{ov}) using Equation (47).

$$P_{ov} = \exp \left[- \left(\sqrt{-\ln(0.02)} \frac{R_c}{R_{u2\%}} \right)^2 \right] = \exp \left[- \left(\sqrt{-\ln(0.02)} \frac{(2.2\text{ m})}{(5.62\text{ m})} \right)^2 \right] = 0.55$$

9. Calculate the wave volume cumulative probability distribution scale factor (a) from Equation (46).

$$a = 0.84 \cdot T_m \cdot \left(\frac{q}{P_{ov}} \right) = 0.84 (7.27 \text{ s}) \left(\frac{0.1 \text{ m}^3/\text{s}/\text{m}}{0.55} \right) = 1.11 \text{ m}^3/\text{m}$$

10. Calculate the total number of waves in the storm event (N_W) and the number of overtopping waves (N_{ow}) from Equation (48). These values need to be rounded down to integers.

$$N_W = \frac{t_E}{T_m} = \frac{(4.0 \text{ hr})(3,600 \text{ s/hr})}{(7.27 \text{ s})} = 1,980.7 = 1,980 \text{ waves}$$

and

$$P_{ov} = \frac{N_{ow}}{N_W} \Rightarrow N_{ow} = P_{ov} \cdot N_W = 0.55 \cdot (1,980 \text{ waves}) = 1,089.0 = 1,089 \text{ waves}$$

11. Calculate the 2-percent overtopping duration ($T_{02\%}$) from Equation (51).

$$T_{02\%} = 1.15 T_{m-1.0} \sqrt{\frac{(R_{u2\%} - R_c)}{H_{m0}}} = 1.15 (7.27 \text{ s}) \sqrt{\frac{(5.62 \text{ m} - 2.2 \text{ m})}{2.0 \text{ m}}} = 10.93 \text{ s}$$

Monte Carlo simulation of the overtopping event

The following repetitive steps were computed for $N_{ow} = 1,089$ overtopping waves. The example below only shows calculations for step 1.

1. Using a random number generator, select an exceedance probability in the range ($0 < P_{VE} < 1$).
2. For this particular example, the random number generator produced the first value of $P_{VE1} = 0.8092$ for the exceedance probability of the first overtopping wave. This will be a relatively small wave with 80% of the waves being greater.
3. Calculate the volume (V_{W1}) for the individual wave using Equation (49).

$$V_{W1} = a [-\ln(P_{VE1})]^{4/3} = (1.11 \text{ m}^3/\text{m}) [-\ln(0.8092)]^{4/3} = 0.14 \text{ m}^3/\text{m}$$

4. Calculate the associated overtopping duration (T_{ol}) using either Equation (56) or (58).

$$T_{o1} = T_{o2\%} \sqrt{\frac{\ln(P_{TE})}{\ln(0.02)}} = (10.93\text{s}) \sqrt{\frac{\ln(0.8092)}{\ln(0.02)}} = 2.54\text{s}$$

or

$$T_{o1} = 0.56 T_{o2\%} \left(\frac{V_{W1} P_{ov}}{q T_p} \right)^{3/8} = 0.56 (10.93\text{s}) \left[\frac{(0.14 \text{ m}^3/\text{m})(0.55)}{(0.1 \text{ m}^3/\text{s/m})(8.0\text{s})} \right]^{3/8} = 2.54\text{s}$$

Both equations gave the same result.

5. Calculate the excess wave volume as the term inside the summation of Equation (32). This is the contribution of the wave to the running cumulative total. Add this amount to the cumulative excess wave volume total (V_{ET}) in Equation (32). First check that

$$\frac{3 V_{W1}}{T_{o1}} > q_c \quad \text{or} \quad \frac{3(0.14 \text{ m}^3/\text{m})}{2.54 \text{ s}} = 0.165 \text{ m}^3/\text{s/m} > 0.014 \text{ m}^3/\text{s/m}$$

Thus, this wave contributes excess wave volume given as

$$\begin{aligned} V_{E1} &= V_{W1} \left[1 - \left(\frac{q_c T_{o1}}{V_{W1}} \right) + \frac{2}{3^{3/2}} \left(\frac{q_c T_{o1}}{V_{W1}} \right)^{3/2} \right] \\ &= (0.14 \text{ m}^3/\text{m}) \left[1 - \left(\frac{(0.014 \text{ m}^3/\text{s/m})(2.54\text{s})}{0.14 \text{ m}^3/\text{m}} \right) + \frac{2}{3^{3/2}} \left(\frac{(0.014 \text{ m}^3/\text{s/m})(2.54\text{s})}{0.14 \text{ m}^3/\text{m}} \right)^{3/2} \right] \\ &= 0.11 \text{ m}^3/\text{m} \end{aligned}$$

This calculation indicates about 80% of the volume from the first overtopping wave contributed to the cumulative excess wave volume.

6. Terminate the calculation after processing N_{ow} waves.

This same procedure is followed for the rest of the waves, i.e.,

$$V_{ET}(t) = \sum_{n=1}^N V_{En} \leq \left(\frac{E_W}{K_W \beta_W} \right) \left(\frac{f_F}{2g \sin \theta} \right) \leq 1,189 \text{ m}^3/\text{m}$$

Results of the wave-only overtopping example

Table 5 summarizes the calculation parameters for the above example in both SI and English units.

Table 5. Calculated parameters for wave-only overtopping example.

Parameter	SI Units	English Units
Constant Parameters		
<i>Erosion index</i>	1,189 m ³ /m	12,800 ft ³ /ft
<i>q_c</i>	0.014 m ³ /s/m	0.15 cfs/ft
<i>T_{m-1,0}</i>	7.27 s	7.27 s
<i>L_{m-1,0}</i>	82.6 m	271 ft
<i>ξ_{m-1,0}</i>	1.607	1.607
<i>R_{u2%}</i>	5.62 m	18.44 ft
<i>R_c</i>	2.2 m	7.22 ft
<i>P_{ov}</i>	0.55	0.55
<i>a</i>	1.11 m ³ /m	11.95 ft ³ /ft
<i>N_w</i>	1,980	1,980
<i>N_{ow}</i>	1,089	1,089
<i>T_{o2%}</i>	10.93 s	10.93 s
Parameters of First Overtopping Wave		
<i>P_{VE1}</i>	0.8092	0.8092
<i>V_{w1}</i>	0.14 m ³ /m	1.5 ft ³ /ft
<i>T_{o1}</i>	2.54 s	2.54 s
<i>V_{E1}</i>	0.11 m ³ /m	1.18 ft ³ /ft

Figure 16 is a plot of the calculated cumulative excess wave volume over the 4-hr duration of the specified storm event. The horizontal dashed line at wave volume of 1,189 m³/m is the erosion damage index that represents the Hewlett et al. (1987) curve for good grass. The no-damage threshold is also shown on the figure. This simulation indicated that the limiting state was reached after about 3.7 hours of the overtopping event. Recall that elapsed event time is greater than the summation of all of the individual overtopping wave durations. The cumulative excess wave volume is almost a straight line trend even though the individual wave volumes varied according to the Weibull exceedance probability of Equation (45).

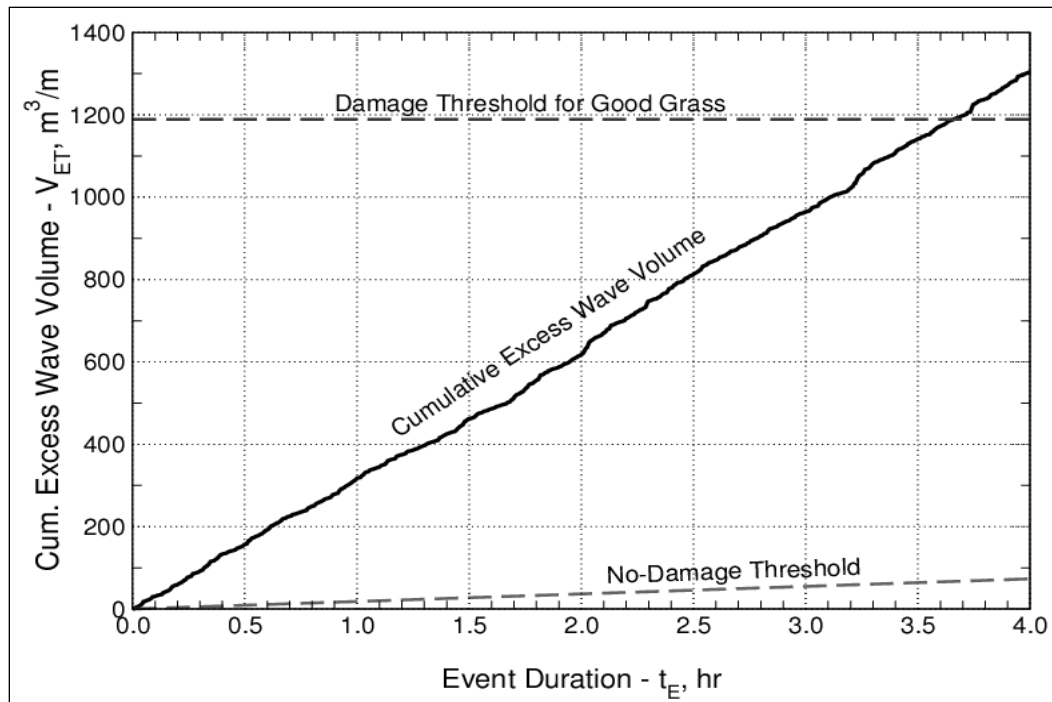


Figure 16. Results of the wave-only overtopping example.

The result shown in Figure 16 is from a single Monte Carlo simulation in which the exceedance probability of each wave in the progression was randomly sampled from the exceedance probability distribution. Variations are expected between simulations.

Figure 17 shows results from twenty Monte Carlo simulations using the same parameters that were used in the wave-only overtopping example. The heavy line is the first simulation performed as part of the example. This first simulation is near the lower bound of the simulations; and thus, it gives a less conservative result than the majority of the simulations.

Because of the spread that is obtained using the Monte Carlo procedure, it is recommended that at least 20 simulations be performed. For each simulation the average wave overtopping discharge can be calculated as the total cumulative wave volume divided by the time of the event, i.e., $q = (\sum V_{wn})/t_E$. The simulation having average discharge closest to the specified target discharge should be selected. Results could also be presented for the most conservative simulation (largest slope), least conservative simulation (smallest slope), or the standard deviation could be determined. Figure 18 is a plot of the best and limiting simulations for the same storm and levee parameters used in the wave-only overtopping example. The time to reach the damage threshold for good grass was 3.4 hrs.

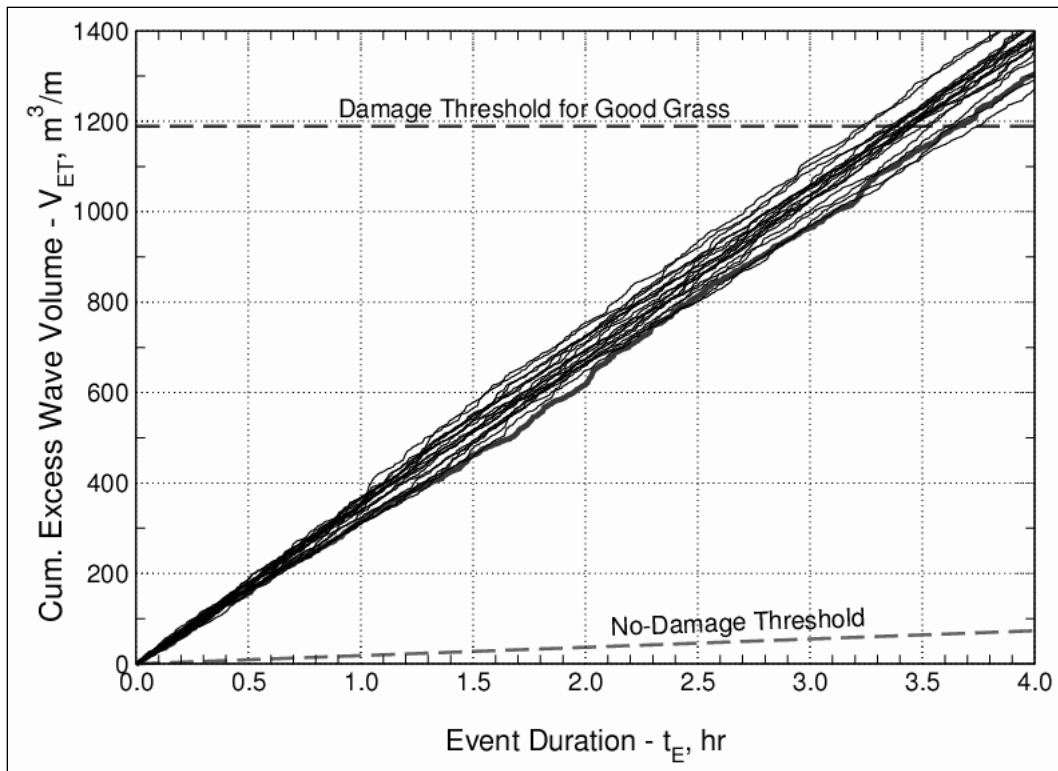


Figure 17. Twenty repeats of the wave-only overtopping example.

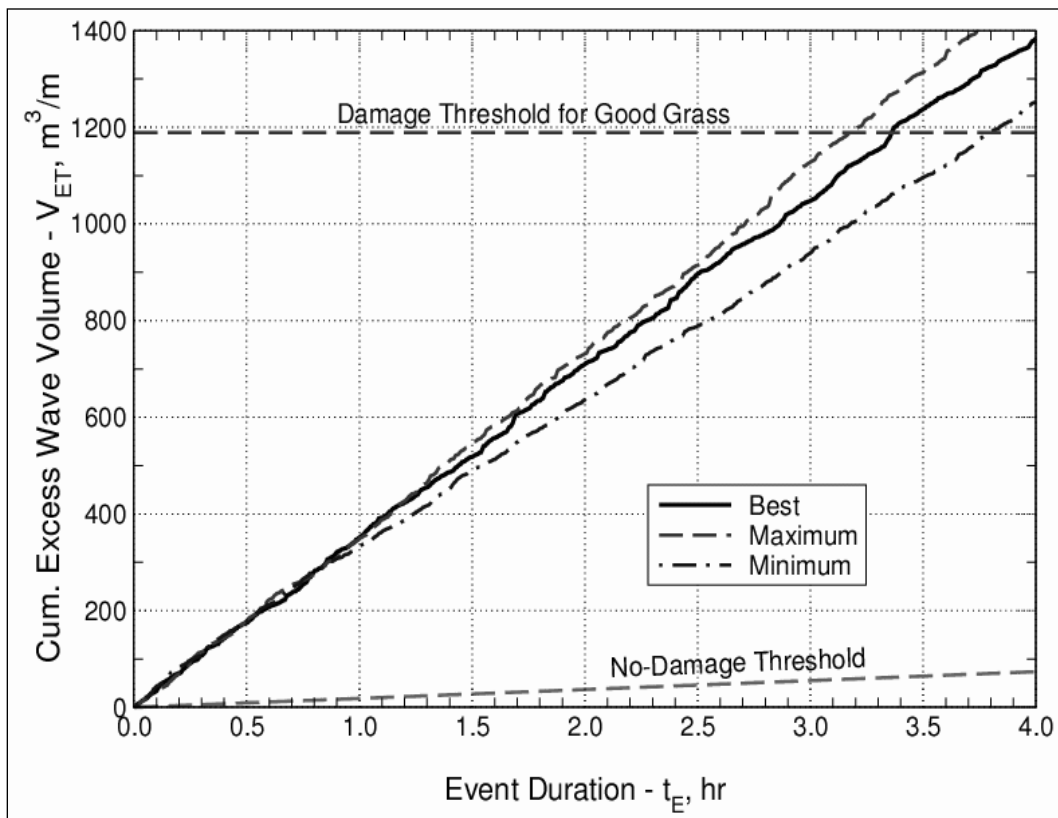


Figure 18. Best simulation and limits from the wave-only overtopping example.

The time histories of individual wave volumes and corresponding overtopping durations are shown on the bar graphs of Figure 19 for one of the Monte Carlo simulations. Two of the wave volumes exceeded $15 \text{ m}^3/\text{m}$, but most volumes did not exceed 4 or $5 \text{ m}^3/\text{m}$. There very well may be physical constraints that prevent the highest overtopping volumes to occur; but any constraints are presently unknown, and thus, are not included in the random selection of overtopping volumes. Also, any grouping of larger waves is not captured by the simulation technique.

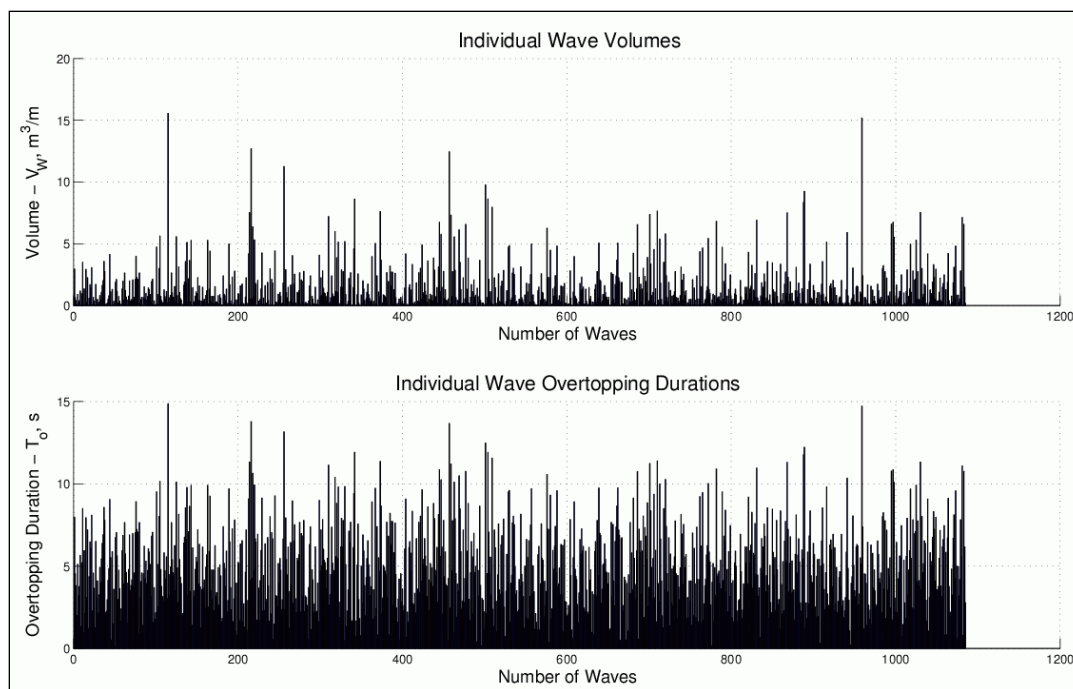


Figure 19. Time histories of individual wave volumes and durations for a simulation.

This particular simulation had 1,085 overtopping waves out of the 1,980 total waves, giving a probability of overtopping, $P_{ov} = 0.55$. The total summation of all individual wave overtopping durations was 1.5 hr. So during the 4-hr duration of the storm event, waves were overtopping just over 37 percent of the time. As mentioned previously, the overtopping durations were evenly distributed over the 4-hr event duration for plotting purposes. The average overtopping duration per wave was 4.98 s, whereas the mean incident wave period was 7.27 s. The smaller overtopping duration is due to the fact that overtopping does not occur during portions of the wave runup and rundown cycle when the runup level is below the levee crown elevation. Dean et al. (2010) recognized this fact, and they applied an overtopping duration reduction factor in their analysis. Estimation of the

total overtopping duration as the event duration times the probability of overtopping (2.2 hr in this case) is not a correct procedure to follow.

Equivalent steady flow

For cases with constant freeboard and constant incident wave conditions, the accumulation of excess wave volume from irregular wave overtopping produces a nearly linear trend in time as seen by the plots of Figures 16 – 18. The Hewlett et al. (1987) limiting velocity curves also produce linear duration relationships (see Figure 4) because the overflow discharge is constant. Therefore, it is possible to theoretically equate these two cases to determine what level of steady overflow will produce the same cumulative excess volume result as a given wave-only overtopping scenario. Keep in mind that this does not guarantee that the assumption of erosional equivalence is correct!

A necessary assumption for equating steady overflow work to intermittent wave overtopping work is that erosion and subsequent slope damage is due to accumulated excess flow work on the slope. Furthermore, it must be assumed that the excess flow work is driving essentially the same erosion mechanism for the two cases. If, however, slope damage from overtopping waves is the result of strong impacts and perhaps high turbulence caused by the larger waves, the equivalence becomes more uncertain.

For steady overflow Equation (11) reduces to

$$V_{ET}(t) = (q - q_c) t \leq \frac{E_W}{K_W \beta_W} \left(\frac{f_F}{2g \sin \theta} \right) \quad \text{with } q > q_c \quad (61)$$

where

$$q_c = \left(\frac{f_F u_c^3}{2g \sin \theta} \right) \quad (62)$$

and

$$q = \left(\frac{f_F u^3}{2g \sin \theta} \right) \quad \text{or} \quad u = \left[\left(\frac{2g \sin \theta}{f_F} \right) q \right]^{1/3} \quad (63)$$

The slope of the excess overflow volume versus duration curve can be given as the damage threshold divided by the duration (t_F) when the line intersects the damage threshold, so Equation (61) becomes

$$q = \frac{E_W}{K_W \beta_W} \left(\frac{f_F}{2g \sin \theta} \right) \frac{1}{t_F} + q_c \quad (64)$$

Therefore, the steady overflow discharge, having the same excess flow volume slope as the wave overtopping simulation, can be estimated using Equation (64), and the corresponding steady overflow velocity can be calculated from Equation (63). In fact, substituting Equation (63) into Equation (64) recovers a rearranged version of the Dean et al. (2010) original equation for excess work given by Equation (3), i.e.,

$$u = \left[\left(\frac{E_W}{K_W \beta_W} \right) \frac{1}{t_F} + u_c^3 \right]^{1/3} \quad (65)$$

As an illustration, consider the previous wave-only overtopping example. Using the erosion index and critical discharge from Table 5, and taking the mean duration to slope damage from Figure 18 as $t_F = 3.4$ hr, Equation (64) gives the equivalent steady overflow as

$$\begin{aligned} q &= \frac{E_W}{K_W \beta_W} \left(\frac{f_F}{2g \sin \theta} \right) \frac{1}{t_F} + q_c \\ &= \frac{1,189 \text{ m}^3/\text{m}}{(3.4 \text{ hr})(3,600 \text{ s/hr})} + 0.014 \text{ m}^3/\text{m} = 0.11 \text{ m}^3/\text{s/m} \end{aligned}$$

The equivalent steady overflow velocity is found from Equation (63) with the values of landward-side levee slope and friction factor from Table 4, i.e.,

$$u = \left[\left(\frac{2g \sin \theta}{f_F} \right) q \right]^{1/3} = \left[\left(\frac{2(9.815 \text{ m/s}^2) \sin(18.43^\circ)}{0.015} \right) (0.11 \text{ m}^3/\text{s/m}) \right]^{1/3} = 3.58 \text{ m/s}$$

The slopes of the maximum and minimum excess wave volume curves in Figure 18 ($t_F = 3.2$ hr and 3.8 hr) produce equivalent steady overflow velocities of $u = 3.65$ and 3.47 m/s, respectively.

Looking at the Dean et al. (2010) fit to the Hewlett et al. (1987) curves shown in Figure 3, it is seen that the curve for good grass corresponds to the above-estimated limiting velocities at the durations specified. At damage durations shorter than about 2.5 hrs, the equivalence will follow the dashed line for good grass rather than the original Hewlett curve because they represent the best-fit parameters used in this methodology. Of course, the easiest method is to read the limiting velocity from Figure 3 directly.

The equivalent steady overflow discharge estimated in the above example ($0.11 \text{ m}^3/\text{s}/\text{m}$ or $1.18 \text{ cfs}/\text{ft}$) is about the same magnitude as the average wave overtopping ($0.10 \text{ m}^3/\text{s}/\text{m}$ or $1.08 \text{ cfs}/\text{ft}$). This is not surprising because the erosional equivalence methodology is based on the assumption of similar excess flow work on the slope. There is still considerable uncertainty as to whether this equivalence is correct. The erosion physical processes occurring during wave overtopping are being studied; and there are indications that high levels of turbulence in the larger overtopping waves, coupled with the impact of the wave leading edge as it moves down the slope might be the primary erosional mechanisms (J. W. van der Meer, personal communication, 2010).

Even if the assumed equivalence between steady overflow and wave overtopping is not correct, the cumulative excess wave volume methodology is still a viable analysis tool. However, use of the methodology requires that appropriate values for the critical threshold velocity and the erosional damage limit can be established from field and/or full-scale laboratory observations. In other words, slope damage due to high turbulence levels in larger waves can be successfully parameterized in terms of the excess overtopping wave volumes to give a time-dependent estimation of slope damage initiation.

Influence of storm and levee parameters

The influence of several key storm event and levee parameters was examined by conducting Monte Carlo simulations based on the parameters used for the above wave-only overtopping example. The results are discussed in the following paragraphs.

Effect of average wave overtopping discharge

A major storm parameter is the average wave overtopping discharge, or alternately, the levee freeboard. Simulations were run with the same

incident wave and levee parameters as the wave-only example (see Table 4) with the only exception being the value of average wave overtopping discharge. For each case, 20 simulations were run; and the simulation closest to the correct average discharge was selected.

Figure 20 presents the excess wave volume versus duration simulations for three values of average discharge. As expected, the time to reach the damage threshold decreased as average overtopping discharge increased. For a storm event lasting 4 hrs, damage of good grass did not occur for $q = 80$ l/s/m, whereas damage did occur at higher average discharges (based on erosional damage limit as defined by the Hewlett et al. curves).

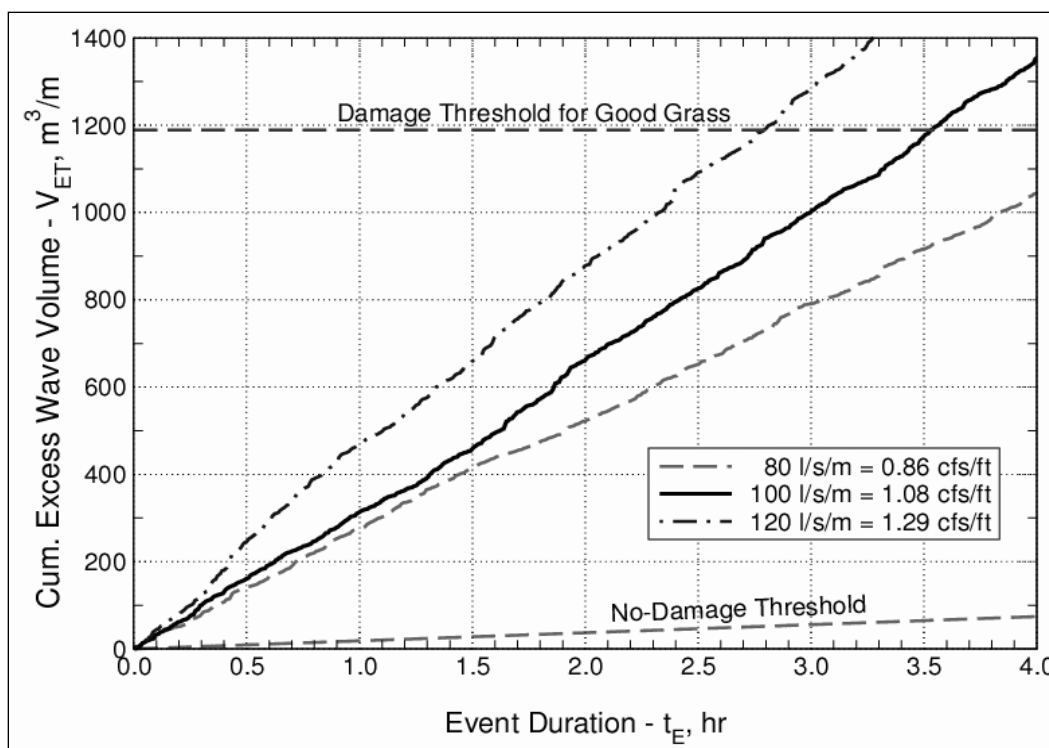


Figure 20. Effect of average overtopping discharge for wave-only overtopping example.

Effect of grass quality

It is well known that grass quality is a major factor contributing to the resiliency of grass-covered levees. This is reflected in both the original Hewlett curves and in simulations of wave overtopping based on erosional equivalence to the Hewlett curves. Figure 21 displays simulation results for good, average, and poor grass cover using the same conditions as the wave-only overtopping example.

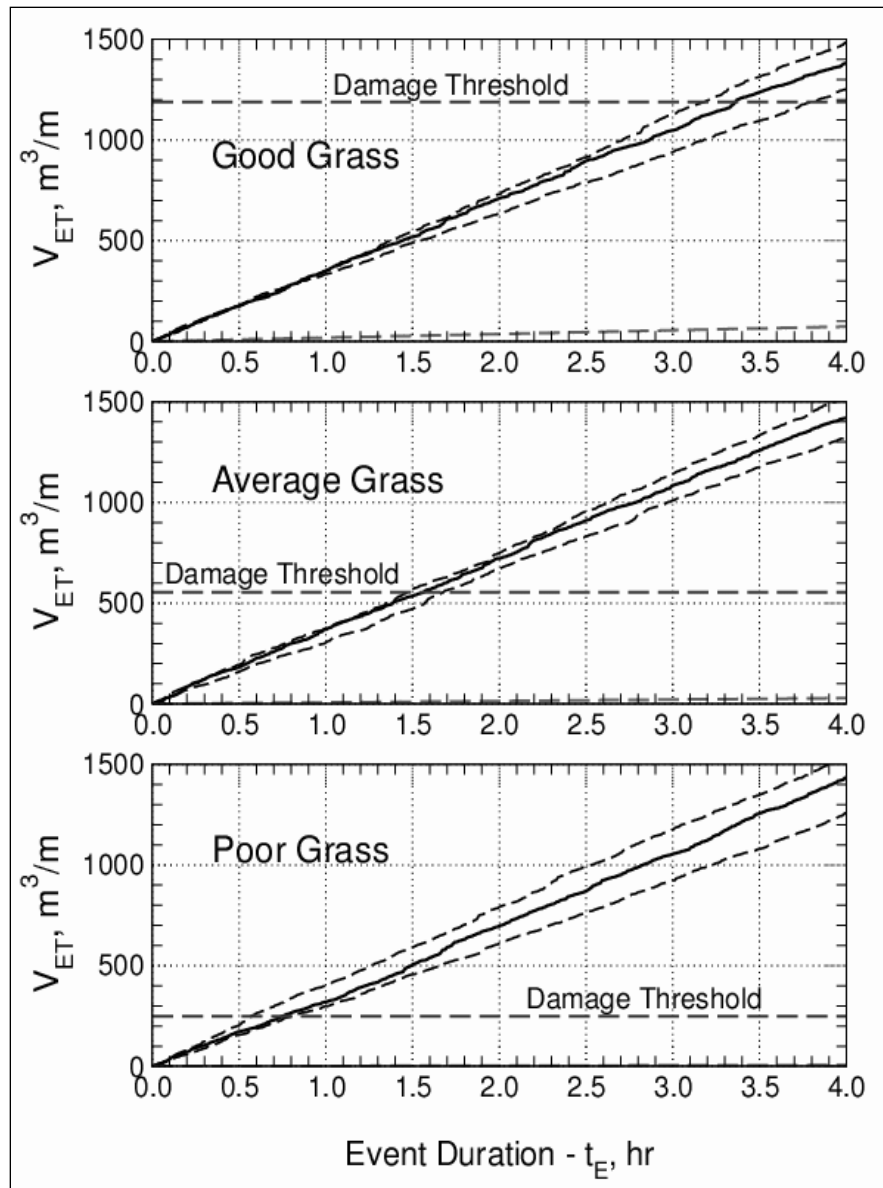


Figure 21. Effect of grass quality on levee resiliency for wave-only overtopping example.

In each plot, the best excess wave volume line is shown as the heavier line, and it is flanked by the maximum and minimum of the Monte Carlo simulations. The relative fragility of the average and poor grass is indicated by the much lower damage thresholds and corresponding shorter times before damage occurs. The good grass cover is capable of withstanding the erosive conditions for over 3 hrs, whereas the average grass can only survive 1.5 hrs and the poor grass will fail before an hour passes. There is little difference in the cumulative excess wave volume curves because the critical threshold velocities are so low compared to the overtopping wave velocities.

Effect of significant wave height

Average wave overtopping discharge depends mostly on the magnitudes of significant wave height and freeboard. It is possible for large wave heights and large freeboards to have the same average discharge as smaller wave heights and smaller freeboards. The main difference is that the high wave height/high freeboard case has less overtopping waves, but the waves that do overtop have greater volumes. It is believed by some (e.g., Hughes and Shaw 2011; J. W. van der Meer, personal communication, 2010) that more levee slope damage will occur for higher wave height and freeboard combinations when compared to lower wave height and freeboard combinations that produce the same average wave discharge. Figure 22 is a test of this hypothesis for the erosional equivalence between steady overflow and wave-only overtopping.

Monte Carlo simulations were run for three different significant wave heights with the freeboard adjusted so that the average wave discharge remained the same. All other parameters of the simulations were unchanged from those of the wave-only example. The number of overtopping waves was estimated to be 1,561 waves, 1085 waves, and 910 waves for $H_{m0} = 1.0$ m, 2.0 m, and 3.0 m, respectively. Excess wave volume curves representing the best result for each test are plotted in Figure 22, and the difference between the curves is minor and well within the variations observed for the Monte Carlo simulation technique.

The initial implication from this result might be that the combination of wave height and freeboard that produces the average discharge makes no difference to the result. However, there is one huge caveat. The erosional equivalence concept is based on the premise that levee slope damage is the result of cumulative excess flow work on the slope above a certain, relatively low, velocity threshold. For low values of critical threshold velocity, the relative sizes of the overtopping waves are not as important so long as the summation of excess wave volume is the same. In reality, there is still a reasonable possibility that initiation of damage and subsequent protective cover damage is also linked to the severe loading and energetic turbulence that result from the largest of the overtopping waves.

The magnitude of the critical threshold velocity plays a pivotal role in the similarity of the curves shown in Figure 22. Because the threshold velocity is relatively low ($u_c = 1.8$ m/s), most of the volume of many overtopping waves was determined to be “excess volume,” and relatively few of the waves were

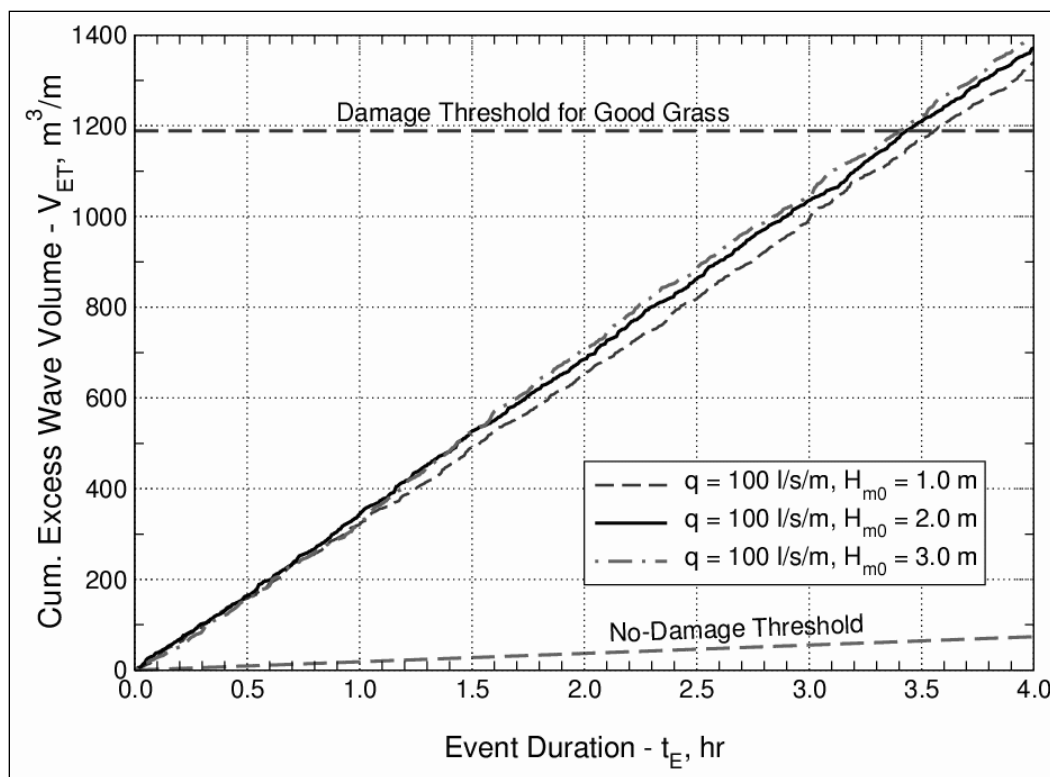


Figure 22. Effect of different wave heights for same average overtopping discharge.

so small that they did not contribute to the cumulative excess wave volume. If the threshold velocity is larger than the value determined for the erosional equivalence to steady flow, then fewer waves will contribute to the excess volume, the contributions will be less for most waves, and the contributions of the larger waves will become more influential.

The same three simulations of different wave height/freeboard combinations shown in Figure 22 were re-run using a higher critical threshold velocity of $u_c = 4.0$ m/s. Results are shown in Figure 23. The higher velocity threshold resulted in distinct differences between the three simulations with equal average discharge. When significant wave height is larger, there are fewer overtopping waves for the same average discharge; but the waves that do overtop have more volume above the critical discharge threshold. Therefore, accumulation of excess wave volume is more rapid than when significant wave height is less and the more numerous overtopping waves are smaller. Also, the grass slope will remain undamaged longer for this second set of simulations because the grass has greater erosion resistance as indicated by the higher threshold velocity.

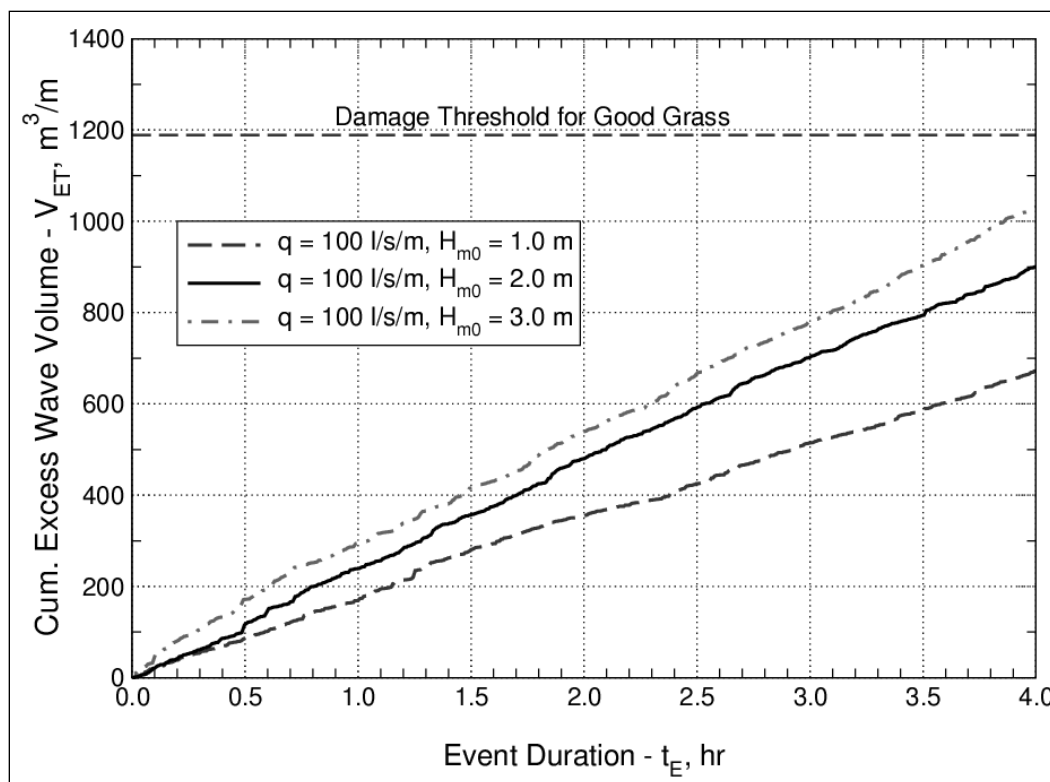


Figure 23. Effect of different wave heights for threshold velocity, $u_c = 4$ m/s.

The different rates of excess wave volume accumulation shown in Figure 23 (compared to the almost identical accumulation rates shown in Figure 22) indicate the importance of determining the critical threshold velocity for various levee grass covers and slope protection alternatives. Thus, the initial implication (see Figure 22) that there is little difference in cumulative excess wave volume when average discharge is the same for different wave height/freeboard combinations is only true when the threshold velocity is small. For more resilient levee covers with higher threshold velocities, damage will occur more rapidly for the case of high waves and high freeboard. Full-scale testing up to the damage limit will help to establish appropriate values of critical threshold velocity for the HSDRRS.

Effect of friction factor

The erosional damage threshold, given as the right-hand side of Equation (32), is a function of the original grouping $[E_W/(K_W \beta_W)]$ derived by Dean et al. (2010) multiplied by the factor $[f_F/(2g \sin \theta)]$. Thus, the damage threshold is directly proportional to the friction factor and inversely proportional to the sine of the landward-side levee slope angle. Physically, greater slope friction means greater flow resistance, and this decreases

flow velocity. Slower flows produce less flow work, so it takes longer to accumulate the excess flow work needed to damage the slope.

The potential importance of the friction factor is illustrated by Figure 24 that shows three Monte Carlo simulations using the same input variables as the wave-only overtopping example, but with different friction factors. The time to damage the slope is significantly different for the variation in friction factors. Note that the friction factor is also used to estimate the critical discharge, q_c ; but the critical discharge for these examples is relatively small, so it only has a minor influence on the overall result.

It appears that a practical solution for application to the HSDRRS is to include the friction factor as part of the empirically-determined erosional index and critical discharge, and then adjust these parameters based on results from full-scale testing. In other words, eventually it will not be necessary to specify a value of f_F because it will already be implicitly included in the erosional index and critical discharge, q_c , determined for specific grasses and armoring alternatives. In essence, this is how slope friction is included in the Hewlett et al. curves.

Effect of landward-side slope

As mentioned above, the erosional index is inversely proportional to the sine of the landward-side levee slope angle. As the slope angle decreases, the erosional damage index increases, and a specified overtopping condition can persist for longer durations before damage occurs. Physically, the slope term ($\sin\theta$) represents the slope of the energy-grade line at terminal velocity conditions. Therefore, milder slopes have a slower terminal velocity; and will take longer to accumulate excess flow work.

Figure 25 illustrates the effect of milder landward-side slopes using the same input parameters as the wave-only example. The only change was the landward-side slope angle. Each cumulative excess wave volume line is the simulation closest to the specified average overtopping discharge for that slope angle. Landward-side slope angle has an obvious importance in determining the duration until the erosional damage limit is reached. Furthermore, the slope angle is unambiguous and easily determined, so it should remain in the erosional index and the critical discharge as a specified parameter.

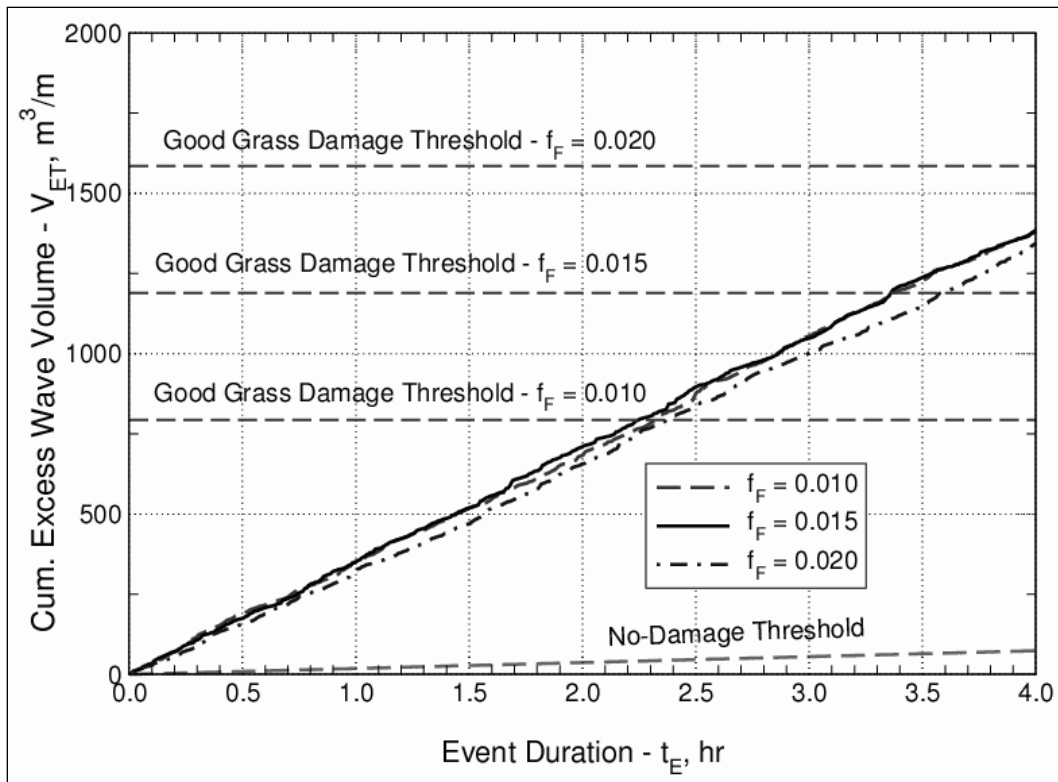


Figure 24. Effect of different landward-side slope friction factors.

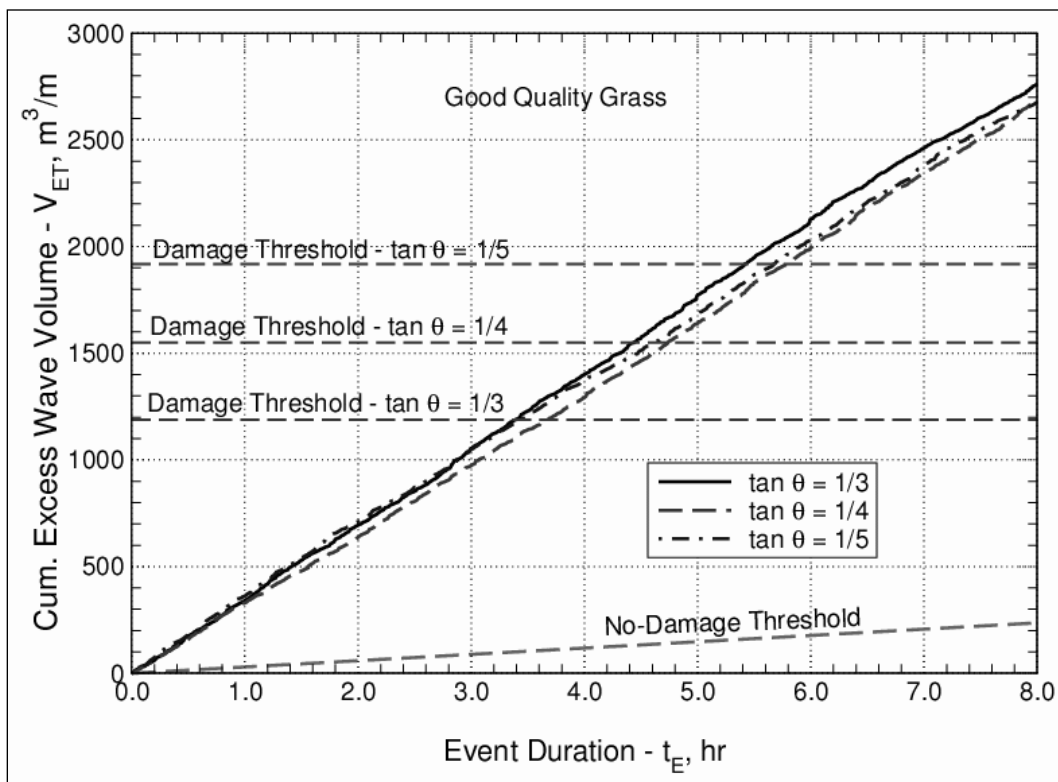


Figure 25. Effect of different landward-side slopes.

6 Application for Combined Wave Overtopping and Surge Overflow

The two key variables needed for application of the cumulative excess overtopping wave volume given by Equations (32) and (33) are the individual overtopping wave volume (V_{Wn}) and the associated overtopping duration (T_{on}). In this section, these required inputs will be specified for the case of combined wave overtopping and storm surge overflow when the levee crown elevation is below the still water elevation of the storm surge (negative freeboard).

Estimation of individual overtopping wave volumes (V_{Wn})

The distribution of overtopping wave volumes (V_{Wn}) for the combined wave and surge overtopping is a function of the following variables:

- H_{m0} = Energy-based significant wave height
- T_p = Incident peak spectral wave period
- T_m = Mean wave period
- R_c = Negative freeboard (levee crown elev. minus SWL elev.)

For a given reach of the HSDRRS, it is necessary to specify H_{m0} , T_p , and R_c . The rest of the parameters are calculated.

Hughes and Nadal (2009) performed small-scale laboratory tests of combined wave overtopping and steady overflow due to a storm surge level higher than the levee crown elevation. They developed empirical equations to estimate the average combined wave/surge overtopping discharge (q_{ws}) as a function of incident significant wave height (H_{m0}) and the negative freeboard (R_c). Peak wave period (T_p) was not included in the formulation because period was found to have minor influence over the range of periods tested. Hughes and Nadal also proposed a Weibull distribution to represent the cumulative probability distribution of overtopping wave volumes.

Below are the equations needed for estimating the individual overtopping wave volumes. The equations are in the approximate order in which they are used in the application to combined wave and surge overtopping. The

application procedure is described after the equations are presented and discussed.

Steady overflow discharge (q_s)

The steady overflow discharge per unit levee length that would occur for negative freeboard in the absence of waves is estimated using the broad-crested weir formulation found in standard hydraulics textbooks (e.g., Henderson 1966)

$$q_s = \left(\frac{2}{3}\right)^{3/2} \sqrt{g} (-R_c)^{3/2} = 0.5443\sqrt{g} (-R_c)^{3/2} \quad \text{for } R_c < 0 \quad (66)$$

Note that freeboard MUST be a negative number so that the value inside the brackets can be raised to the 3/2 power.

Average combined wave overtopping and surge overflow discharge (q_{ws})

Hughes and Nadal (2009) proposed that the average discharge due to combined wave overtopping and surge overflow can be estimated using the empirical formula

$$\frac{q_{ws}}{\sqrt{g} H_{m0}^3} = 0.034 + 0.53 \left(\frac{-R_c}{H_{m0}}\right)^{1.58} \quad \text{for } R_c < 0 \quad (67)$$

The same requirement applies that freeboard must be entered as a negative number. In the unusual case that the total combined overtopping discharge is specified, Equation (67) can be solved for negative freeboard.

Individual wave overtopping volume (V_w)

Hughes and Nadal (2009) fit the following Weibull distribution to the wave volume cumulative probability distributions obtained from their experimental measurements. This equation gives the probability that a wave volume per unit levee length will be less than the specified volume, V_w .

$$P_v = P(V \leq V_w) = 1 - \exp \left[- \left(\frac{V_w}{c_v} \right)^{b_v} \right] \quad (68)$$

In Equation (68), the scale factor is given by the expression

$$c_V = 0.79 \cdot q_{ws} \cdot T_p \quad (69)$$

and the shape factor was found to be a function of the wave parameters and the steady overflow discharge, i.e.,

$$b_V = 15.7 \left(\frac{q_s}{g T_p H_{m0}} \right)^{0.35} - 2.3 \left(\frac{q_s}{\sqrt{g H_{m0}^3}} \right)^{0.79} \quad (70)$$

Equation (68) is very similar to the cumulative distribution given for wave-only overtopping (Equation 44) with nearly the same scale factor (see Equation 46) considering that $T_m = T_p/1.1$ and $P_{ov} = 1$ for combined wave/surge overtopping. The main difference between the wave-only and combined overtopping distributions is that Equation (68) has a shape factor that varies whereas the shape factor for the wave-only overtopping probability distribution is a constant equal to 0.75. The shape factor influences the extreme tail of the distribution.

The corresponding exceedance probability (defined as $P_{VE} = 1 - P_V$) that an overtopping wave volume, V , is greater than a specified volume, V_W , is given as

$$P_{VE} = P(V > V_W) = \exp \left[- \left(\frac{V_W}{c_V} \right)^{b_V} \right] \quad (71)$$

Inverting the exceedance probability function of Equation (71) gives the individual wave volume associated with a given probability of exceedance, P_{VE} , i.e.,

$$V_W = c_V \left[-\ln(P_{VE}) \right]^{1/b_V} \quad (72)$$

Estimation of individual wave overtopping durations (T_{on})

The duration of overtopping for each individual wave is the other key parameter needed for implementation of the methodology. For combined wave overtopping and surge overflow Hughes and Nadal (2009) proposed the following equation for individual wave overtopping duration.

$$\frac{T_o}{T_p} = 0.9 \left(\frac{V_W}{q_{ws} T_p} \right)^{3/5} \quad \text{for } R_c < 0 \quad (73)$$

Equation (73) is quite similar in form to Equation (60) that was derived from the original Bosman (2007) equation and extrapolated for negative freeboard. When the levee crest goes dry between waves, T_o is defined as shown in Figure 12. At higher surge levels, the duration is the time between flow thickness minimums between wave peaks.

Figure 26 shows individual wave overtopping data collected during experiments of combined wave overtopping and surge overflow (Hughes and Nadal 2009). The 5,903 data points were from tests with the surge levels approximately 0.3 m, 0.8 m, and 1.3 m above the levee crown (scaled to prototype). The heavy solid line is Equation (73) that represents the best-fit through all of the data points.

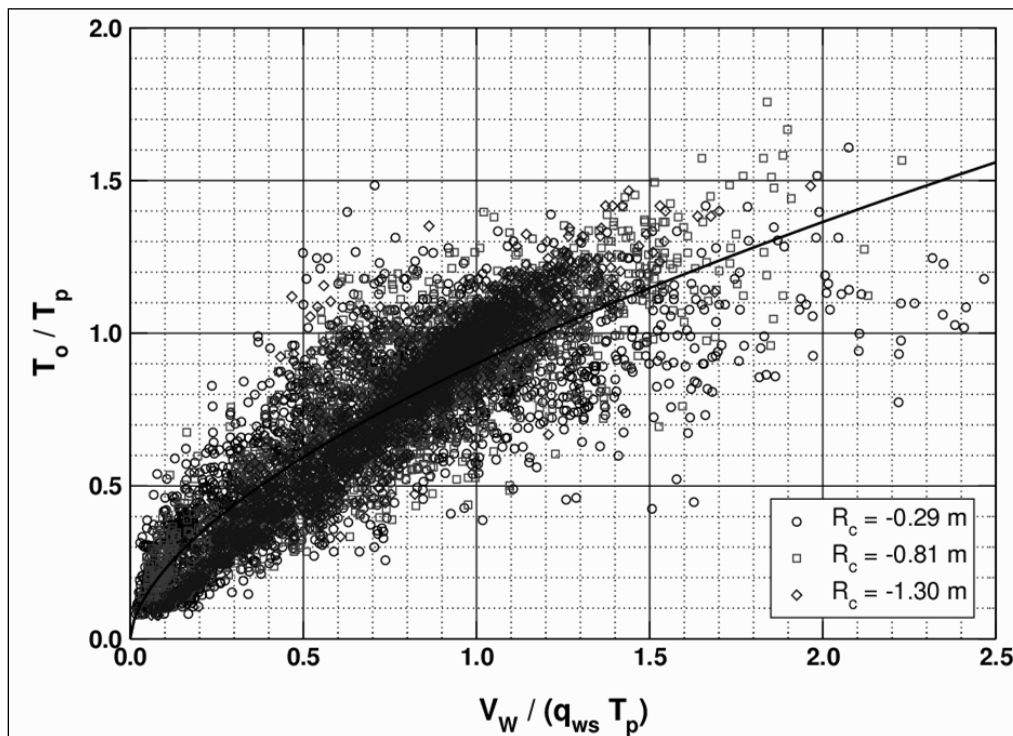


Figure 26. Individual overtopping volumes for combined wave and surge overtopping.

Combined wave and surge overtopping calculation procedure

Just as for wave-only overtopping, estimation of the cumulative excess wave volume contributing to levee landward-side slope erosion and damage is a two-phase process. The first phase is calculation of

parameters that remain constant throughout the overtopping event duration (assuming the incident wave conditions and surge elevation do not change). The second phase is repeated calculation of individual overtopping wave volumes, durations, and excess wave volumes in the style of a Monte Carlo simulation. The result is a plot of cumulative excess wave volume as a function of storm event duration.

Required parameters

This calculation procedure requires specification of the parameters listed in Table 6. The first 4 parameters pertain to the storm event. Freeboard is specified as a negative value for this case. The next 2 parameters are related to levee geometry and slope roughness. The final two parameters quantify the initial and limiting erosion criteria for the specific type of levee protection alternative being evaluated.

Table 6. Required input parameters for combined wave and surge overtopping.

H_{m0}	–	Energy-based significant wave height
T_p	–	Incident peak spectral wave period
t_E	–	Duration of storm event
R_c	–	Levee (negative) freeboard [note: $R_c < 0$]
$\tan \theta$	–	Slope of the landward-side levee face
f_F	–	Landward-side levee face friction factor
u_c	–	Threshold velocity for levee grass or armoring alternative
$E_w / (K_w \beta_w)$	–	Erosion limit for levee grass or armoring alternative

Calculation of constant parameters

The following steps give the procedure for calculating the constant parameters for a storm event simulation.

1. Calculate the erosional limit from the rightmost side of Equation (32) for the type of levee protection.
2. Calculate the critical discharge (q_c) based on threshold velocity from Equation (33).
3. Calculate the mean wave period (T_m) from Equation (35).
4. Estimate the steady overflow discharge (q_s) associated with the levee freeboard (R_c) from Equation (66).

5. Estimate the combined wave overtopping and surge overflow average discharge (q_{ws}) using Equation (67).
6. Calculate the wave volume cumulative probability distribution scale factor (c_V) from Equation (69).
7. Calculate the wave volume cumulative probability distribution shape factor (b_V) from Equation (70).
8. Calculate the total number of waves in the storm event (N_W) from Equation (48) and round down to the nearest integer. Because every wave overtops when the surge level is higher than the levee crown, the number of overtopping waves (N_{ow}) equals the number of waves, and the probability of overtopping is unity (i.e., $P_{ov} = 1$).

Monte Carlo simulation of the overtopping event

Once all of the constant parameters for the simulation are computed, a Monte Carlo procedure is used to simulate the overtopping of individual waves. We assume that the ordering of the waves selected from the overtopping wave volume cumulative distribution is completely random, provided the distribution of volumes is correctly represented. The following repetitive steps are required for the total number (N_{ow}) of overtopping waves.

1. Using a random number generator, select an exceedance probability in the range ($0 < PVE < 1$).
2. Calculate the volume (V_{Wn}) for the individual wave using Equation (72).
3. Calculate the associated overtopping duration (T_{on}) using Equation (73).
4. Calculate the excess wave volume as the term inside the summation of Equation (32) for each wave in which $(3VW / T_o) > q_c$. This is the contribution of the wave to the running cumulative total. Add this amount to the cumulative excess wave volume total (VET) in Equation (32). Note that waves not meeting this criterion contribute zero volume.
5. Terminate the calculation after processing N_{ow} waves.
6. Compare the cumulative excess wave volume to the erosion limit excess wave volume determined for the levee slope protection.

The overtopping of N_{ow} waves takes place over a storm event duration that is slightly longer than the summed overtopping durations, i.e., $t_E > \sum (T_{on})$ even with every wave overtopping. For plotting purposes, we will distribute the contributions of individual overtopping waves evenly over the total storm event duration, even though the overtopping waves are not evenly distributed in nature.

Example 2: Combined wave and surge overtopping calculation

Determine if a levee protected with an open-mat TRM will suffer damage during a specified storm. Assume that the storm surge and incident wave conditions are constant during a storm lasting 4 hours, and use the threshold velocity and erosional damage limit for open mats shown in Table 2. The calculation input parameters are shown on Table 7. Calculations were performed using a MatLab[®] script.

Table 7. Input parameters for combined wave and surge overtopping example.

Parameter	SI Units	English Units
H_{mo}	2.0 m	6.56 ft
T_p	8.0 s	8.0 s
t_E	4.0 hr	4.0 hr
R_c	-0.5 m	-1.64 ft
$\tan \theta$	1/3	1/3
f_F	0.015	0.015
u_c	4.23 m/s	13.9 ft/s
$E_W/(K_W \beta_W)$	1.231 (10) ⁶ m ³ /s ²	43.47 (10) ⁶ ft ³ /s ²

Calculation of constant parameters

The following steps give the procedure for calculating the constant parameters for a storm event simulation. SI units are used for this example.

1. Calculate the erosional limit from the rightmost side of Equation (32) for the open mat levee protection.

$$\left(\frac{E_W}{K_W \beta_W} \right) \left(\frac{f_F}{2g \sin \theta} \right) = \left[1.231(10)^6 \text{ m}^3/\text{s}^2 \right] \left[\frac{0.015}{2(9.815 \text{ m/s}^2) \sin(18.4^\circ)} \right] = 2,975 \text{ m}^3/\text{m}$$

2. Calculate the critical discharge (q_c) based on threshold velocity from Equation (33).

$$q_c = \left(\frac{f_F u_c^3}{2g \sin \theta} \right) = \left[\frac{0.015 (4.23 \text{ m/s})^3}{2(9.815 \text{ m/s}^2) \sin(18.4^\circ)} \right] = 0.183 \text{ m}^3/\text{s}/\text{m}$$

3. Calculate the mean wave period (T_m) from Equation (35).

$$T_m = \frac{T_p}{1.1} = \frac{8.0\text{s}}{1.1} = 7.27\text{s}$$

4. Estimate the steady overflow discharge (q_s) associated with the levee freeboard (R_c) from Equation (66).

$$q_s = \left(\frac{2}{3}\right)^{3/2} \sqrt{g} (-R_c)^{3/2} = 0.5443 \sqrt{(9.815\text{ m/s}^2)} [-(-0.5\text{ m})]^{3/2} = 0.603\text{ m}^3/\text{s}/\text{m}$$

5. Estimate the combined wave overtopping and surge overflow average discharge (q_{ws}) using Equation (67).

$$\begin{aligned} q_{ws} &= \sqrt{g H_{m0}^3} \left[0.034 + 0.53 \left(\frac{-R_c}{H_{m0}} \right)^{1.58} \right] \\ &= \sqrt{(9.815\text{ m/s}^2)(2.0\text{ m})^3} \left[0.034 + 0.53 \left(\frac{-(-0.5\text{ m})}{2.0\text{ m}} \right)^{1.58} \right] = 0.83\text{ m}^3/\text{s}/\text{m} \end{aligned}$$

6. Calculate the wave volume cumulative probability distribution scale factor (c_v) from Equation (69).

$$c_v = 0.79 \cdot q_{ws} \cdot T_p = 0.79 (0.83\text{ m}^3/\text{s}/\text{m})(8.0\text{ s}) = 5.24\text{ m}^3/\text{m}$$

7. Calculate the wave volume cumulative probability distribution shape factor (b_v) from Equation (70).

$$\begin{aligned} b_v &= 15.7 \left(\frac{q_s}{g T_p H_{m0}} \right)^{0.35} - 2.3 \left(\frac{q_s}{\sqrt{g H_{m0}^3}} \right)^{0.79} \\ &= 15.7 \left(\frac{(0.603\text{ m}^3/\text{s}/\text{m})}{(9.815\text{ m/s}^2)(8.0\text{ s})(2.0\text{ m})} \right)^{0.35} - 2.3 \left(\frac{(0.603\text{ m}^3/\text{s}/\text{m})}{\sqrt{(9.815\text{ m/s}^2)(2.0\text{ m})^3}} \right)^{0.79} = 1.97 \end{aligned}$$

8. Calculate the total number of incident waves in the storm event (N_w) from Equation (48) and round down to the nearest integer. Because every wave overtops when the surge level is higher than the levee crown, the number

of overtopping waves (N_{ow}) equals the number of incident waves, and the probability of overtopping is unity (i.e., $P_{ov} = 1$).

$$N_w = N_{ov} = \frac{t_E}{T_m} = \frac{(4.0 \text{ hr})(3,600 \text{ s/hr})}{(7.27 \text{ s})} = 1,980.7 = 1,980 \text{ waves}$$

Monte Carlo simulation of the overtopping event

The following repetitive steps were computed for $N_{ow} = 1,980$ overtopping waves. The example below only shows calculations for step 100.

1. Using a random number generator, select an exceedance probability in the range ($0 < P_{VE} < 1$).

For this particular example, the random number generator produced the value of $P_{VE100} = 0.3371$ for the exceedance probability of the 100th overtopping wave in the sequence. This will be a relatively larger wave with only 1/3 of the waves being greater.

2. Calculate the volume (V_{W100}) for the individual wave using Equation (72).

$$V_{W100} = c_v [-\ln(P_{VE})]^{1/b_v} = (5.24 \text{ m}^3/\text{m})[-\ln(0.3371)]^{1/1.97} = 5.47 \text{ m}^3/\text{m}$$

3. Calculate the associated overtopping duration (T_{o100}) using Equation (73).

$$T_{o100} = 0.9 T_p \left(\frac{V_{W100}}{q_{ws} T_p} \right)^{3/5} = 0.9 (8.0 \text{ s}) \left(\frac{(5.47 \text{ m}^3/\text{m})}{(0.83 \text{ m}^3/\text{s/m})(8.0 \text{ s})} \right)^{3/5} = 6.41 \text{ s}$$

4. Calculate the excess wave volume as the term inside the summation of Equation (32). This is the contribution of the wave to the running cumulative total. Add this amount to the cumulative excess wave volume total (V_{ET}) in Equation (32). First check that

$$\frac{3 V_{W100}}{T_{o100}} > q_c \quad \text{or} \quad \frac{3(5.47 \text{ m}^3/\text{m})}{6.41 \text{ s}} = 2.56 \text{ m}^3/\text{s/m} > 0.183 \text{ m}^3/\text{s/m}$$

Thus, this wave contributes excess wave volume given as

$$\begin{aligned}
 V_{E100} &= V_{W100} \left[1 - \left(\frac{q_c T_{o100}}{V_{W100}} \right) + \frac{2}{3^{3/2}} \left(\frac{q_c T_{o100}}{V_{W100}} \right)^{3/2} \right] \\
 &= (5.47 \text{ m}^3/\text{m}) \left[1 - \left(\frac{(0.183 \text{ m}^3/\text{s/m})(6.41 \text{ s})}{5.47 \text{ m}^3/\text{m}} \right) + \frac{2}{3^{3/2}} \left(\frac{(0.183 \text{ m}^3/\text{s/m})(6.41 \text{ s})}{5.47 \text{ m}^3/\text{m}} \right)^{3/2} \right] \\
 &= 4.50 \text{ m}^3/\text{m}
 \end{aligned}$$

This calculation indicates that about 82% of the volume from the 100th overtopping wave contributed to the cumulative excess wave volume.

5. Terminate the calculation after processing N_{ow} waves.

This same procedure is followed for the rest of the waves, i.e.,

$$V_{ET}(t) = \sum_{n=1}^N V_{En} \leq \left(\frac{E_w}{K_w \beta_w} \right) \left(\frac{f_F}{2g \sin \theta} \right) \leq 2,975 \text{ m}^3/\text{m}$$

Results of the combined wave and surge overtopping example

Table 8 summarizes the calculation parameters for the above example in both SI and English units.

Figure 27 is a plot of the cumulative excess wave volume over the 4-hr duration of the specified storm event during which the surge level exceeded the levee crest by 0.5 m. Shown are the simulation results with average discharge closest to the specified value and limiting results from the 20 Monte Carlo simulations. The horizontal dashed line at a wave volume of 2,975 m³/m is the erosion damage index that represents the Hewlett et al. (1987) curve for open mats (see Figure 6). The no-damage threshold corresponding to open mats is also shown in Figure 27.

If we can believe the Hewlett et al. (1987) curve for open mats, this simulation indicated that the limiting state was reached after about 1.6 hours of the combined wave and surge overtopping event. Recall that elapsed event time is greater than the summation of all the individual overtopping wave durations. The cumulative excess wave volume is almost a straight line trend, even though the individual wave volumes varied according to the Weibull exceedance probability of Equation (71).

Table 8. Calculated parameters for combined wave and surge overtopping example.

Parameter	SI Units	English Units
Constant Parameters		
Erosion index	2,975 m ³ /m	32,023 ft ³ /ft
q_c	0.183 m ³ /s/m	1.97 cfs/ft
T_m	7.27 s	7.27 s
q_s	0.603 m ³ /s/m	6.49 cfs/ft
q_{ws}	0.83 m ³ /s/m	8.93 cfs/ft
c_v	5.24 m ³ /m	56.4 ft ³ /ft
b_v	1.97	1.97
N_W	1,980	1,980
N_{ow}	1,980	1,980
Parameters of 100th Overtopping Wave		
P_{VE100}	0.3371	0.3371
V_{W100}	5.47 m ³ /m	58.9 ft ³ /ft
T_{o100}	6.41 s	6.41 s
V_{E100}	4.50 m ³ /m	48.4 ft ³ /ft

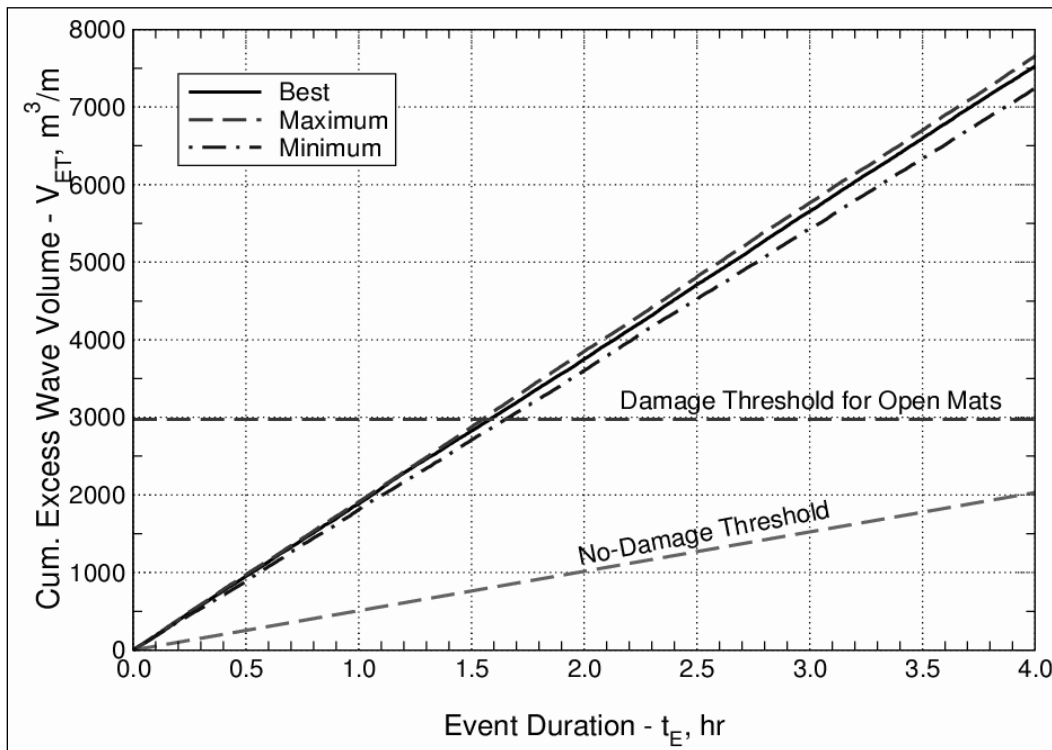


Figure 27. Results from the combined wave and surge overtopping example.

The time histories of individual wave volumes and corresponding overtopping durations are shown on the bar graphs of Figure 28 for one of the Monte Carlo simulations. The largest wave volume exceeded $15 \text{ m}^3/\text{m}$, but most volumes did not exceed 7 or $8 \text{ m}^3/\text{m}$. There very well may be physical constraints that prevent the highest predicted overtopping volumes to occur; but any constraints are presently unknown, and thus, not included in the random selection of overtopping volumes. Also, any grouping of larger waves is not captured by the simulation technique.

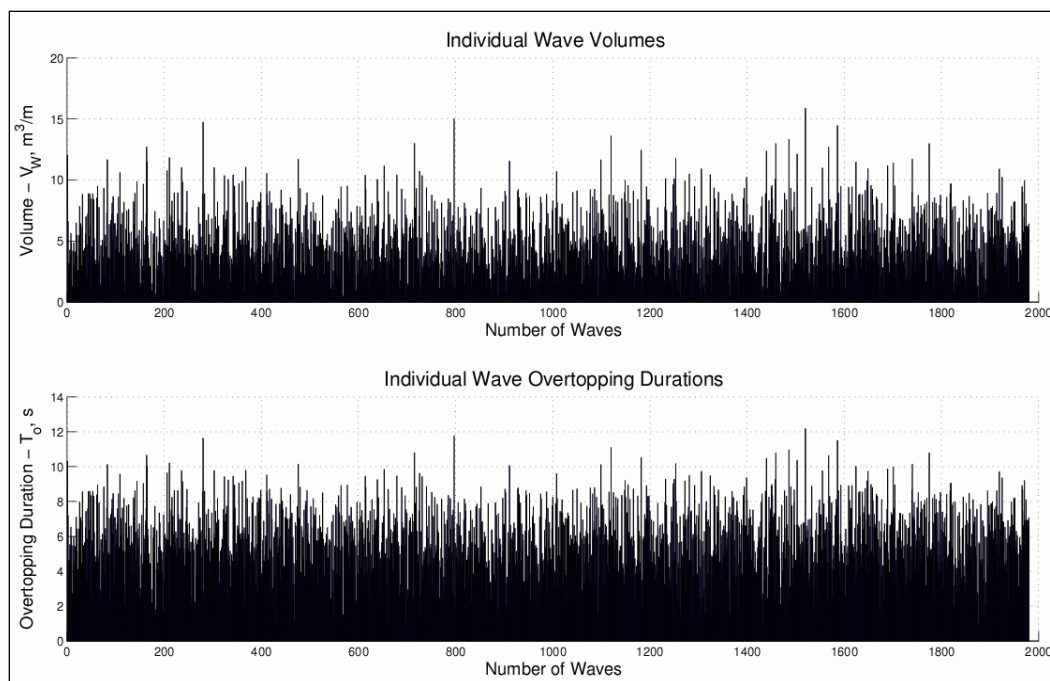


Figure 28. Time histories of wave volumes and durations for combined example.

Because the probability of overtopping, $P_{ov} = 1.0$, all of the 1,980 waves in this particular simulation overtopped the levee. The total summation of all individual wave overtopping durations was 3.1 hr. So during the 4-hr duration of the storm event, waves were overtopping just over 77 percent of the time. (As mentioned previously, the overtopping durations were evenly distributed over the 4-hr event duration for plotting purposes.) The average overtopping duration per wave was 5.6 s, whereas the mean incident wave period was 7.27 s. The smaller overtopping duration is due to the fact that overtopping does not occur during portions of the wave cycle when the wave trough level is below the levee crown elevation.

The equivalent limiting velocity of steady overflow on open mats is found easily from Equation (65) using the time-to-damage of 3.1 hr, i.e.,

$$u = \left[\left(\frac{E_W}{K_W \beta_W} \right) \frac{1}{t_F} + u_{c,W}^3 \right]^{1/3} = \left[\frac{1.231(10)^6 \text{ m}^3/\text{s}^2}{(1.6 \text{ hr})(3,600 \text{ s/hr})} + (4.23 \text{ m/s})^3 \right]^{1/3} = 6.6 \text{ m/s}$$

This limiting velocity corresponds to the dashed best-fit line shown in Figure 6 for open mats, and not the solid line that represents the original Hewlett et al. curve.

7 Application for Time-Varying Waves and Surge

Chapters 5 and 6 described the application of the concept of excess wave volume (or work) for the cases of wave-only overtopping and wave overtopping combined with steady surge overflow. Both of these cases were developed for a constant still water elevation. This short chapter illustrates how a real storm scenario with waves and surge levels that vary in time can be simulated as a series of discrete steps having relatively short durations. The procedure was coded using a MatLab[®] script.

Simulation method for time-varying waves and surge

It is proposed that simulation of a storm in which the wave parameters and the surge level (i.e., freeboard) vary in time can be accomplished by discretizing the storm surge hydrograph into a series of steps having durations of about one hour each. Using shorter step durations might be possible, but a shorter duration may impact the random selection of wave volumes from the distribution because the number of overtopping waves could become quite small. At each step, it is assumed that freeboard, significant wave height, and peak spectral wave period remain at the same constant values throughout the step.

Simulations are run for each discrete time step, and the cumulative excess wave volume (as represented by the best Monte Carlo simulation conducted at each step) is added to the value of the previous step. This results in a time history of cumulative excess wave volume over the entire duration of the modeled storm event.

Simulation of a hypothetical storm

The above-described procedure is best illustrated by an example. Table 9 lists time-varying storm parameters for a hypothetical hurricane. In this example the 9-hr duration of the storm centered on the storm peak is represented by discrete 1-hr steps. Figure 29 gives a graphical representation of the parameters listed in Table 9. A simulation was conducted of the hypothetical storm for a typical HSDRRS levee having a flood-side slope of 1-on-4 and landward-side slope of 1-on-3. Good grass was assumed as the protective cover. The simulation result is shown in Figure 30.

Table 9. Parameters for hypothetical time-varying hurricane.

Step Duration - Δt (hr)	Freeboard - R_c (m)	Wave Height - H_{m0} (m)	Peak Period - T_p (s)
1.0	3.50	1.5	6.0
1.0	3.00	1.5	6.0
1.0	2.50	2.0	7.0
1.0	2.25	2.5	8.0
1.0	2.00	3.0	8.0
1.0	2.25	2.5	8.0
1.0	2.50	2.0	7.0
1.0	3.00	1.5	6.0
1.0	3.50	1.5	6.0

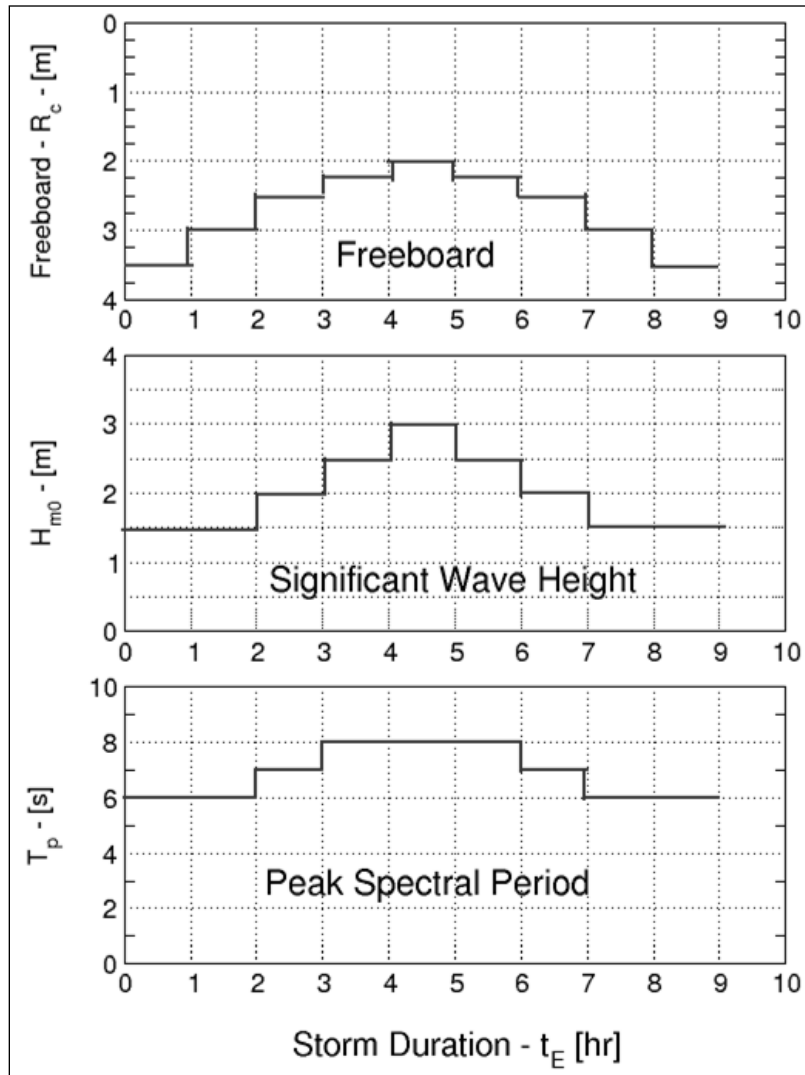


Figure 29. Storm parameters represented as discrete 1-hr steps.

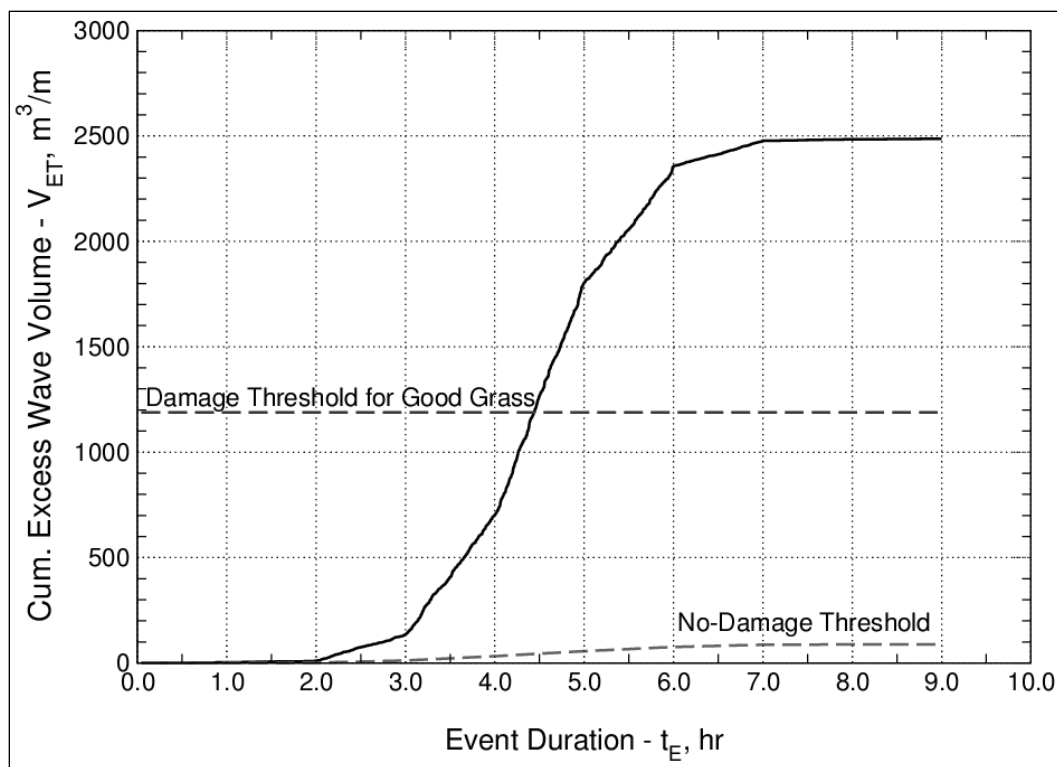


Figure 30. Result of hypothetical hurricane simulation for good grass.

The simulation shows that there was very little overtopping occurring during the first two hours and the last two hours when the conditions were the mildest. Beginning at about hour 3, overtopping became significant; and the excess wave volume accumulated at a fast rate. Cumulative excess wave volume exceeded the damage criterion (based on the Hewlett et al. 1987 steady overflow curves) for good grass right at the peak of the storm, and additional excess wave volume accumulation occurred after the peak of the storm while the small freeboard still allowed significant overtopping. If the good-grass damage threshold is representative of HSDRRS levees, then this hypothetical storm would have had another 2 or 3 hrs to erode the exposed underlying clay of the levee.

Figure 31 is a plot of all of the individual wave volumes and associated overtopping durations for the entire 9-hr simulation of the hypothetical storm. Notice the minor overtopping volumes at the far left and far right of the plot that occurred during the mildest portions of the simulation storm sequence.

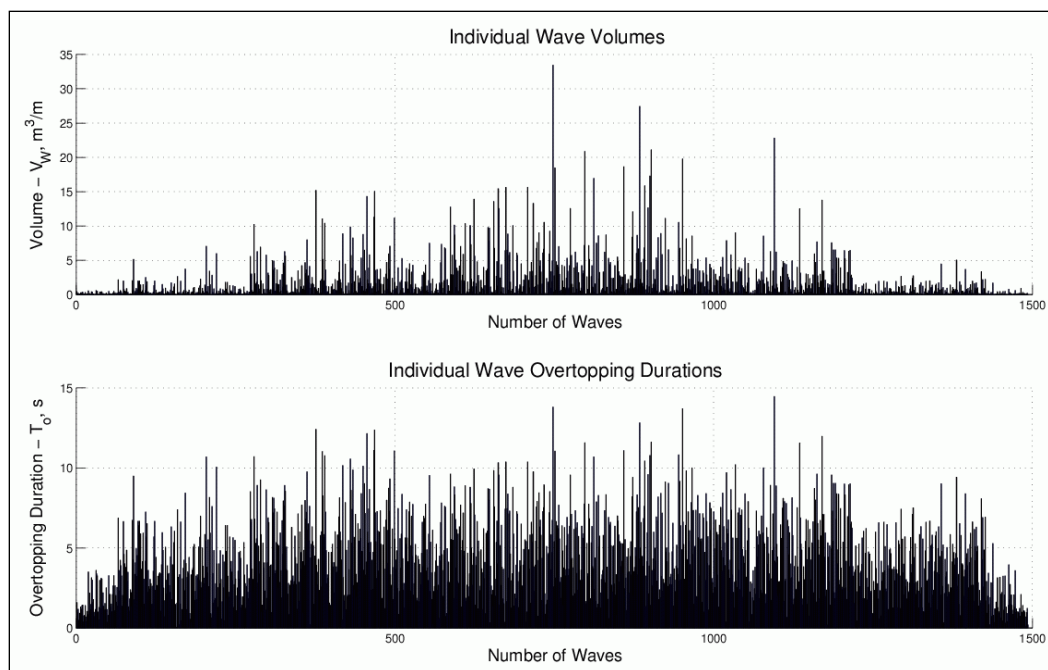


Figure 31. Individual wave volumes and overtopping durations for storm simulation.

Simulation variations due to slope protection types

The influence of the critical discharge parameter for the three different grass qualities was investigated by re-running the same simulation for average- and poor-quality grass. The result is shown in Figure 32. Generally, it can be surmised that the variation in q_c for the different grasses is relatively insignificant compared to the variation in erosional damage threshold. The variation between simulations is within the boundaries witnessed for the Monte Carlo simulation technique. This lack of difference is the result of the values of q_c for the different grasses (see Table 1) being quite small relative to typical velocities in overtopping waves.

However, the difference between q_c for grass and open mats is significant (threshold velocity = 1.8 m/s versus 4.2 m/s), and this does make a difference in simulation results. Figure 33 shows the result for an open mat using the same hypothetical storm example compared to the result for good grass. The cumulative excess wave volume is substantially less for the open mat because the critical threshold velocity for no damage is much higher for open mats. This simulation indicates that the levee protected with an open mat will survive the hypothetical storm with a good margin to spare. This result, of course, assumes that the damage threshold velocity for open mats is correct.

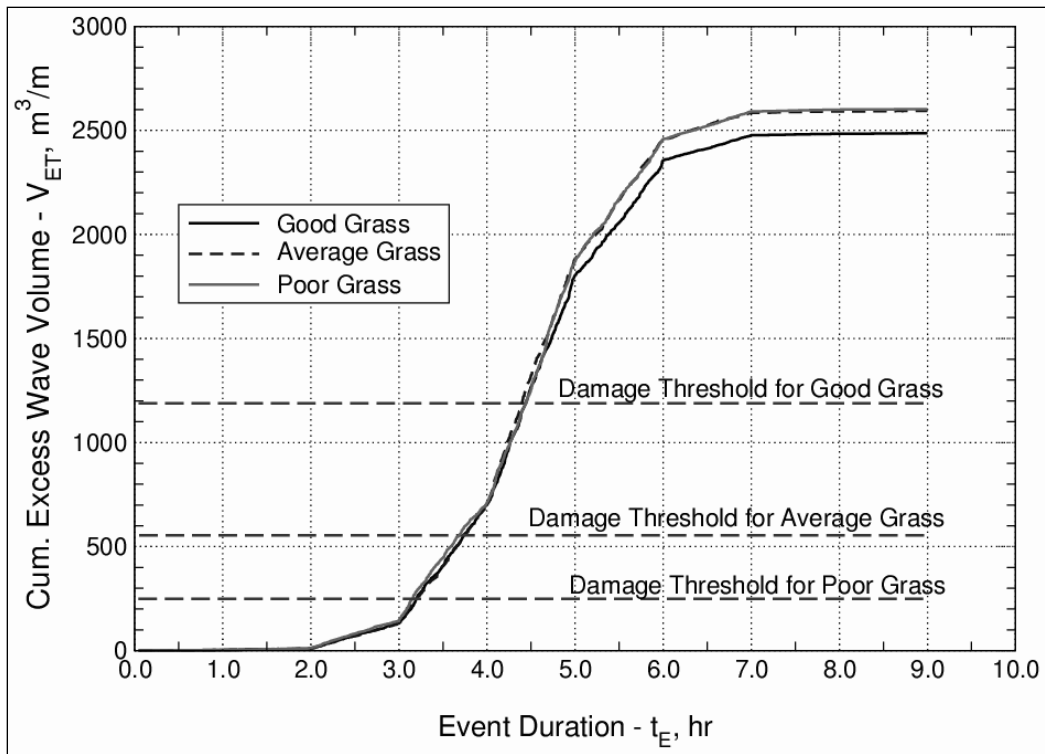


Figure 32. Variations between different grass qualities.

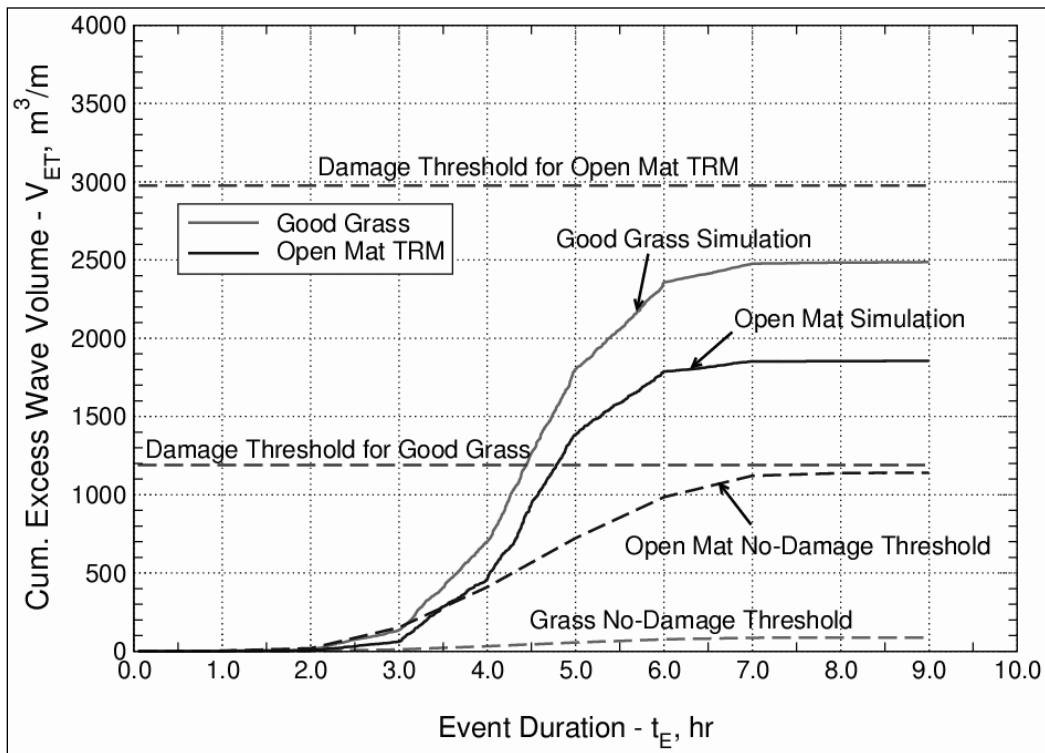


Figure 33. Comparison between good grass and open mat simulations.

8 Comparison of Methodology to Wave Overtopping Simulator Results

This chapter qualitatively compares the erosional equivalence methodology to field test results obtained in The Netherlands using the Wave Overtopping Simulator.

The Dutch Wave Overtopping Simulator

The Wave Overtopping Simulator (OTS) was invented in The Netherlands by Dr. Jentsje van der Meer (van der Meer, 2006). In simple terms, the OTS is a large water containment structure that is transported to an earthen dike and erected on the dike crest. A pump fills the OTS from a nearby water source, and at prescribed intervals the water is released so that it flows down the dike slope.

The OTS is designed and operated in a manner that simulates the periodic overtopping of waves. Each water release represents the volume of an individual overtopping wave with the approximately correct flow velocity and flow thickness at the leading edge of the released volume. A key advantage of the OTS is the capability of testing in-situ dike slopes at overtopping conditions that cannot be replicated by even the largest wave flumes. Figure 34 shows an earlier version of the OTS releasing a large water volume (14 m³) in just a few seconds. Notice the significant turbulence and air entrainment in the flowing water.

The sequence of released water volumes is such that the distribution of released volumes is the same as the distribution of individual overtopping wave volumes that would occur for a given storm condition and dike freeboard. In fact, the development used in this report to link the wave and surge parameters to the wave overtopping volumes and durations (Equations 34 - 58) are nearly the same equations used to operate the OTS. The levee overtopping test facility at Colorado State University uses a super-sized version of the OTS shown in Figure 34.

Van der Meer et al. (2008) summarized results after three years of Dutch field tests using the Wave Overtopping Simulator. An expanded version of the conference paper is given in van der Meer (2008). Their description



Figure 34. The Dutch Wave Overtopping Simulator in action (from van der Meer 2008).

included an overview of OTS operation, a listing of parameters of the design storm that was simulated by the OTS, and a discussion of the response of grass-covered slopes of dikes that were subjected to wave overtopping simulations.

Dutch overtopping simulator test conditions

In their summary paper, van der Meer et al. (2008) included a table that listed parameters of the individual overtopping wave distribution for the following conditions:

$$\begin{aligned}
 H_{m0} &= 2.0 \text{ m} \\
 T_p &= 5.66 \text{ s} \\
 \tan \alpha &= 1/4 \\
 q &= 0.1, 1.0, 10, 30, 50, 75, 100, 125 \text{ l/s/m} \\
 t_E &= 2.0 \text{ hr}
 \end{aligned}$$

The peak spectral wave period was determined from a wave steepness of $s_{op} = H_{m0}/L_{op} = 0.04$ with $L_{op} = (g/2\pi) \cdot (T_p)^2$.

These same conditions were simulated using the erosional equivalence procedure described in this report for three average overtopping

discharges to confirm that the erosional equivalence methodology produces approximately the same wave overtopping conditions as were used in the Dutch field tests. Table 10 shows the comparison.

Table 10. Comparison of wave overtopping parameters for three average discharges.

Parameter	van der Meer et al. (2008)	This report
q = 30 l/s/m (0.32 cfs/ft)		
Freeboard	2.03 m	2.01 m
Number of overtopping waves	561	514
Percent of overtopping waves	37%	37%
Maximum wave volume	3.79 m ³ /m	3.41 m ³ /m
q = 50 l/s/m (0.54 cfs/ft)		
Freeboard	1.76 m	1.74 m
Number of overtopping waves	720	660
Percent of overtopping waves	47%	47%
Maximum wave volume	5.18 m ³ /m	6.14 m ³ /m
q = 75 l/s/m (0.81 cfs/ft)		
Freeboard	1.54 m	1.53 m
Number of overtopping waves	858	785
Percent of overtopping waves	56%	56%
Maximum wave volume	6.75 m ³ /m	8.84 m ³ /m

Generally, the methodology produced similar parameters. The maximum wave volume listed for this methodology was the one associated with the Monte Carlo simulation having average wave overtopping discharge closest to the value specified. Variation of maximum volumes for all 20 simulations was substantial. However, if we believe that cumulative excess wave volume is governing the damage process, differences in the maximum wave volume should not be too critical.

Van der Meer et al. (2008) described all field tests performed during 2007 and 2008. The 2007 tests were limited to maximum average wave overtopping of $q = 50$ l/s/m (0.54 cfs/ft). In 2008, the OTS was enlarged to a capacity that allowed simulations up to $q = 75$ l/s/m (0.81 cfs/ft). The landward-side dike slope was usually 1-on-3, but there was one site with a slightly steeper landward-side slope of 1-on-2.5.

At each test site, the OTS simulated a sequence of overtopping events lasting six hours each ($t_E = 6$ hr). During each 6-hr segment the average overtopping discharge was kept constant, and then the average overtopping discharge level was increased for the next 6-hr segment. The progressively increasing average overtopping discharges were: 0.1, 1.0, 10.0, 30.0, 50.0, and 75.0 l/s/m. Thus, when a test reached the maximum average discharge of 75 l/s/m, the dike slope has already been subjected to 30 hrs of progressively larger wave overtopping conditions.

Comparison of the erosional equivalence methodology to OTS results

The erosional equivalence methodology assumes that the slope protection damage threshold is reached through an accumulation of excess wave volume (or flow work). Therefore, it seems logical that excess wave volume accumulated during the 6-hr steps with smaller average overtopping should be added to the total. In other words, it would not be correct to simulate only the 6-hr segment where $q = 50$ l/s/m when, in fact, excess wave volume could have been eroding the soil during the 6-hr segments when $q = 10$ and 30 l/s/m.

Figure 35 shows the aggregate composition of five 6-hr simulations, each at a progressively larger average overtopping discharge. Results from each step were added to produce a composite cumulative excess wave volume versus duration curve as described in the previous chapter. The particular segments shown in Figure 35 were computed for “good grass” (as defined by Dean et al. based on the Hewlett et al. curves) using the appropriate value of $u_c = 1.8$ m/s from Table 1 and a friction factor of $f_F = 0.015$. Similar curves were generated for average and poor grass with the smaller values of u_c , and it was found that the curves are very nearly the same (as demonstrated in Chapter 7). This indicates that the critical threshold velocity is not too important for the estimation of cumulative excess wave volume for the three grass types using the range of critical velocities determined from the Hewlett et al. (1987) curves. The cumulative wave volume curves will show a distinct difference when the critical velocity is larger, say in the range of 4 - 6 m/s.

Because of the minor differences in the resulting curves for the three grass types, it was permissible to show the damage threshold criteria for the three grass types on the same plot. These damage thresholds are shown by the horizontal dashed lines. As seen in Figure 35, the methodology predicts damage to poor grass at the end of the $q = 10$ l/s/m test segment, damage to

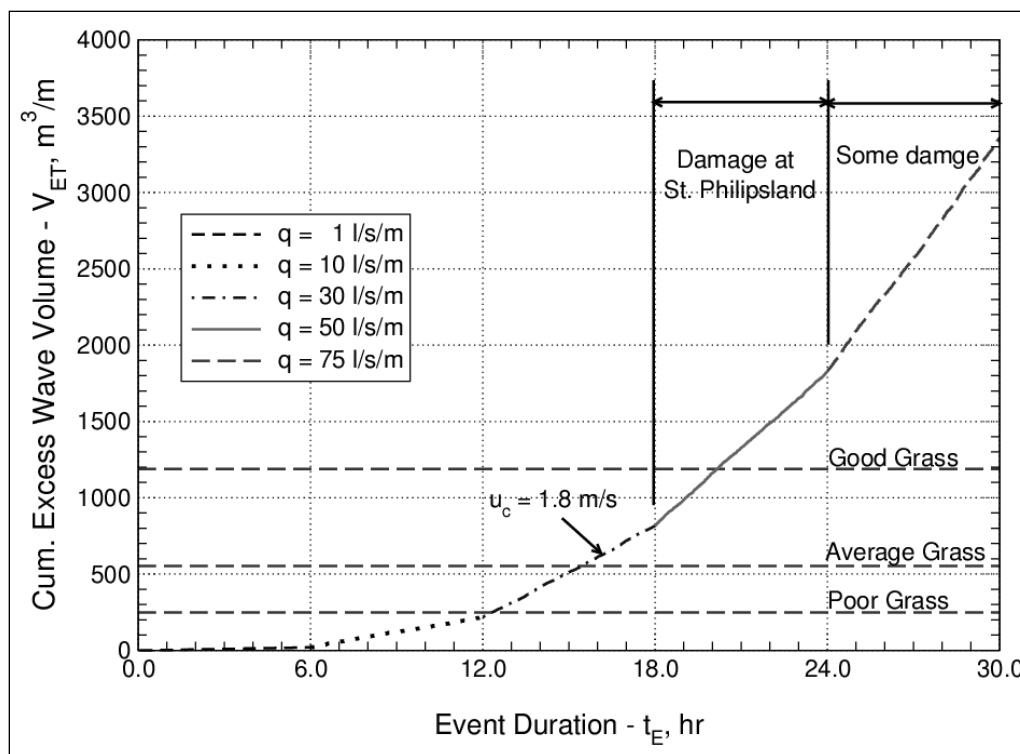


Figure 35. Wave Overtopping Simulator experiments.

average grass midway through the $q = 30$ l/s/m segment, and damage to good grass during the $q = 50$ l/s/m segment. Once again, the definition of damage is not precisely clear, and this issue has been addressed initially by van der Meer et al. (2010).

Figure 35 also indicates zones in which slope damage (or no damage) was documented during the Dutch OTS tests based on some of the general observations reported by van der Meer et al. (2008) and summarized below.

1. None of the grass-covered test sections showed significant damage during the 30 l/s/m segment (between 12 and 18 hrs in Figure 35). Figure 35 seems to be in agreement with this observation provided the grass could be considered better than “average.”
2. One test section (St. Philipsland) had significant damage at the $q = 50$ l/s/m overtopping level. This dike section was described as having a steeper landward-side slope (1-On-2.5) with a fairly open grass cover over sandy clay. (See the photograph in Figure 36.) According to the simulation, this damage was at the criterion for good grass, but it seems clear from the description that the St. Philipsland section would be more aptly classified as average or poor grass.



Figure 36. Slope damage at St. Philipsland after $q = 50$ l/s/m test (from van der Meer 2008).

3. At the highest average wave overtopping discharge of $q = 75$ l/s/m, some test sites had extensive damage, but a significant portion withstood the wave loading very well. From the simulation of Figure 35, it is seen that this portion of the test sequence had cumulative excess wave volume substantially higher than the Dean et al. (2010) damage criterion for good grass. Figure 37 shows the severely damaged slope at Boonweg, Friesland, after testing. The damage was thought to be caused by a loose soil layer under the sod that allowed water to collect beneath the sod. The vertical roots gave way, but the strong lateral thatching of the sod held together. This led to formation of a bubble-type soil structure that eventually was torn away by the overtopping waves (van der Meer, personal communication, 2010).
4. The most prevalent grass damage occurred at the transition between the dike slope and adjacent horizontal land. Significant damage occurred in 6 of the 9 tests, sometimes at $q = 30$ l/s/m, but especially at $q = 50$ l/s/m. This slope transition situation is not covered by the Hewlett et al. curves; and thus, is not yet incorporated into the erosional equivalence methodology. Erosion occurring at the transition at the toe of a solid clay levee must “head-cut” a long distance before damage to the levee crest (and possible breaching) could occur. Damage progression for a sand-core dike protected by a grass-covered clay layer will be somewhat different.

Figure 38 shows the entire sequence of individual wave volumes and overtopping durations that resulted from the simulations of the OTS stepped increases in average wave overtopping discharge.

Comparison using larger critical threshold velocity

Throughout this report the importance of critical threshold velocity to the cumulative excess wave volume calculation has become apparent. The values of u_c used in the previous section were those determined from the Dean et al. (2010) analysis of the Hewlett et al. (1987) limiting velocity versus duration curves. These threshold values might not be correct for wave overtopping, and it was demonstrated in Chapter 5 that higher threshold velocities yield differences in cumulative excess wave volume for the same discharge, but different wave heights. This seems rational.

Recent analysis of Dutch Wave Overtopping Simulator results by Dr. Jentsje van der Meer and colleagues (van der Meer et al. 2010) has indicated that critical threshold velocities associated with the initiation of erosion are significantly higher than those derived from the Hewlett et al. curves.



Figure 37. Slope damage at Boonweg after $q = 75$ l/s/m test (from van der Meer 2008).

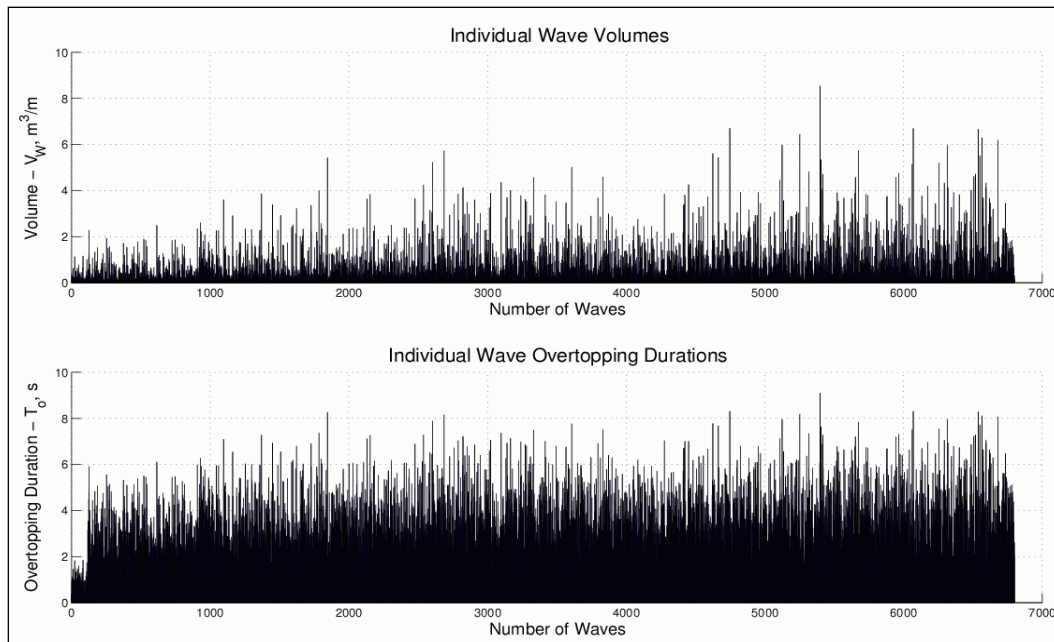


Figure 38. Individual wave volumes and overtopping durations for the OTS simulation.

Van der Meer et al. (2010) suggested that the threshold velocity at St. Philipsland was on the order of $u_c = 5$ m/s, almost 2.8 times greater than the value of 1.8 m/s used to generate the simulation shown in Figure 35.

Figure 39 shows a repeat simulation of the Overtopping Simulator test sequence with the only difference being an increase of the critical threshold velocity from $u_c = 1.8$ m/s to $u_c = 5.0$ m/s. The new simulation is shown by the solid (blue) curve. For comparison, the original simulation for the lower value of u_c is also included.

The new simulation indicates that the damage at St. Philipsland that occurred with the average discharge at 50 l/s/m (between hours 18 and 24) corresponds to the damage criterion for average grass. The damage threshold for good grass is near the end of the 6-hr period when the average discharge was 75 l/s/m.

The simulation with $u_c = 5.0$ m/s compares favorably with actual observed performance of Dutch dikes tested using the OTS. The fact that erosional damage limit thresholds established using the Hewlett et al. curves seem to correspond to OTS results may be coincidence, but at least these thresholds appear qualitatively correct for these specific sites. Refinement of both the critical threshold velocity and the erosional damage limit threshold will require additional testing and analyses.

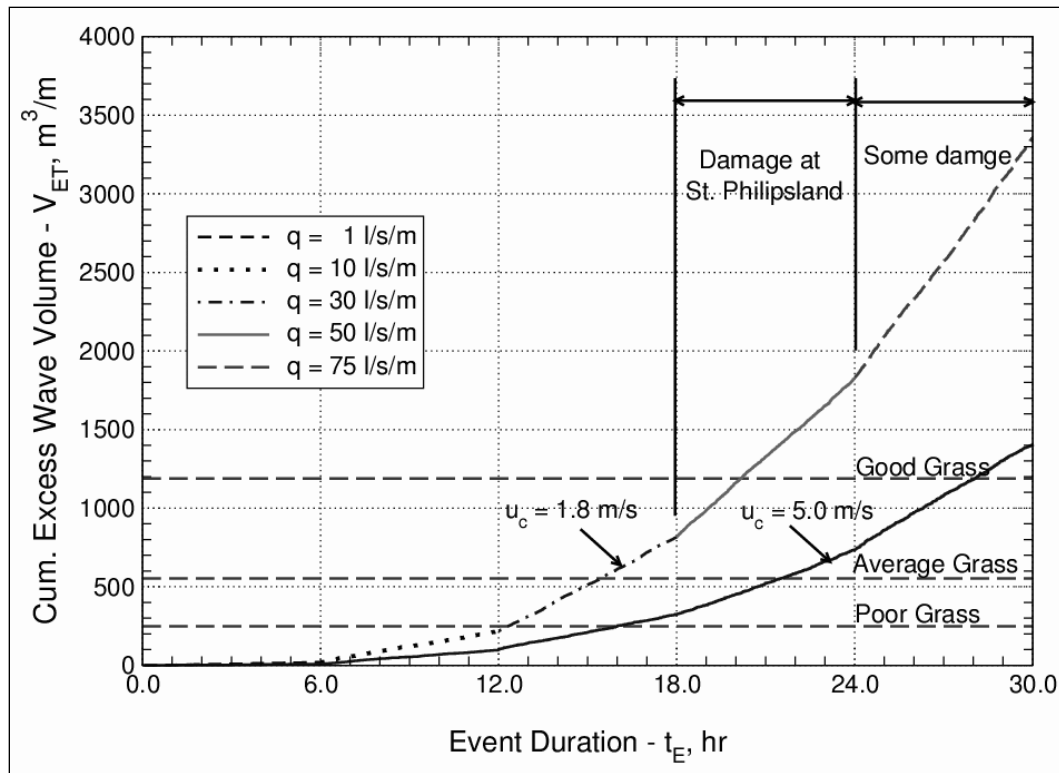


Figure 39. Wave Overtopping Simulator experiments with $u_c = 5.0$ m/s.

Dutch cumulative hydraulic load methodology

Concurrent to the original development of the erosional equivalence methodology by Dean et al. (2010), Dutch researchers led by Dr. Jentsje van der Meer developed a similar methodology independently for evaluating grass cover damage and dike resiliency. Van der Meer et al. (2010) proposed that dike erosion and damage results from accumulated “hydraulic loading” caused primarily by the impact by the leading edge of the overtopping wave. They expressed the concept of accumulated hydraulic loading by the following equation.

$$H_L = \sum_{n=1}^N (u_{p_n}^2 - u_c^2) \quad (74)$$

In Equation (74) the velocity u_p is the maximum (or peak) velocity at the leading edge of the individual overtopping waves, and u_c is the threshold velocity. Equation (74) is the summation of the hydraulic loading contribution from all overtopping waves. The cumulative hydraulic loading has units of velocity squared which is the same as specific energy

(energy or work per unit mass). Multiplying the hydraulic load by water density gives units of energy density (energy per unit volume).

Equation (74) is quite similar to Equation (8) that was proposed by Dean et al. (2010) as the erosional equivalence based on excess shear stress. However, Equation (74) uses the peak velocity of the individual waves rather than the average velocity, and it does not include the time associated with the overtopping. Van der Meer et al. (2010) observed that the duration over which the highest velocities in the overtopping wave exceeded the threshold velocity was on the order of 1-3 s, and this is quite a bit shorter than the total overtopping duration. Furthermore, this short interval appeared to be fairly consistent for all overtopping waves, and they stated that erosional damage was likely caused by the impact of the highest velocity over a short duration. For this reason, they dropped the time interval that is still included in the Dean et al. Equation (8).

One interpretation of Equation (74) is that cumulative hydraulic loading is similar to the accumulation of peak shear stress occurring over 1-s duration. In some sense, the Dutch cumulative hydraulic loading can also be thought of as “erosional equivalence” because the accumulation of hydraulic loading can be achieved by many different sets of overtopping conditions, all leading to the same result. So the cumulative hydraulic loading can be thought of as erosional equivalence based on excess specific energy or excess energy density at the peak of the wave, whereas the methodology described in this report is erosional equivalence based on excess work over the entire wave. In essence, the two methods are quite similar.

Van der Meer et al. (2010) used field observations from four different tests performed on dikes using the Wave Overtopping Simulator to determine appropriate values for the threshold velocity and the erosional limit in terms of cumulative hydraulic loading. They also considered four distinct damage levels that were identified as follows:

- First damage: First development of a small hole in the grass.
- Various damage locations: Grass cover damage at multiple locations.
- Failure: Loss of grass and sufficient clay erosion to expose the sand core (approximately 0.15 m for the specific site).
- Non-Failure: Some grass damage, but the clay layer was intact after testing.

Results of the analysis, as presented by van der Meer et al. (2010), indicated that a threshold velocity of $u_c = 4$ m/s gave the best cumulative hydraulic loading correspondence of the various damage criteria among the four different tests. Note that this velocity is significantly higher than the 1.8 m/s derived by Dean et al. for good grass. Cumulative hydraulic load limits were also given for each of the damage criteria.

Strictly, this calibration of the cumulative hydraulic loading methodology is valid only for the site tested by the Overtopping Simulator, but accumulation of additional test results will lead ultimately to generalized design guidance spanning a range of soil and grass conditions. This is precisely the type of calibration that is needed for the erosional equivalence based on excess wave volume.

Conclusions

Based on a comparison between actual field tests using the Dutch Wave Overtopping Simulator (van der Meer et al. 2008; van der Meer et al. 2010) and predictions based on the erosional equivalence methodology, it can be tentatively concluded that the critical threshold velocity determined from the Hewlett et al. (1987) curves for steady overflow limiting velocity are probably somewhat conservative. The Hewlett et al. curves are design recommendations, and they may have some conservatism included in the damage assessment. Another possibility is the Hewlett et al. data correspond to grass-covered flow channels with less compacted soils and/or grass species with less grass erosion resistance than typical soils and grass found on well-constructed dikes and levees.

The simulation of tested dike slopes in The Netherlands with $u_c = 1.8$ predicted that the dike slopes would experience damage at lower average overtopping discharge than they actually were able to withstand, assuming the erosional limit criteria of the methodology is correct. However, when the simulation was repeated with critical threshold velocity increased to a value of $u_c = 5.0$ m/s, the damage predicted by the erosional limit thresholds corresponded fairly well with the field observations. This is an important indication that the critical threshold velocity needs to be corrected using field and full-scale observations. Furthermore, the erosional limit threshold derived from the Hewlett et al. curves might be reasonable; but additional analyses of field and full-scale data are needed to assure that the good correspondence between the erosional damage limits and observed damage was not just coincidence.

Thus, the comparison between the Overtopping Simulator tests and the erosional equivalence methodology is similar enough to support the methodology and perhaps even justify using the erosional damage limit thresholds given by the Hewlett et al. curves. The Dutch cumulative hydraulic loading methodology, which is erosional equivalence based on excess energy density, was successfully calibrated to field data; and this encourages additional development and perhaps merging of the two techniques.

9 Uncertainties of the Methodology

This chapter briefly discusses the major uncertainties associated with the erosional equivalence methodology based on the steady overflow limiting velocity curves of Hewlett et al. (1987).

Assumed damage mechanism

The entire concept of the erosional equivalence methodology introduced by Dean et al. (2010), and developed herein, is based on the premise that erosion of the soil for a grass cover layer occurs whenever the flow velocity exceeds a critical threshold velocity. A certain amount of soil erosion is permissible; but at some point, the grass cover begins to lose enough grass that bare clay is exposed, and (by definition) damage of the grass cover occurs.

This damage mechanism has logic, and the development ties back to the classic steady overflow limiting velocity versus duration of Hewlett, et al. (1987). The erosional equivalence method also accounts for duration of overtopping by determining the cumulative amount of excess wave volume as a function of time. For example, grass covers capable of withstanding a certain level of overtopping for 4 hrs might experience damage after an additional 2 hrs of overtopping at the same intensity level. The cumulative aspect of the methodology also allows engineers to assess potential slope protection failure for a second hurricane striking before the grass can recover from the first hurricane.

In theory, the methodology predicts damage throughout the grass cover at the point where the accumulated excess wave volume surpasses the defined damage threshold. However, this would assume homogeneous soil/grass everywhere, and that is never the case. Instead, the damage occurs at localized weak spots on the levee slope, and some resulting percentage of bare soil was defined as the erosional damage threshold of the grass cover.

Whereas the erosional equivalence method makes a good deal of sense, there is still the possibility that other damage mechanisms might play important roles in the degradation of a grass cover layer. Overtopping waves are highly turbulent with a high percentage of entrained air. Soil

erosion and plant loss might be more a function of flow turbulent energy than the rate of flow work being done on the soil through shear stresses. If damage is tied to turbulence levels, then we would expect that larger overtopping wave volumes with greater turbulence would be more harmful. Therefore, the combination of high significant wave height and high freeboard would be worse than a combination of lower wave height and freeboard having the same average overtopping discharge because the former combination has more turbulent energy in the larger overtopping waves. Note, however, that this is entirely speculation at this point.

The erosional equivalence method does not distinguish between different wave height and freeboard combinations that produce the same average discharge when applied using the low values of critical threshold velocity derived from the Hewlett et al. curves (see Figure 22). However, there is a distinct difference between the combinations when larger values of threshold velocity are used (see Figure 23). Full-scale testing on Dutch dikes examined the grass response equivalent average discharge conditions corresponding to (1) high wave height and freeboard, and (2) low wave height and freeboard. These tests showed that the two conditions will evoke different responses when the threshold velocity is higher. Additional full-scale tests at Colorado State University (CSU) will possibly shed some additional insight into this question.

If turbulent flow intensity is the primary causative erosion force, the level of turbulence should be characterized adequately by the individual wave peak velocities (van der Meer, personal communication, 2010). Thus, the cumulative excess wave volume methodology would seem to capture the cumulative effect of turbulence level provided the critical threshold velocity and the erosional damage limit have been properly determined.

Another damage mechanism observed during Dutch tests of the Wave Overtopping Simulator was overtopping water being trapped between the grass and underlying soil after the vertical roots had given way. This created a bubble in the grass cover that soon was ripped off, forming the start of a major damage area. Whereas this is a real damage mechanism where the underlying soil was weak, it would be exceedingly hard to quantify and predict. The most likely occurrence would be at places where grass growing in the thin soil layer over a turf reinforcement mat failed to push roots through the mat.

For levees having a landward-side slope of 1-on-3 and milder, the risk of the grass cover sliding down the slope is not as great as it is on steeper slopes. However, slopes protected with TRMs may suffer a sudden slippage of the TRM if the mat has not been properly anchored and the grass has not been able to establish a healthy root system that penetrates through the mat into the underlying soil.

Finally, there is the possibility that grass cover damage is initiated in many cases by a single overtopping wave that just happens to exhibit the right combination of turbulence, impact, and force to rip a small portion of the grass cover out of place. This might be analogous to damage of a rubble-mound structure. Damage mechanisms based on a single (rogue?) wave are the most difficult to predict. In the case of rubble-mound structures, hundreds of tests are needed to derive a predictive capability. Furthermore, hundreds of levee overtopping tests could be conducted without actually simulating the singular damaging wave event.

In conclusion, there are multiple damage mechanisms that may act singularly or in concert to damage the overtopping slope protection. The damage mechanism tied to erosional equivalence methodology is certainly feasible and rational, but there is a risk that other damage mechanisms could be equally damaging. However, the erosional equivalence method provides an easy and rational method for evaluating potential levee damage for a wide range of input storm conditions. Furthermore, the method can be improved in the future as better full-scale overtopping response data become available.

Definitions of damage and failure

The calculation of cumulative excess wave volume as detailed in this report is relatively useless if there is no damage threshold with which it can be compared. The erosional equivalence methodology provides damage thresholds for three qualities of grass cover and two types of turf reinforcement mats. These damage criteria were derived directly from the limiting velocity versus duration curves provided in the report by Hewlett et al. (1987). Therefore, the criteria are linked directly to the definition of failure given by Hewlett et al. Failure for grass was defined as follows:

“The condition when soil is directly exposed to flowing water is classified as the onset of failure and is unacceptable.” (Hewlett et al. 1987)

The reason for this definition is that exposed soil erodes more rapidly, and gullies and head-cuts begin to form. Hewlett et al. defined mat failure as the point where the overlying grass cover erodes enough that mats can be uplifted by the flowing water.

The Hewlett et al. curves provided an initial provisional set of damage criteria, and it is fully expected that these criteria will be adjusted as full-scale overtopping tests conducted at CSU and on actual dikes become available. A key aspect of any criteria adjustment will be clear definitions of damage that are applicable for any type of slope protection used at any location throughout the HSDRRS. The damage levels described by van der Meer et al. (2010) provide a good start toward developing logical and consistent damage categories.

The HSDRRS levees are being rebuilt or strengthened using high-quality lean and fat clays compacted to a minimum of 90 percent at optimum water content. The percentage of sand is below 35 percent, and the bare clay is expected to have low erodibility characteristics if exposed to overtopping flows. Therefore, on landward-side slopes where the grass cover layer has been eroded at places and the clay exposed, the resiliency of the bare clay is expected to be quite substantial.

The Armoring Team of Task Force Hope has developed several definitions for the HSDRRS that will be used in the context of refining the erosional equivalence method using full-scale test results.

Failure: Breaching of a levee (or levee component such as a T-wall or transition) that causes catastrophic flooding.

Resiliency: Capability for any component of the HSDRRS to maintain its intended functionality without failure when subjected to overtopping forces greater than those of the design level. Damage can occur; but the damage should not interfere with the component functionality, and the damage should be repairable.

Damage: Degradation of the levee slope or component due to overtopping conditions either above or below the design level.

Decisions about whether or not to strengthen various reaches of the HSDRRS with armoring to provide protection beyond that provided by

grass will be based on the above definitions. Evaluation of the estimated degree of damage that could occur without additional protection will require that the erosional equivalence method have damage thresholds that conform to the above definitions. This will be difficult to achieve fully, and there will be some degree of uncertainty in any criteria developed.

The erosional equivalence method by itself cannot predict levee breaching. This has to be done using other predictive models; many of which are being developed, and none of which can be considered to be accurate, particularly for the clay levees of the HSDRRS. The erosional equivalence method should eventually be able to register some degree of resiliency based on further full-scale testing and practical field experience.

Presently, the methodology of this report has erosional damage limits derived from the steady overflow curves of Hewlett et al. The uncertainty of these damage thresholds relates to how they compare to the grass and soil used for the HSDRRS. Tests conducted with the Dutch Overtopping Simulator indicate that the damage criteria based on the Hewlett et al. curves is conservative, so this may indicate that the present methodology using the original critical threshold velocity and erosional damage limits will be conservative when applied to the HSDRRS.

Most likely, full-scale testing will provide multiple damage thresholds that can be incorporated into the methodology such as determined by van der Meer et al. (2010). The first damage level for grass-only cover might be when a certain percentage of the grass plants have been eroded in a localized area. A second damage level might be when bare clay is exposed over a certain percentage of the cover layer. A third level might be when an erosion hole of a given size develops, and a final damage level might be wide-scale loss of grass cover. For TRMs, we will probably have somewhat different damage thresholds that depend on how the TRMs perform and suffer damage. Initial damage will be related to loss of grass from the slope, and the more severe damage would be tearing or removal of the mat.

Once the grass cover or TRM is damaged, the underlying clay will experience erosion if overtopping conditions persist. The CSU tests using bare clay will provide an indication of erosion rate up to the depth of clay in the trays. It should be possible to incorporate this information into the methodology to give at least a rough estimate of resiliency beyond the loss of slope protection.

Even without any further improvements to the erosional equivalence methodology, the present damage thresholds for grass and open mats provide a means of comparative analysis for all reaches of the HSDRRS. This analysis would indicate which reaches will experience the greatest cumulative excess wave volume during overtopping; and thus, are in most need of additional slope protection beyond just grass.

Friction factors

The damage thresholds given in terms of m^3/m are directly proportional to the Fanning friction factor, f_F . As noted in Chapter 3, there is considerable uncertainty about the appropriate value for the friction factor because it changes with flow depth. Figure 24 in Chapter 5 gives an example of how the damage threshold changes with friction factor; however, there is some uncertainty regarding the validity of this plot.

When applying the methodology using the erosion damage limits and critical threshold velocities given in Tables 1 and 2, a friction factor must be specified. A value of $f_F = 0.015$ was deemed reasonable. As new full-scale data become available, it will be possible to determine values of the damage threshold and the critical discharge that include the friction factor in the empirical parameters. Thus, in the future there will be no need to specify friction factor so long as the levee surface is similar to the surface on which the empirical parameters are based.

Individual overtopping wave duration

Overtopping duration of individual waves is the other key piece of the erosional equivalence method. The equations of Bosman (2007) for wave-only overtopping and Hughes and Nadal (2009) for combined wave and surge overtopping appear to give reasonable overtopping durations based on the example simulations. Average overtopping durations were less than the average incident wave periods, as would be expected.

Effect of shorter overtopping durations

The following sensitivity analysis was performed to examine the effect of individual wave overtopping durations shorter than those predicted by Equation (56) or (58) for wave-only overtopping.

The total individual overtopping wave volume (per unit length of levee), given by Equation (24) and repeated here, is estimated as

$$V_w = \frac{q_p T_o}{(m+1)} = \frac{q_p T_o}{3} \quad (75)$$

where q_p is the peak discharge per unit length, and $m = 2$. The corresponding equation for estimating the excess wave volume per unit length, given by Equation (30) and repeated here, is estimated as

$$V_E = V_w \left[1 - 3 \left(\frac{q_c}{q_p} \right) + 2 \left(\frac{q_c}{q_p} \right)^{3/2} \right] \quad (76)$$

where q_c is the threshold discharge that can be equated to the critical threshold velocity by specifying a friction factor and assuming terminal flow. For a wave to contribute to the cumulative excess wave volume, the ratio q_c/q_p must be less than q .

Equation (75) gives the relationship between wave volume (V_w), peak discharge (q_p), and overtopping duration (T_o). For the same wave volume, a decrease in overtopping duration means there is a corresponding increase in peak discharge. This means that velocity and/or flow thickness must increase.

Consider two waves having equal volume, i.e.,

$$V_w = \frac{q_{p1} T_{o1}}{3} \quad \text{and} \quad V_w = \frac{q_{p2} T_{o2}}{3} \quad (77)$$

Let the overtopping duration of the second wave be some fraction, γ_T , of the first wave, i.e.,

$$T_{o2} = \gamma_T \cdot T_{o1} \quad (78)$$

For the case of equal wave volumes,

$$q_{p2} = \frac{q_{p1}}{\gamma_T} \quad (79)$$

The excess wave volume for each wave is given from Equation (76) as

$$V_{E1} = V_W \left[1 - 3 \left(\frac{q_c}{q_{p1}} \right) + 2 \left(\frac{q_c}{q_{p1}} \right)^{3/2} \right] \quad (80)$$

and

$$V_{E2} = V_W \left[1 - 3 \left(\frac{q_c \gamma_T}{q_{p1}} \right) + 2 \left(\frac{q_c \gamma_T}{q_{p1}} \right)^{3/2} \right] \quad (81)$$

In Equation (81) the peak discharge was substituted using Equation (79).

The non-dimensional difference in the excess wave volume due to the difference in overtopping duration is found as

$$\frac{\Delta V_E}{V_W} = \frac{(V_{E2} - V_{E1})}{V_W} = \left[3 \left(\frac{q_c}{q_{p1}} \right) (1 - \gamma_T) - 2 \left(\frac{q_c}{q_{p1}} \right)^{3/2} (1 - \gamma_T^{3/2}) \right] \quad (82)$$

The solution for Equation (82) is plotted in Figure 40 for the entire viable range of $0 < q_c/q_p < 1$ for values of the duration reduction factor, γ_T , between 0.5 and 0.9. The larger overtopping waves are to the left side of the plot, and the smaller waves are to the right. Waves with the ratio $q_c/q_p > 1$ do not contribute to the excess wave volume.

The difference increases as the duration fraction decreases, and the difference varies according to the size of the wave relative to the critical discharge, q_c . Thus, it is impossible to provide a single “percent difference” value for an overtopping event simulation because each overtopping wave has a different percent reduction.

As an illustration of the influence of reducing the individual wave overtopping durations, simulations were run using the Monte Carlo technique described in this report. The simulation parameters were the same as those used for the wave-only overtopping Example 1, as summarized in Table 4. The levee cover was assumed to be good grass.

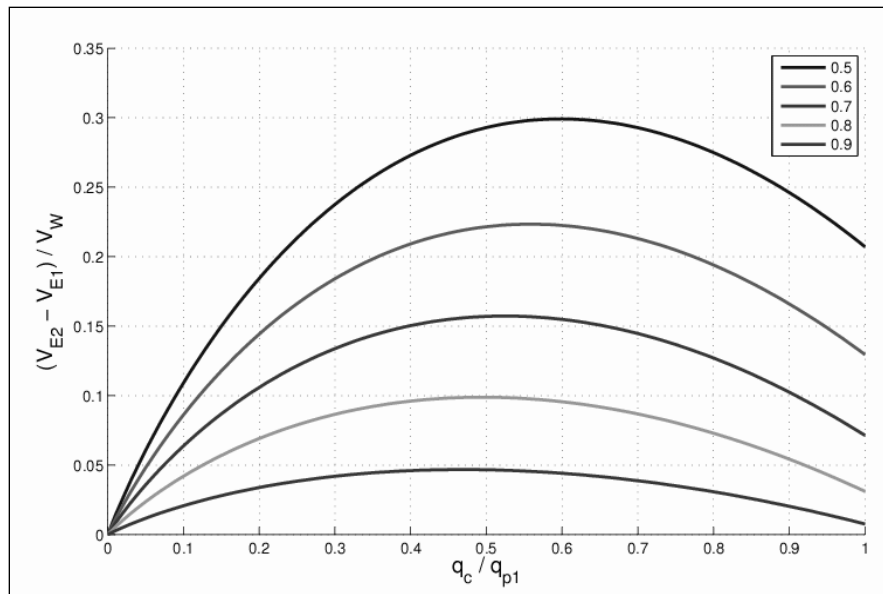


Figure 40. Difference due to overtopping duration reduction.

Case 1: Critical threshold velocity, $u_c = 1.8$ m/s

These simulations used the value of critical threshold velocity derived by Dean et al. (2010). This is considered to be a low threshold velocity, and nearly all of the waves had peak discharge greater than the critical discharge. Therefore, nearly all waves contributed substantially to the cumulative excess wave volume.

Two simulations were run. The first simulation used individual wave overtopping durations determined using the Bosman Equation (56). Figure 41 shows a time history of the computed overtopping durations. The mean overtopping duration was 4.86 s, whereas the mean period of the incident waves was about 7.27 s.

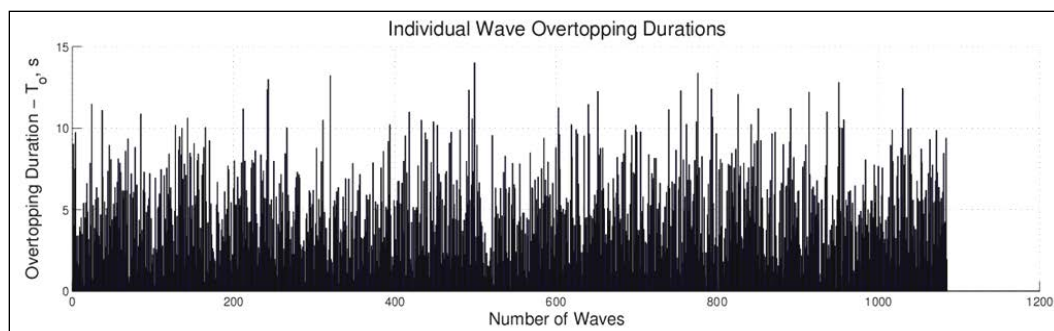


Figure 41. Wave periods from Bosman Equation (56) for Case 1 first run.

The second simulation used all of the same parameters, but the computed overtopping durations were halved. In other words, $\gamma_T = 0.5$ in Equation (81). The mean overtopping duration for the second simulation was 2.44 s, and the time history is shown in Figure 42.

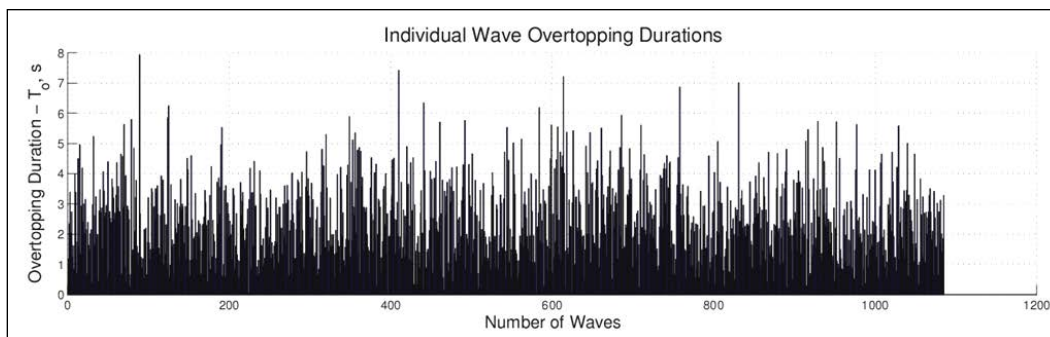


Figure 42. Wave periods from Bosman Equation (56) reduced using $\gamma_T = 0.5$ for Case 1.

Figure 43 compares the computed cumulative excess wave volume versus event duration for the two simulations. The solid line is the simulation that used the Bosman equation to estimate overtopping durations, and the dashed line is the simulation in which the overtopping durations were half of what the Bosman equation estimated.

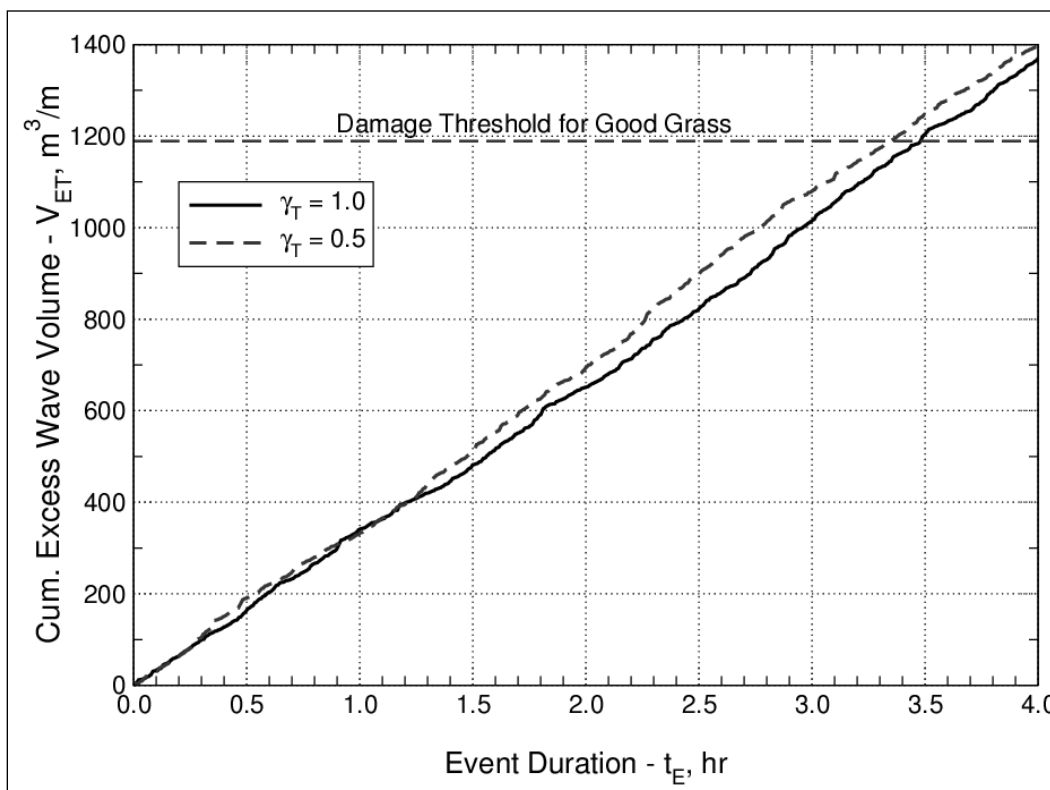


Figure 43. Cumulative excess wave volume estimates for $u_c = 1.8$ m/s.

There is some difference in the cumulative excess wave volume; but for the case of a low value of critical threshold velocity, this difference would not be considered significant. The relatively minor difference is caused by the fact that most of the overtopping waves had small values of the ratio q_c/q_p that correspond to less difference, as seen on the left-hand side of Figure 40. In other words, most of the wave volume turns out to be excess wave volume.

The rank-ordered values of q_c/q_p for the first simulation are shown in Figure 44. With the low critical discharge, only 12 of the 1085 overtopping waves did not contribute to the excess wave volume, and about 900 waves had values of q_c/q_p less than 0.1. Thus, most of the excess wave volumes varied between the two simulations by less than 10 percent as seen from the sensitivity analysis results of Figure 40.

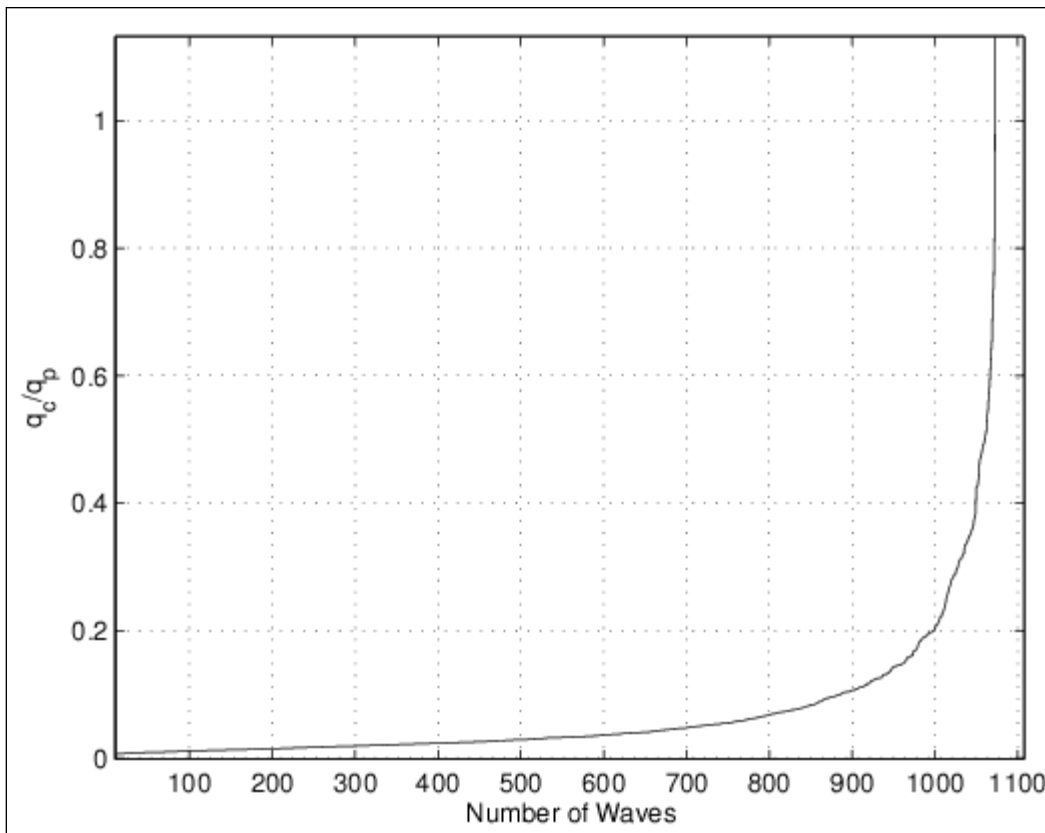


Figure 44. Rank-ordered values of q_c/q_p from the first Case 1 simulation.

The values of q_c/q_p from the second simulation with overtopping durations halved were very similar.

Case 2: Critical threshold velocity, $u_c = 5.0$ m/s

These simulations used a much higher value of critical threshold velocity than that derived by Dean et al. (2010). This critical velocity was suggested by Dr. van der Meer based on preliminary analysis of Dutch tests using the Wave Overtopping Simulator (van der Meer, personal communication, 2010). With such a relatively large critical velocity, many of the overtopping waves will not contribute at all to the excess wave volume because the peak discharge, q_p , will be less than the critical discharge, q_c . Because the peak discharge will increase as overtopping duration decreases, we should expect to see greater differences between simulations.

The same two simulations were run as in Case 1. The first simulation used individual wave overtopping durations determined using the Bosman Equation (56). The time history of the overtopping durations was nearly the same as for Case 1. The mean duration was 4.96 s, whereas the mean period of the incident waves was about 7.27 s. The second simulation used all of the same parameters, but the computed overtopping durations were halved. The mean overtopping duration for the second simulation was 2.43 s (same as Case 1).

Figure 45 compares the computed cumulative excess wave volume versus event duration for both simulations. As before, the solid line is the simulation that used the Bosman equation to estimate overtopping durations, and the dashed line is the simulation in which the overtopping durations were half of what the Bosman equation estimated.

This time there is substantial difference in the cumulative excess wave volume, and the second simulation with the shorter overtopping durations develops excess wave volume more rapidly. The shorter individual wave durations means that the overtopping wave forms are more peaked with more of the wave volume above the relatively high critical discharge threshold. Therefore, a greater percentage of the wave volume is contributed to the cumulative excess volume when compared to a wave with the same volume, but longer overtopping duration. As seen for Case 1, this effect is not dramatic when the critical discharge threshold is low, but Case 2 shows that overtopping duration is a significant factor when the critical discharge threshold is higher.

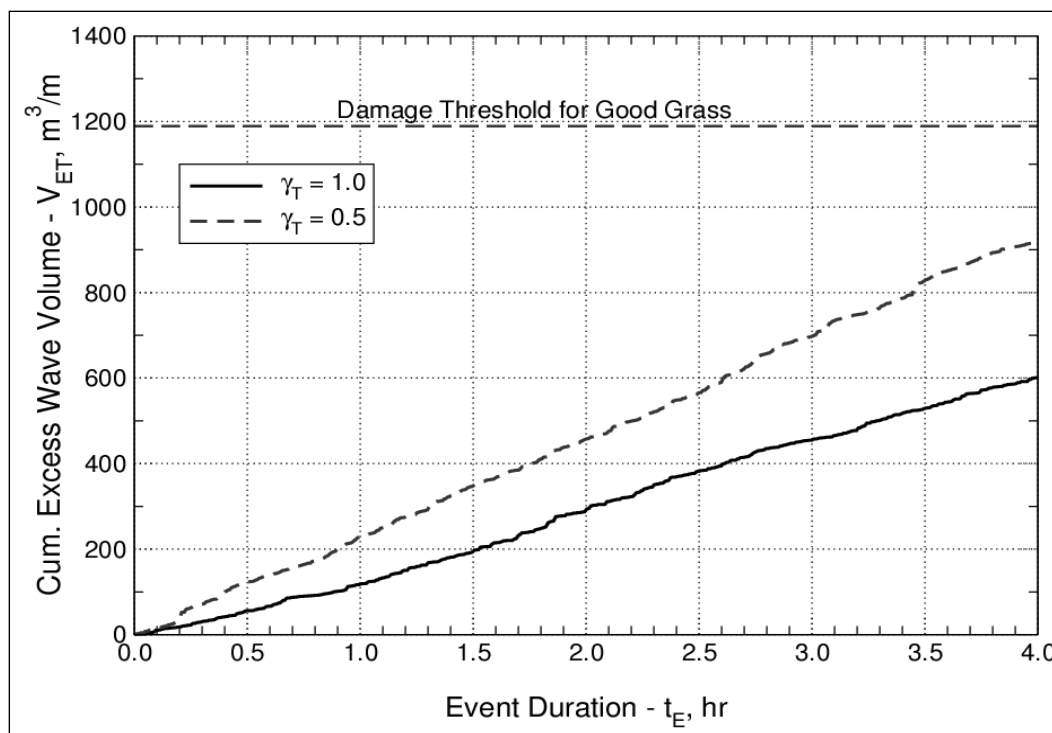


Figure 45. Cumulative excess wave volume estimates for $u_c = 5.0$ m/s.

The higher critical discharge threshold resulted in individual waves having significantly higher values of the ratio q_c/q_p as seen in the rank-order values shown in Figure 46 for the first simulation. The majority of the q_c/q_p -values are in the range of maximum difference seen on the sensitivity analysis of Figure 40. For the Case 2 simulations, about 700 of the 1085 waves contributed to the excess wave volume.

Finally, the higher critical discharge threshold used in Case 2 means that the accumulation of excess wave volume is slower than that seen for Case 1 (compare Figures 43 and 45). This is logical because a levee surface with greater resiliency to erosion should take longer to experience damage.

Conclusions

This simple sensitivity study examined the influence of individual wave overtopping durations on the cumulative excess wave volume (excess work) methodology. It showed that overtopping duration is definitely important when the critical threshold velocity (critical discharge) is high. We should expect high values of critical discharge for well-prepared and maintained levee and dike slopes. Individual wave overtopping durations are not as crucial for weaker levee slopes that have a low critical threshold velocity.

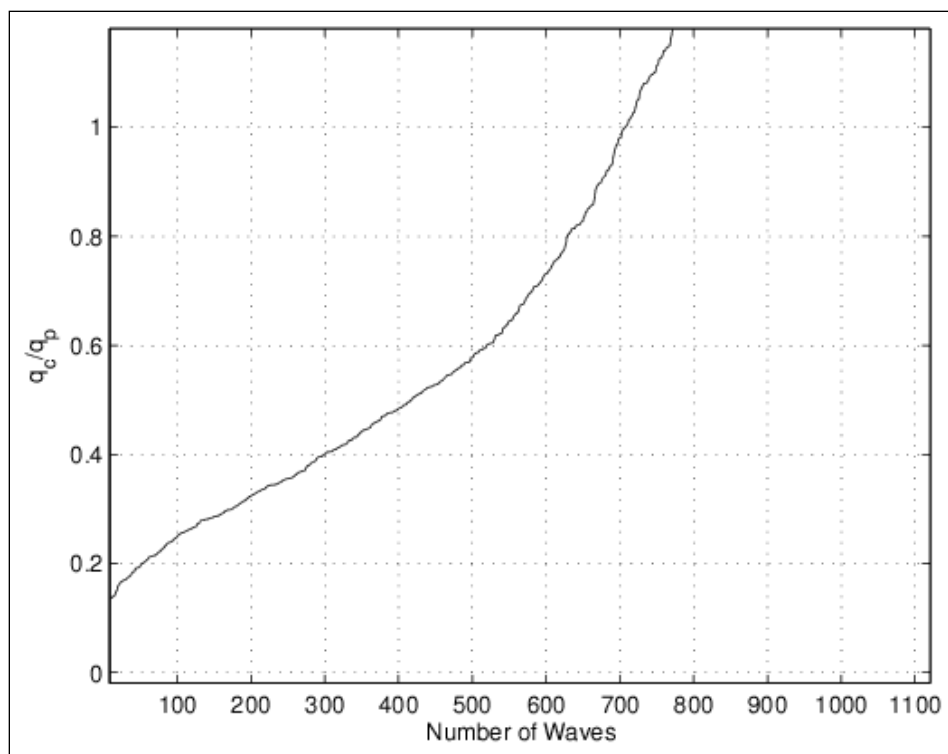


Figure 46. Rank-ordered values of q_c/q_p from the first Case 2 simulation.

Obviously, there is a need to examine/verify/improve the Bosman equation that has been tentatively adopted for use in the Corps' wave overtopping studies. First, the CSU overtopping simulator needs to produce overtopping conditions that replicate, to the greatest extent possible, the physics of intermittent wave overtopping. Second, the Monte Carlo simulation methodology, once calibrated using full-scale test results, needs an accurate estimation of individual wave overtopping durations to predict armoring requirements.

Other uncertainties

The other identified uncertainties are those related to prediction and probabilities of the storms expected to impact the HSDRRS, and the accuracy of the methods used to link storm parameters to wave overtopping. Storm prediction and probability of occurrence is well outside the scope of this study, and these topics are being addressed elsewhere.

The key elements for linking the incident wave conditions to the cumulative excess wave volume are the distribution of individual overtopping wave volumes and the associated overtopping durations.

(Overtopping durations were analyzed in the previous subsection.) The equations used for the overtopping wave distribution were established using laboratory experiments. The cumulative distribution equation for wave-only overtopping is used to program the Dutch Wave Overtopping Simulator.

The main uncertainty in the overtopping wave volume distribution is at the extreme tail of the distribution. This tail is critical for design of the Overtopping Simulator because it determines the maximum size of the water volume container. However, with the erosional equivalence method, estimating the rare extreme wave volume precisely is not crucial because of the cumulative nature of the method. If, on the other hand, we had a method in which damage was known to be initiated only by the largest waves; then correctly estimating the extreme tail would be critical.

Development of the methodology presented in this report centers on the concept of erosional equivalence between steady overflow and irregular wave overtopping. The equivalence is expressed in terms of cumulative excess wave volume (or work). There is uncertainty about whether or not the same magnitudes of critical threshold velocity and erosional damage limits determined for steady overflow are appropriate for wave overtopping. Physically, both situations involve turbulent flow on the levee slope, but the turbulence levels for wave overtopping will have significant variations within an overtopping wave and between different waves. Furthermore, the sudden flow acceleration at the overtopping wave leading edge might enhance the erosion processes. Because of these differences in erosion mechanics, we should not be surprised if the critical threshold velocity and/or the erosional damage limits are different for wave overtopping.

Finally, assumptions were made about the characteristic sawtooth shape of the time series of individual overtopping wave velocity, flow thickness, and discharge. This resulted in an equation for estimating excess wave volume above the no-damage (critical) discharge threshold. This characterization may not be entirely accurate, but it does give a slightly better accounting for excess wave volume than the difference between average discharge and critical discharge multiplied by the overtopping duration.

10 Improvement of the Methodology

Sensitivity analyses in previous chapters of this report have suggested that strict erosional equivalence between wave overtopping and steady overflow may not be valid because of different erosional flow physics. However, the overall concept of excess flow work remains sound; and the methodology framework described in this report does not have to be altered, it only needs to be calibrated for the particular situation.

The most productive improvements to the erosional equivalence methodology would be establishing reliable values for the critical threshold velocity (u_c) and the erosional limit ($E_w/(K_w\beta_w)$) for each of the protective levee alternatives (grass, TRMs, ACMs, and strengthened soil). The only values of these parameters presently available for use in the methodology are those that arise from the fitting of “excess work” curves to the Hewlett et al. (1987) limiting velocity curves. Appropriate values of critical threshold velocity and erosional limits need to be determined using results from full-scale tests using the Wave Overtopping Simulator, supplemented with field observations of HSDRRS levee performance during Hurricane Katrina. Some thoughts on how this could be achieved are given in the following sections.

Improvements based on Colorado State University testing program

A new test facility at Colorado State University has been outfitted with an improved Wave Overtopping Simulator (WOS) that is larger than previous machines. The increased WOS size permits the simulation of wave overtopping having values of average overtopping discharge substantially larger than previously tested. The new WOS also provides greater control on the release times for the individual wave volumes. This section discusses calibration of the erosional equivalence method based on WOS test results. Whereas the discussion centers on trays prepared for Task Force Hope, the general concepts apply for other similar types of overtopping tests using different soils and grasses.

Large tray sets (one straight tray and one bent tray) containing a 10-inch-thick layer of compacted clay protected by either grass or other slope protection alternative were placed in the CSU test facility and subjected to increasing levels of average discharge. Monitoring of the grass surface

during testing was intended to identify various thresholds related to the initiation and progression of damage to the levee protection. Figure 47 illustrates the placement of the two trays to replicate the landward-side slope of an earthen levee, and Figure 48 shows the CSU Overtopping Test Facility in operation.

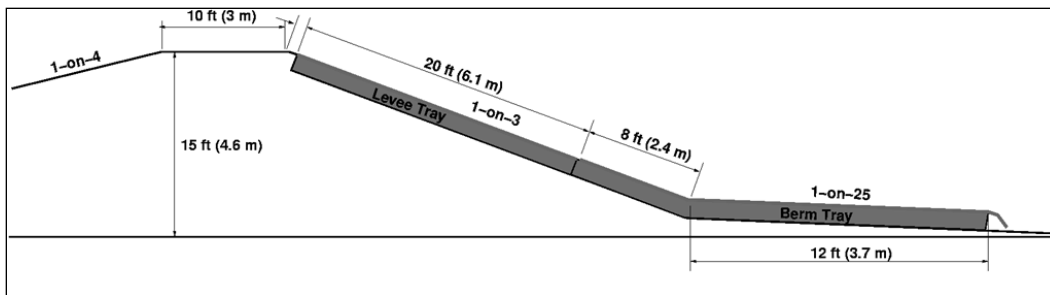


Figure 47. Dimensions and orientation of test trays.



Figure 48. Colorado State University Overtopping Test Facility.

Testing sequences

A wide variety of testing sequences is possible using the WOS. The discussion below focuses mainly on the testing sequence used for the first

test series run at CSU, and it was written prior to the start of those tests. Other testing sequences are equally viable, and the flexibility to alter the sequence based on initial results is imperative. The key objective of the testing (related to erosional equivalence) is to obtain the necessary information to calibrate the methodology for the specific type of grass or slope reinforcement installed in the test trays.

For a given wave condition, the WOS initially produced a 1-hr sequence of wave volumes representing an average overtopping discharge of 0.1 cfs/ft (9.3 l/s/m). This was followed by additional 1-hr sequences, each with the average discharge increased by some increment. At each stopping point, the slope was inspected for signs of erosion initiation and various stages of erosion damage (as yet undefined). The objective was for testing to be continued until the final damage state was reached.

Each of the slope protection alternatives was installed in two tray sets. This means that each protection alternative could be subjected to two independent test sequences. The first test sequence would produce the required average overtopping discharge hydrograph using a low wave height and low freeboard combination. The second test sequence would produce the same discharge hydrograph assuming a high wave height and high freeboard combination. Comparison of damage occurrence for the two tests would help answer the questions about wave height influence discussed in Chapter 5, and it will provide the basis for erosional equivalence calibration. Hopefully, the grass/soil quality between tray sets is consistent, and variations due to differences in how the average discharge hydrographs were produced would not be adversely affected by variations in grass/soil quality.

Acquired test information

For each step of the test sequence, the WOS is operated using a predetermined sequence of individual overtopping wave volumes and associated overtopping durations. These sequences can be directly applied in the erosional equivalence simulation methodology to determine the cumulative excess wave volume associated with a given critical threshold discharge (q_c). In other words, there is no need to develop a sequence of wave volumes by randomly sampling from the overtopping volume distribution because this is already known for each test.

Identification of damage on the slope (or at the transition between the levee slope and berm slope) and the time when damage occurred is the other crucial piece of information. The duration-to-damage is used to establish the appropriate value of the erosion damage limit associated with the wave volume sequence and the selected critical discharge threshold.

Additional acquired data included time series of measured flow depth and flow velocity on the levee crown and possibly at selected locations on the levee slope. Total discharge and average discharge are known a priori, and they can serve as validation of the instantaneous time series measurements.

Analysis of test results

During the analysis phase of the testing, the sequence of released volumes and corresponding overtopping durations are used to estimate the cumulative excess wave volume curve for the full-scale test using an assumed critical threshold discharge. The intersection of the curve with the time of damage yields a value for the erosional damage limit.

The problem with applying this procedure to only a single test is essentially having one equation with two unknowns. If we re-compute the cumulative excess wave volume curve for the same simulation using a different critical threshold discharge, a different value of erosional damage limit will result. And, we do not know which set of thresholds is correct. However, with results of two independent tests that simulated the discharge hydrograph using different wave height and freeboard combinations, it should be possible to select the critical threshold discharge to give nearly the same erosional damage limit for both tests. Van der Meer et al. (2010) achieved successful calibration of their cumulative hydraulic loading method in precisely this manner.

Once all of the tests are complete, it should be possible to assess the simulation results as a whole with the goal of developing rational and consist values for critical threshold discharge and erosional damage limit for each type of levee slope protection. This was expected to be a challenging task, and there is no guarantee that all tests will fit a concise and narrow trend. However, the values of the two key thresholds determined from the experiments that produce failure should provide improved reliability and predictive capability when applying the methodology of this report to analyses of levees. The ultimate goal is to assess the need for levee slope protection beyond that provided by grass-only covers.

Determination of the two key threshold parameters (q_c and erosional damage limit) directly from the full-scale tests alleviates the difficulty of having to specify a reasonable value for the friction factor. In essence, the friction factor would be implicitly included in the critical discharge threshold and the erosional damage limit. This means that the threshold parameters will be specific for the tested protection alternative. Given the potential sensitivity of the erosional damage limit to the friction factor (see Chapter 5), this will be a positive aspect of the proposed calibration of the erosional equivalence method.

Roadblocks

Potential roadblocks to calibration of the erosional equivalence methodology using full-scale test results include: (1) quantifying various damage progression states for the different slope protection alternatives; (2) identifying the initial erosion critical discharge; (3) differentiating between systematic and chaotic erosion variations; (4) limited number of test variations; and (5) not reaching the unacceptable damage level because of strong grass covers with robust erosion resistance that is stronger than the loading that can be produced by the WOS.

Damage to the levee protection alternatives will depend on local weaknesses in the grass and soil, and these weaknesses are not expected to be consistent between the different tray sets. Thus, initiation and progression of damage on one tray set will probably be somewhat different on the other tray set having the same levee protection installed. Hopefully, the soil and grass have been prepared with enough uniformity to minimize these expected differences.

Trays with TRMs installed will be more difficult to damage, and the damage (if it occurs) could progress in two phases. The first phase would be loss of soil and grass plants as overtopping increases. The second phase might be mechanical failure of the TRM that exposes the underlying bare soil to erosion. Mechanical failure of the TRM will likely be different between the types of TRM being tested.

With only two tests being conducted for each unique type of slope protection, the robustness of the calibration is fragile. For this reason, we should provide a reasonable factor of safety to the methodology if it is applied to the HSDRRS to allow for experiment anomalies.

Postscript on the 2010 CSU Wave Overtopping Simulator tests

Between the first and second drafts of this report, testing was completed on the tray sets designed to represent the HSDRRS levees. Details of the testing and testing results are not discussed here, but the main finding was that the grass/clay prepared in the test trays had very high erosion resistance. Testing in the WOS subjected the grass surfaces to many hours of wave overtopping having average overtopping discharges greater than 3 and 4 ft³/s per ft (0.28 and 0.37 m³/s per m). The grass slopes showed little if any damage, and never was bare clay exposed anywhere on the levee grass surface. This astounding grass performance was entirely unexpected, and initial thoughts attribute the grass strength to its dense root structure and the thatching between grass stems.

The erosional equivalence methodology cannot be effectively calibrated with these test results because failure was never reached during any of the testing. It is possible to estimate the rate of excess wave volume accumulation for assumed values of threshold velocity and friction factor, but this accumulation far exceeds the erosional limits based on the Dean et al. analysis of the Hewlett et al. curves. Lacking accurate calibration, the most effective use of the erosional equivalence methodology would be performing a comparative analysis for the different levee reaches in the HSDRRS, and using the methodology to help determine appropriate safety factors to accommodate lesser-quality grass covers.

Improvements based on Hurricane Katrina observations

Dean et al. (2010) suggested in their paper that the validity of the erosional equivalence method could be improved by examining the performance of the HSDRRS levee system during Hurricane Katrina. Sufficient information to complete this evaluation may be available in reports compiled by the Interagency Performance Evaluation Task Force (IPET) and other sources in the New Orleans District.

The basic idea would be to calculate the cumulative excess wave volume curve as a function of time for various reaches of the HSDRRS. For each reach the necessary input information has already been hindcast using numerical models. This includes the time histories of storm surge (freeboard) and incident wave characteristics (H_{m0} and T_p). Initially, the values of critical threshold velocity and erosional limit derived from the Hewlett et al. curves would be applied in the calculations.

The estimates of cumulative excess wave volume for selected reaches would be assessed in terms of observed damage for that reach. Damage at locations where the levees were constructed of sandy, hydraulically-placed soils would not be very useful because the HSDRRS will not use these types of soil in construction. Selected reaches would have to have good soil and grass quality, but still have suffered damage due to large overtopping discharge. If enough candidate sites are analyzed, a trend might become apparent with the erosional equivalence method giving relative indications of when slope damage occurred. The final step would be an iterative manipulation of the critical discharge threshold parameter (where justified) to develop some rational consistency between the quality of levee protection afforded by various grass covers and the erosional damage thresholds.

There is no guarantee that such an analysis would produce definitive results; but on the other hand, the Hurricane Katrina observations could significantly help to improve the validity of the erosional equivalence method and lend confidence to the predictions.

Improvements based on Dutch overtopping simulator results

Dutch researchers have been testing the strength of in-situ dikes for over three years using progressively larger versions of the Wave Overtopping Simulator invented by Dr. Jentsje van der Meer. Testing has ranged from dikes protected with high-quality clay and fairly long grass stems to dikes constructed with sandier soils. Although dike construction and grass maintenance in The Netherlands may be different in some aspects as compared to the HSDRRS, there are enough similarities in soil and grass specifications to warrant looking at the Dutch results.

Once data become available from the Dutch OTS tests, the same analysis proposed for the Colorado State University full-scale test results could be applied to the Dutch test results. The Dutch OTS was operated in a manner similar to what was used in the CSU tests, so that application of the erosional equivalence methodology should not be challenging.

Appropriate values for the critical threshold discharge and the erosional damage limits determined for Dutch test results might not be applicable to the grass species and construction methods used for the HSDRRS. Nevertheless, the grass on some Dutch dikes may have similar characteristics to New Orleans grass, and this would supply at least some validity to the erosional equivalence methodology. In addition, it would be possible to

examine similarities and differences between the excess work (this report) and the excess energy density (Dutch) versions of the erosional equivalence methods.

Summary

The erosional equivalence methodology could be applied using the thresholds developed from the steady overflow limiting velocity curves of Hewlett et al. (1987). However, rational adjustment of the critical discharge thresholds and the erosional damage limits based on full-scale testing and possibly Hurricane Katrina field observations is needed to improve the methodology and make it more reliable for the specific grass covers of the HSDRRS. This is critical for three reasons: (1) accurate estimates of levee landward-side resiliency and potential damage due to overtopping could potentially save millions of dollars in levee armoring costs; (2) the methodology must be able to withstand technical scrutiny and challenges; and most importantly, (3) the people and property landward of the levees must be protected.

11 Summary and Conclusions

Summary

This report describes a rational methodology for evaluating the strength and resiliency of earthen levee protection against wave overtopping forces during severe hurricanes. The new methodology was developed by applying and extending the concept of “cumulative excess work” originally proposed by Dean et al. (2010). They hypothesized that damage to grass-covered slopes was caused by cumulative work done by the overtopping waves on the levee slope, in excess of some tolerable work level. Once the initiation of erosion threshold has been exceeded during an overtopping event, there is a certain amount of allowable erosion that can occur without causing damage to the slope protection. However, if overtopping persists, at some point the cumulative erosion results in slope damage.

Dean et al. (2010) analyzed the allowable steady overflow curves of Hewlett et al. (1987) that give limiting flow velocity as a function of flow duration. Dean et al. tested whether the shape of the Hewlett et al. curves was best explained in terms of excess velocity above a critical threshold, excess shear stress above a critical threshold, or excess flow work above a critical threshold. Their best-fit analyses suggested that excess flow work best explained the loading versus duration characteristics of the Hewlett et al. curves. Dean et al. (2010) adapted the excess work concept for intermittent wave overtopping, and they gave two examples illustrating application of the methodology to earthen levees.

In this report, the “erosional equivalence” methodology of Dean et al. (2010) has been extended and adapted for use in analyzing the levees in the Hurricane Storm Damage Risk Reduction System (HSDRRS). The characteristic sawtooth shape of individual overtopping wave velocity and flow thickness variations in time was idealized so that a mathematical expression could be developed for the time variation of instantaneous discharge. This allowed a reasonably accurate estimation of the excess wave volume above a critical threshold discharge for each overtopping wave. Multiplication of excess wave volume by unit weight of water gives excess work. The cumulative excess wave volume is simply the summation of the contributions for all the individual overtopping waves.

A predictive capability for estimating the cumulative excess wave volume (or excess work) as a function of time for prescribed wave, surge, and levee parameters was developed for the case of wave-only overtopping. For a given significant wave height, peak spectral wave period, levee freeboard, and flood-side levee slope, accepted empirical equations are used to estimate wave runup, average overtopping discharge, and the distribution of overtopping wave volumes. The sequence of overtopping wave volumes is simulated by randomly sampling the calculated wave volume cumulative distribution similar to the Monte Carlo method. Associated overtopping durations for each wave are also estimated, and the cumulative excess wave volume as a function of storm event duration is calculated. The best procedure is to perform the calculations for several simulations, and then select the simulation that comes closest to matching the target average wave overtopping discharge. Application of the methodology for wave-only overtopping was illustrated by a worked example.

The influence of several key parameters was explored by performing simulations using the values of critical threshold velocity and erosional damage limit derived from the steady overflow curves of Hewlett et al. (1987). It was noted that the assumed value for friction factor affects the erosional damage limit, so it would be best if further calibration of the methodology include friction factor implicitly. There appeared to be little difference between the cumulative excess wave volume curves created using different wave height and freeboard combinations that produced the same average overtopping discharge. However, this was due to using a relatively small value for the critical threshold velocity ($u_c = 1.8$ m/s). When the critical velocity was increased to 4 m/s, a pronounced difference between simulations occurred.

The erosional equivalence predictive method was also developed for the case of combined wave overtopping and steady overflow that occurs when the still water elevation exceeds the levee crown elevation. This method uses a slightly different set of equations for representing the distribution of individual wave volumes and overtopping durations; but for the most part, the same steps are followed in the Monte Carlo simulations. Application of the methodology for combined wave and surge overtopping was illustrated with a worked example.

The erosional equivalence methodology was applied in a step-wise manner to simulate the realistic case of storm surge and incident storm wave

characteristics that vary in time. It was assumed that storm surge and wave parameters remained constant in one-hour increments before increasing or decreasing to the next step.

Descriptions and provisional results from the Dutch testing of actual dike slopes using the Wave Overtopping Simulator (OTS) provided insight into the progression of slope damage. The sequence of progressively larger average discharges used during the OTS tests was simulated using the erosional equivalence methodology. According to the simulations, the erosional damage limit should have been reached earlier than what actually transpired during field testing. In other words, the Dutch dikes were stronger than predicted using the methodology with critical threshold velocity of $u_c = 1.8$ m/s. However, Dr. Jentsje van der Meer (leader of the Dutch testing) indicated that they believe the critical threshold velocity is around $u_c = 5.0$ m/s. When the simulation was repeated with the higher value of u_c , the predicted damage showed much better correspondence to observed field damage at two locations.

There are several uncertainties in the erosional equivalence predictive methodology. One uncertainty pertains to how we define the conditions of initial erosion, damage progression, and damage limit for the various types of levee slope protection. Another uncertainty is whether or not the physical processes causing damage for wave overtopping are similar to the damage processes for steady overflow. The turbulence levels in overtopping waves are higher, and this could accelerate the erosion processes. The key uncertainty is using the values of critical threshold velocity and erosional damage limit derived for steady overflow. These important thresholds will need to be adjusted based on full-scale testing and analysis of field observations. Further discussion of the uncertainties is given in the following section.

The erosional equivalence methodology should be improved and extended using results from full-scale testing at Colorado State University. The proposed testing procedures lend themselves to calibration of the methodology using the limited data that will come from the tests. The resulting improvement should provide better simulations that more accurately depict the erosional resistance of the HSDRRS levees and the robustness of the various armoring alternatives to be tested as CSU.

Additional improvement of the erosional equivalence methodology might be achieved by a post-mortem examination of the levee performance during Hurricane Katrina. Estimation of the cumulative excess wave volume function using Hurricane Katrina hindcast wave and surge parameters would provide a basis for looking at levee performance for specific reaches of the HSDRRS. These comparisons could help to further adjust the prediction methodology to reflect the damage limits with better reliability. Also, analysis of the Dutch OTS experiment data would also be very beneficial.

Caveats and uncertainties

The erosional equivalence method is based on the capability of the slope protection to resist the cumulative excess work being done on the slope by the overtopping waves. The methodology, as developed in this report, gives predictions that can be used to assess the need for additional levee armoring beyond the protection provided by grass-only covers. However, application of the methodology should be made only after careful consideration of the following caveats and uncertainties.

1. The predictive methodology presented in this report initially uses thresholds for initiation of erosion and the onset of damage that were derived from limiting velocity versus duration curves for stability of grass slopes exposed to steady overflow. Application of these steady overflow thresholds to unsteady overtopping by irregular waves assumes an “erosional equivalence” between the two diverse types of hydrodynamic loading, and there is uncertainty about the veracity of these thresholds. Fortunately, the methodology developed here can be adjusted using more reliable thresholds for the initiation of erosion and onset of damage that arise from full-scale wave overtopping tests at the CSU facility and from field observations.
2. In adapting the thresholds suitable for steady overflow, the erosional equivalence methodology implicitly assumes that similar physical processes are dominating the initiation of soil erosion, progression of erosion, and the type of damage for intermittent wave overtopping. This may not be the case. Dutch researchers have commented that turbulence intensity is higher in overtopping waves, and turbulence may be more important to the erosional processes than flow work or shear stress. Also, there is abrupt flow acceleration at the leading edge of the overtopping waves that could contribute to the degradation of the slope and tearing loose of grass plants through some impact mechanism. Nevertheless, the

- turbulent intensity in an overtopping wave might be well represented by the excess wave volume. In other words, there is hope that the excess wave volume (excess flow work) accumulation is proportional to the excess turbulent energy levels in overtopping waves.
3. Weak spots on levee grass cover will exist because no grass surface can be homogeneous. Damage will be initiated at these weak spots, and damage progression will extend outward. It is the intention that test trays used in the CSU experiments will be representative of construction used throughout the HSDRRS; but there is the possibility that actual levees will have greater variation in grass/soil consistency, and this may lead to damage at less cumulative excess wave volume than predicted by the methodology.
 4. The initial CSU tests were intended to replicate to the extent possible the attributes of real levees. However, the sod placed in the trays proved to be very robust, despite having limited time to establish mature root system connection to the underlying clay. Consequently, the grass in the trays did not fail during testing when subjected to extreme overtopping loads. Without failure, calibration of the erosional equivalence method could not be accomplished based on these test results. However, before judging the resiliency of the entire HSDRRS relative to the CSU test results, it will be necessary to determine whether the actual grass has the same characteristics as the grass tested in the trays at CSU.
 5. The critical threshold discharge and erosional damage limits based on the steady overflow curves implicitly include a value for the friction factor. The included value is probably reasonable, but it may not be correct. Once the methodology is calibrated with full-scale tests, it will not be necessary to specify a value of friction factor.
 6. Overtopping durations of individual waves are estimated using a formula that has not been extensively verified. Differences could arise in the predictions if the overtopping durations are actually shorter than those estimated by the selected equation.

The above caveats and uncertainties are not extreme, and most could be resolved if full-scale test results become available that include failure of the grass or other slope protection alternative. The most overriding concern is establishing the correct value for the critical threshold discharge (or velocity) for each of the distinct types of levee protection (grass, TRMs, ACM, bare clay, etc.).

Conclusions

Armoring portions of the HSDRRS to provide greater resiliency for storm events that exceed the established design level is a critical mission for Task Force Hope. Previously, no design guidance existed that would provide a rational method for assessing where levee armoring should be placed to provide adequate resiliency against extreme storm events. Furthermore, no methods existed that could estimate the duration of overtopping that can be tolerated before slope damage becomes problematic.

This report has adapted and extended the erosional equivalence concept first introduced by Dean et al. (2010). This concept is based on the notion that once soil erosion is initiated; there is a certain amount of erosion that can be tolerated before unacceptable damage occurs on the slope. As each wave overtops the levee crown, there can be an excess amount of flow work (excess wave volume) above a certain threshold level that contributes to the slope erosion. The duration of tolerable overtopping is determined by the accumulation of excess flow work in time.

The erosional equivalence method is able to account for the fact that (1) earthen levees can tolerate certain levels of wave overtopping without any soil erosion, (2) earthen levees can survive some duration of increased wave overtopping with a certain amount of allowable erosion, and (3) earthen levees will eventually suffer damage to the slope protection if the overtopping level is high enough and the overtopping persists for sufficient duration.

A predictive tool based on the erosional equivalence concept was developed to simulate the accumulation of excess wave volume for the cases of wave-only overtopping, combined wave and surge overtopping, and time-varying wave and surge conditions. The methodology provisionally uses critical threshold velocity and erosional limits derived from steady overflow conditions. However, these thresholds are most likely conservative and will predict damage sooner than it should be expected because the critical threshold velocities are smaller than necessary for good-quality grass on clay slopes. Fortunately, the methodology can be adjusted using more reliable thresholds for initiation of erosion and onset of damage that arise from full-scale wave overtopping tests. In the meantime, the methodology provides a useful (but perhaps conservative) tool for comparative analyses of different reaches of the HSDRRS to identify which reaches will be likely candidates for additional slope armoring.

If fully validated using full-scale test results and other comparisons, the erosional equivalence methodology could provide a logical basis for selecting appropriate armoring options for all reaches of the HSDRRS exposed to potential wave overtopping. Like any engineering design tool, it would be prudent to include some factor of safety when analyzing predictions to account for the fact that the methodology can only truly be tested by gauging the performance of strengthened levee slopes during actual hurricane events.

References

- Bagnold, R. A. 1960. Sediment discharge and stream power, *Preliminary Announcement*, U.S. Geological Survey Circular 421, Menlo Park, CA.
- Bagnold, R.A. 1966. An approach to the sediment transport problem from general physics, U.S. Geological Survey, Professional Paper 422-J.
- Bosman, G. 2007. Velocity and flow depth variations during wave overtopping, "Masters Thesis, Delft University of Technology, The Netherlands, 163p.
- Bosman, G., J. W. van der Meer, G. Hoffmans, H. Schuttrumpf, H. Verhagen. 2008. Individual overtopping events at dikes. *Proceedings of the 31st International Conference Coastal Engineering*, American Society of Civil Engineers, Vol 4, pp 2944-2956.
- DCR 2004. Virginia stream restoration and stabilization best management practices guide. Department of Conservation and Recreation, Division of Soil and Water Conservation, Richmond, VA.
- Dean, R. G., J. D. Rosati, T. L. Walton, and B. L. Edge. 2010. Erosional equivalences of levees: Steady and intermittent wave overtopping. In: Demirbilek (editor), Special issue of *Ocean Engineering*, Elsevier, Vol 37, pp 104-113.
- de Waal, J. P., and J. W. van der Meer. 1992. Wave run-up and overtopping on coastal structures, *Proceedings of the 23rd International Coastal Engineering Conference*, American Society of Civil Engineers, Vol 2, pp 1758-1771.
- Franco, L., M. de Gerloni, and J. W. van der Meer. 1994. Wave overtopping on vertical and composite breakwaters, *Proceedings of the 24th International Coastal Engineering Conference*, American Society of Civil Engineers, Vol 1, pp 1030-1045.
- Henderson, F. M. 1966. *Open channel flow*, MacMillian Publishing Co., New York.
- Hewlett, H. W. M, L. A. Boorman, and M. E. Bramley. 1987. Design of reinforced grass waterways, CIRIA Report 116, Construction and Industry Research and Information Association, London.
- Hughes, S. A., and N.C. Nadal. 2009. Laboratory study of combined wave overtopping and storm surge overflow of a levee. *Coastal Engineering*, Vol 56. No. 3, Elsevier, pp 244-259.
- Hughes, S. A., and J. M. Shaw. 2011. Continuity of instantaneous wave overtopping discharge with application to stream power concepts. *Journal of Waterway, Port, Coastal, and Ocean Engineering*, American Society of Civil Engineers, Washington, D.C., Vol 137, No. 1, pp 12-25.
- Knighton, A.D. 1999. Downstream variation in stream power. *Geomorphology*, Vol 29, pp 293-306.

- Nadal, N. C. 2007. Shear stress and stream power. Unpublished white paper, U.S. Army Engineer Research and Development Center, Vicksburg, Mississippi.
- Pullen T., N.W.H. Allsop, T. Bruce, A. Kortenhuis, H. Schüttrumpf, J.W. van der Meer. 2007. EurOtop: Wave overtopping of sea defences and related structures: Assessment Manual, www.overtopping-manual.com.
- Schüttrumpf, H., J. Möller, and H. Oumeraci. 2002. Overtopping flow parameters on the inner slope of seadikes, *Proceedings of the 28th International Coastal Engineering Conference*, World Scientific, Vol 2, pp 2116-2127.
- Schüttrumpf, H., and H. Oumeraci. 2005. Layer thicknesses and velocities of wave overtopping flow at seadikes, *Coastal Engineering*, Elsevier, Vol 52, pp 473-495.
- TAW. 2002. Technical Report - Wave run-up and wave overtopping at dikes, Technical Advisory Committee for Flood Defence in the Netherlands (TAW), Delft, The Netherlands.
- USDA 2001. Stream corridor restoration: principles, processes, and practices, The Federal Interagency Stream Restoration Working Group, United States Department of Agriculture (USDA) - Natural Resources Conservation Service, Part 653 of the *National Engineering Handbook*.
- van der Meer, J. W., W. and Janssen. 1995. Wave run-up and wave overtopping at dikes, In: Kabayashi and Demirbilek (Eds.), *Wave Forces on Inclined and Vertical Wall Structures*, American Society of Civil Engineers, pp 1-27.
- van der Meer, J. W., P. Bernardini, W. Snijders, and E. Regeling. 2006. The wave overtopping simulator, *Proceedings of the 30th International Conference on Coastal Engineering*, World Scientific, Vol 5, pp 4654-4666.
- van der Meer, J. W., G. J. Steendam, G. de Raat, and P. Bernardini. 2008. Further developments on the wave overtopping simulator, *Proceedings of the 31st International Conference Coastal Engineering*, American Society of Civil Engineers, Vol 4, pp. 2957-2969.
- van der Meer, J. W., B. Hardeman, G.J. Steendam, H. Schüttrumpf, and H. Verheij. 2010. Flow depths and velocities at crest and inner slope of a dike, in theory and with the wave overtopping simulator, *Proceedings of the 32st International Conference Coastal Engineering*, American Society of Civil Engineers, (in press).
- van Gent, M. R. 2002. Wave overtopping events at dikes, *Proceedings of the 28th International Coastal Engineering Conference*, World Scientific, Vol 2, pp 2203-2215.
- Whitehead, E., M. Schiele, and W. Bull. 1976. A guide to the use of grass in hydraulic engineering practice, *CIRIA Technical Note 71*, Construction and Industry Research and Information Association, London.

Appendix: The Relationship Between Flow Work and Stream Power

Hughes and Shaw (2011) provided the following discussion of stream power and how it relates to wave overtopping. The text has been extracted and reproduced with only minor editing.

The concept of stream power was introduced by Bagnold (1960, 1966). He considered the relationship between the rate of energy available and the rate of work being done in transporting sediments. Bagnold defined stream power (P_s) as power per unit area of stream bed, which could be expressed as shear stress (τ_0) times the free-stream flow velocity (u), i.e.,

$$P_s = \tau_0 \cdot u \quad (\text{A1})$$

In an unpublished white paper Nadal (2007) summarized some of the literature about stream power as follows:

According to United States Department of Agriculture (USDA 2001), sediment transport rates are directly related to stream power. Stream power is defined as the rate of doing work, or as a measure of the energy available for moving rock, sediment particles, or woody or other debris in the stream channel, as determined by discharge, water surface slope, and the specific weight of water (DCR, 2004). Knighton (1999) explained the origin of the energy as coming from potential or position energy; and as the water flows, the energy is converted into kinetic form.

Given the wide-spread use of stream power as an estimator of sediment transport and erosion in rivers and stream and the fact that Dean et al. (2010) explained the form of the Hewlett et al. (1987) curves in terms of excess work above a threshold, stream power may prove valuable as an indicator of levee slope erosion due to wave overtopping.

Considering only the one-dimensional case of a very wide channel (i.e., a straight and long levee or dike with uniform crest elevation) with the major axis aligned with the landward-side levee slope (s -coordinate), the momentum equation applicable to steep slopes is given by

$$\frac{\partial u}{\partial t} + v \frac{\partial u}{\partial s} + g \frac{\partial h}{\partial s} + g S_f - g \sin \theta = 0 \quad (\text{A2})$$

where u is flow velocity parallel to the slope, g is acceleration of gravity, s is the down-slope coordinate parallel to the slope, h is flow thickness perpendicular to the slope, θ is the angle of levee slope to horizontal, and t is time. The variable S_f is the slope of the energy grade line, also known as the friction slope (net change in energy between two locations on the slope). Substituting for S_f from the usual definition of shear stress given by

$$\tau_0 = \gamma_w h S_f \quad (\text{A3})$$

where γ_w is specific weight of water, Equation (A2) can be rearranged to the form

$$\tau_0 = \gamma_w h \left[\sin \theta - \frac{\partial h}{\partial s} - \frac{\partial}{\partial s} \left(\frac{u^2}{2g} \right) - \frac{1}{g} \frac{\partial u}{\partial t} \right] \quad (\text{A4})$$

In Equation (A4) shear stress, flow thickness and velocity vary in both time and space. From the definition of Equation (A3) it is seen that the friction slope is comprised of the four terms in the square brackets that arise from weight of water on the slope, pressure change due to flow thickness variation along the slope, convective acceleration, and temporal acceleration, respectively. If the flow on the slope reaches a quasi-equilibrium balance between the forcing and slope resistance, then the friction slope reduces to $S_f = \sin \theta = S_0$.

Stream power at a location on the landward-side levee slope can also be expressed in terms of instantaneous overtopping discharge by substituting Equation (A3) or (A4) into Equation (A1) and noting that $u(t) \cdot h(t) = q(t)$, i.e.,

$$P_s(t) = \tau_0(t) \cdot u(t) = \gamma_w [h(t) u(t)] S_f(t) = \gamma_w q(t) S_f(t) \quad (\text{A5})$$

At locations where the instantaneous flow velocity can be well approximated as the terminal velocity (i.e., $S_f = \sin \theta$), discharge can be expressed as

$$q(t) = \frac{P_s}{\rho g \sin \theta} \quad (\text{A6})$$

With Equation (A6) it is possible to cast Dean, et al.'s (2010) summation equation for accumulated flow work in terms of stream power. Substituting Equation (A6) into Equation (11) gives

$$W_{ET}(t) = \sum_{n=1}^N (P_{Sn} - P_{Sc}) \Delta t_n \leq \frac{E_w}{K_w \beta_w} \left(\frac{\rho f_F}{2} \right) \quad \text{with } P_{Sn} > P_{Sc} \quad (\text{A7})$$

where

$$P_{Sc} = \left(\frac{\rho f_F u_c^3}{2} \right) \quad (\text{A8})$$

The bracketed term inside the summation on the left-hand side of Equation (A7) is the excess stream power in a wave that is available to erode the levee slope. It is expressed as difference between the total stream power and some critical steam power. Equation (A7) has units of (kN-m)/m² in the SI system, so it represents excess flow work done on the slope in terms of stream power.

Equations (A7) and (A8) will not be used directly for estimating erosion potential because discharge is easier to estimate for overtopping conditions. However, it is reassuring to know that Dean, et al.'s (2010) methodology conforms to the well-established concept of stream power.

REPORT DOCUMENTATION PAGE

Form Approved
OMB No. 0704-0188

Public reporting burden for this collection of information is estimated to average 1 hour per response, including the time for reviewing instructions, searching existing data sources, gathering and maintaining the data needed, and completing and reviewing this collection of information. Send comments regarding this burden estimate or any other aspect of this collection of information, including suggestions for reducing this burden to Department of Defense, Washington Headquarters Services, Directorate for Information Operations and Reports (0704-0188), 1215 Jefferson Davis Highway, Suite 1204, Arlington, VA 22202-4302. Respondents should be aware that notwithstanding any other provision of law, no person shall be subject to any penalty for failing to comply with a collection of information if it does not display a currently valid OMB control number. **PLEASE DO NOT RETURN YOUR FORM TO THE ABOVE ADDRESS.**

1. REPORT DATE (DD-MM-YYYY) May 2011	2. REPORT TYPE Final report	3. DATES COVERED (From - To)		
4. TITLE AND SUBTITLE Adaptation of the Levee Erosional Equivalence Method for the Hurricane Storm Damage Risk Reduction System (HSDRRS)		5a. CONTRACT NUMBER		
		5b. GRANT NUMBER		
		5c. PROGRAM ELEMENT NUMBER		
6. AUTHOR(S) Steven A. Hughes		5d. PROJECT NUMBER		
		5e. TASK NUMBER		
		5f. WORK UNIT NUMBER		
7. PERFORMING ORGANIZATION NAME(S) AND ADDRESS(ES) U.S. Army Engineer Research and Development Center Coastal and Hydraulics Laboratory Vicksburg, MS 39180-6199		8. PERFORMING ORGANIZATION REPORT NUMBER ERDC/CHL TR-11-3		
		10. SPONSOR/MONITOR'S ACRONYM(S)		
9. SPONSORING / MONITORING AGENCY NAME(S) AND ADDRESS(ES) Task Force Hope, US Army Engineer District, New Orleans P.O. Box 60267, New Orleans, LA 70160-0267		11. SPONSOR/MONITOR'S REPORT NUMBER(S)		
		12. DISTRIBUTION / AVAILABILITY STATEMENT Approved for public release; distribution is unlimited.		
13. SUPPLEMENTARY NOTES				
14. ABSTRACT This report describes a rational methodology for evaluating the strength and resiliency of earthen levees against wave overtopping forces during hurricanes. The new methodology was developed by extending Dean, et al.'s (2010) concept of "cumulative excess work," which hypothesized that damage to grass-covered slopes is caused by cumulative work done by the overtopping waves in excess of some tolerable level. The erosional equivalence method is able to account for the fact that (1) earthen levees can tolerate certain levels of wave overtopping without any soil erosion, (2) earthen levees can survive some duration of increased wave overtopping with allowable erosion, and (3) earthen levees will eventually suffer slope damage if the overtopping level is high and overtopping duration is sufficiently long. A predictive capability for estimating the cumulative excess wave volume (or excess work) as a function of time for prescribed wave, surge, and levee parameters was developed for the cases of wave-only overtopping, combined wave and surge overtopping, and realistic storms with time-varying parameters. Application of the methodology is illustrated by worked examples. The erosional equivalence methodology provides a useful (but perhaps conservative) tool for comparative analyses of different reaches of the HSDRRS to identify which reaches would benefit from additional slope armoring.				
15. SUBJECT TERMS Erosional equivalence Excess work		Levee erosion Levees Overtopping duration	Resiliency Steady overflow Wave overtopping	
16. SECURITY CLASSIFICATION OF:			17. LIMITATION OF ABSTRACT	18. NUMBER OF PAGES 141
a. REPORT UNCLASSIFIED	b. ABSTRACT UNCLASSIFIED	c. THIS PAGE UNCLASSIFIED		
			19b. TELEPHONE NUMBER (include area code)	